Stratigraphic forward modelling for South West Collie Hub

Phase One - Static Model

Cedric M. Griffiths, Zahra Seyedmehdi, Tristan Salles, Chris Dyt
Report Number EP13068
October 2012

Australian National Low Emissions Coal Research and Development (ANLEC R&D).

ANLEC R&D is supported by Australian Coal Association Low Emissions Technology Limited and the Australian Government through the Clean Energy Initiative

CSIRO Earth Science and Resource Engineering, Rock Properties Group, Kensington, Perth, WA

Citation

Griffiths, C. M., Seyedmehdi, Z., Salles, T., Dyt, C., 2012. Stratigraphic forward modelling for South West Collie Hub: Phase One - Static Model. Report for ANLEC R&D Targeted Project 129. CSIRO Open File Report Number EP13068

Copyright and disclaimer

© 2012 CSIRO To the extent permitted by law, all rights are reserved and no part of this publication covered by copyright may be reproduced or copied in any form or by any means except with the written permission of CSIRO.

Important disclaimer

CSIRO advises that the information contained in this publication comprises general statements based on scientific research. The reader is advised and needs to be aware that such information may be incomplete or unable to be used in any specific situation. No reliance or actions must therefore be made on that information without seeking prior expert professional, scientific and technical advice. To the extent permitted by law, CSIRO (including its employees and consultants) excludes all liability to any person for any consequences, including but not limited to all losses, damages, costs, expenses and any other compensation, arising directly or indirectly from using this publication (in part or in whole) and any information or material contained in it.

Contents

Contents iii

Figures v

Tables vii

Acknowledgments viii

Executive summary ix

1 Introduction 1

1.1 The technical basis of the Research Project 2

2 The Sedsim Program 4

2.1 Stratigraphic Forward Modelling Context 4

2.2 Basic Principles of Sedsim Operation 5

2.2.1 Fluid Flow 5

2.2.2 Sediment Transport 6

2.2.3 Temporal aliasing/time sampling sensitivity 7

2.2.4 Tectonic subsidence 7

2.2.5 Compaction 8

2.3 Steps involved in a Sedsim Simulation 8

3 Conceptual Model of the Triassic and Lower Jurassic deposition in the South Perth Basin 10

4 Method 14

4.1 Area and Scope of Investigation 14

4.1.1 Time period of interest 15

4.2 Data sources 17

4.2.1 Topographic/bathymetric surface 17

4.2.2 Tectonic History 17

4.2.3 Seismic 18

4.2.4 Sea level curve 19

4.2.5 Climate 20

4.2.6 Depositional systems 21

4.2.7 Petrographic data 22

4.2.8 Biostratigraphic data 23

4.2.9 Well data (including wireline, cuttings and core) 24

5 Construction of the depositional model 25

5.1 Conceptual models 25

5.2 Computer model 25
5.2.1 Olenekian to Anisian (250 Ma to 237 Ma) [Wonnerup Equivalent] 25
5.2.2 Ladinian to Rhaetian (237 Ma to 198 Ma) [Yalgorup Equivalent] 26
5.2.3 Hettangian to Pliensbachian (198 Ma to 182 Ma) [eneabba Equivalent] 26
5.3 Initial altitude and Sea level curves 26
5.4 Tectonic movement 27
5.5 Manning Coefficients and Porosity Table 27

6 Experimental runs 28

6.1 Initial round of simulations at 5 km resolution 28
6.1.1 Olenekian to Anisian (250 Ma to 237 Ma) [Wonnerup Equivalent] 30
6.1.2 Ladinian to Rhaetian (237 Ma to 198 Ma) [Yalgorup Equivalent] 31
6.1.3 Hettangian to Pliensbachian (198 Ma to 182 Ma) [eneabba Equivalent] 31
6.1.4 Olenekian to Pliensbachian (250 Ma to 182 Ma) [Lesueur and Eneabba Fm.] Sand Fraction. 32
6.2 Nested 500 m grid simulations 32
6.2.1 Olenekian to Anisian (250 Ma to 237 Ma) [Wonnerup Equivalent] Thicknesses 35
6.2.2 Ladinian to Rhaetian (237 Ma to 198 Ma) [Yalgorup Equivalent] 35
6.2.3 Hettangian to Pliensbachian (198 Ma to 182 Ma) [eneabba Equivalent] 36

7 Verification 37

8 Static Model 41

9 Discussion 42

10 Conclusions 44

A.1 Sedsim9 simulation input files 49
A.1.1 Command, Topography, Sealevel, tectonic files 49
A.2 Sedsim9 simulation output files 49
A.2.1 ASCII processed output files 49
A.2.2 ASCII raw output files 50
A.2.3 BINARY output files 51

References and Bibliography 52

Figures

Figure 1 The stratigraphic succession that has been modelled is from 250 Ma to 182 Ma Early Triassic to Early Jurassic. The Lake Preston-1 well is within the simulation area. The orange stratigraphic unit is the Wonnerup Member and equivalent, the type section for which is the interval shown in the Wonnerup-1 well 75 km south west of the simulation area. The green stratigraphic unit is the Yalgorup [previously known as the Myalup] Member and equivalent, the type section for which is in the Lake Preston-1 well in the simulation area. The red stratigraphic unit is the Eneabba Formation and equivalent, the type section for which is in the Eneabba-1 well, 300 km north north west of the simulation area. 13

Figure 2 Present day regional location of the South Perth Basin in south-western Australia, with the 5 km grid simulation area marked by the red rectangle. The higher resolution (500 m grid) area is outlined in green. 14

Figure 3 South Perth Basin and main structural features. The red rectangle marks the 15x8, 5000 m resolution simulation area. (adapted from Crostella and Backhouse (2000)) 15

Figure 4 Stratigraphic intervals with the Haq and Al-Qahtani (2005) sea level curve. Ages on the left of the diagram from Ogg, et al. (2008) and the ICS Chart (2009). The blue curve is the Haq and Al-Qahtani sea level curve, modulated by the Quaternary Milanković frequencies and phase relationships and sampled at 5 ka as used for the Sedsim simulation. Background chart from TimeScale Creator (TSCreator visualization of enhanced Geologic Time Scale 2004 database (Version 5.3; 2012) James Ogg (database coordinator) and Adam Lugowski (software developer) http://www.tscreator.org. Plate reconstructions from Blakey (2008). 16

Figure 5 Initial 5000 m resolution depositional surface with a gradient of 0.0002. Sediment sources are shown as green arrows. Contours in metres..... 17

Figure 6 Top Sabina horizon gridded at 500 m (left), Top Wonnerup horizon gridded at 500 m) (centre), Wonnerup isochore gridded at 500 m (right). All values in metres. 19

Figure 7 Anisian (245 Ma) palaeogeography and the simulation area marked in red (modified after Yan and Zhao, 2001, Figure 3)..... 20

Figure 8 Palaeogeographic reconstructions and major river directions for the Perth Basin (Norvik, 2003). 22

Figure 9 Core petrographic data from Wonnerup Member (PJ1-D4), Yalgorup Member (earlier named Myalup) (PJ1-D2 and PJ1-D3) and Eneabba Fm. (PJ1-D1) in Pinjarra-1. From Schlumberger-TerraTek, 2010. 23

Figure 10 Wells in the simulation area and type wells for Wonnerup Member, Yalgorup (Myalup) member and Eneabba Fm.. Red wireline traces are gamma, and blue wireline traces are sonic logs. Orange boxes are Wonnerup intervals, green boxes demarcate Yalgorup intervals and red boxes mark Eneabba intervals. Depths are mRKB. 24

Figure 11 East-West lithology sections across the simulated area. Grain sizes as shown in the legend..... 28

Figure 12 East-West 'pseudo seismic' sections across the simulated area. Alternate time layers are code red and blue. 28

Figure 13 Sections from the 5 km resolution model, crossing at the Harvey-1 well position, showing Sedsim predicted lithology, pseudo-seismic and porosity distributions. 29

Figure 14 Wonnerup equivalent thickness comparisons with the seismic isochore at 5 km resolution and the well data set. Left-hand image is the Sedsim predicted thickness distribution. The centre image shows the observed well thicknesses. The right-hand image is the seismic isochore. The legend for all maps is shown below. The actual values in metres at the location of the Harvey-1 well are shown in the table. 30

Figure 15 Yalgorup equivalent thickness comparisons with the seismic isochore at 5 km resolution and the well data set. The explanation of columns and legend is otherwise as in Figure 11. 31

Figure 16 Eneabba equivalent thickness comparisons with the seismic isochore at 5 km resolution and the well data set. The explanation of columns and legend is otherwise as in Figure 11. 31

Figure 17 Sedsim sand fraction predictions at 5 km resolution for each of the lithostratigraphic units modelled. The predicted values at the location of the Harvey-1 well are shown in the table. 32

Figure 18 Green rectangle marks the location of the nested Sedsim 500 m grid within the 5000 m Sedsim simulation (fine red rectangle). The pink and blue polygons mark the boundaries of the Schlumberger static and dynamic models respectively. 33

Figure 19 Coarse and fine grid porosity volumes showing the location of the 500 m nested grid. 33

Figure 20 Sedsim predicted 500 m grid volume. Lithology, pseudo-seismic and porosity sections 34

Figure 21 Wonnerup equivalent thickness comparisons with the seismic isochore at 500 m resolution and the well data set. The explanation of columns and legend is otherwise as in Figure 14. 35

Figure 22 Yalgorup equivalent thickness comparisons with the seismic isochore at 500 m resolution and the well data set. The explanation of columns and legend is otherwise as in Figure 14. 35

Figure 23 Eneabba equivalent thickness comparisons with the seismic isochore at 500 m resolution and the well data set. The explanation of columns and legend is otherwise as in Figure 14. 36

Figure 24 Constraint well porosity distribution with lithology and depth. (A) Pinjarra-1 sonic porosity values, Lake Preston-1 sonic porosity (dark orange) and density porosity (light orange) distribution with depth. (B) Sedsim porosity table calibrated against these wells. Rows show the effect of different mud: sand ratios on fractional porosity response to pressure (burial depth). (C) The application of this table to Sedsim prediction of porosity at 5 km grid resolution at these two well locations. 38

Figure 25 Observed and predicted porosity distribution with depth in the Harvey-1 well. The Sedsim porosity values were derived as described above (Section 5.5) from a porosity matrix calibrated against Pinjarra-1 and Lake Preston-1 well data. The observed porosity values in the well were CNC (Neutron porosity), Ødt (sonic porosity), Ørhob (density porosity), Porosity 4300 and Porosity 800 (core plug values), and the Sedsim predicted values (p.u.5). 39

Figure 26 Location of seismic lines . Line '11GA_LL2-mig-final' is shown in red in relation to the Lake Preston-1 well location. 39

Figure 27 Seismic line '11GA_LL2-mig-final' (upper), at the location shown in Figure 26 compared with a 'pseudo-seismic' section (lower) from the Sedsim simulation at approximately the same location..... 40

Figure 28 The area shown is the 500 m resolution static model grid around Harvey-1 well location. A) Sedsim predicted seal potential in the Yalgorup equivalent (75% mud contour shown). B) Sedsim predicted sand fraction in the Wonnerup equivalent. Faults interpreted from the 2011 2D seismic lines are overlain on the Sedsim facies maps. Green lines represent faults with unspecified downthrow to the West and SW, while blue lines represent faults with unspecified downthrow to the North and NE (Langhi et al, 2013). 44

Figure 29 Sedsim predicted risk maps for seal and reservoir for the 500 m grid area (red higher risk, green lower risk). The Common Risk Segment (CRS) map combines the seal and reservoir risk in a simplistic (unweighted) fashion. The green CRS areas are those where the optimum seal and reservoir conditions coincide at the same Sedsim node. Note that this is a conservative case. Faults interpreted from the 2011 2D seismic lines are overlain on the Sedsim CRS maps. Green lines represent faults with unspecified downthrow to the West and SW, while blue lines represent faults with unspecified downthrow to the North and NE (Langhi et al, 2013). 45

Figure 30 The area shown is the 5000 m resolution regional model grid. A) Sedsim predicted sand fraction in the Wonnerup equivalent (60% sand fraction contour shown). B) Sedsim predicted sand fraction in the Yalgorup equivalent (60% sand fraction contour shown). Faults interpreted from the 2011

2D seismic lines are overlain on the Sedsim facies maps. Green lines represent faults with unspecified downthrow to the West and SW, while blue lines represent faults with unspecified downthrow to the North and NE (Langhi et al, 2013). 46

Figure 31 The area shown is the 5000 m resolution regional model grid. A) Sedsim predicted mud fraction in the Yalgorup equivalent (60% mud fraction contour shown). B) Sedsim predicted mud fraction in the Eneabba equivalent (60% mud fraction contour shown). Faults interpreted from the 2011 2D seismic lines are overlain on the Sedsim facies maps. Green lines represent faults with unspecified downthrow to the West and SW, while blue lines represent faults with unspecified downthrow to the North and NE (Langhi et al, 2013). 47

Tables

Table 4-1 Selected wells with unit tops (mRKB). 24

Table 5-1 Sedsim input parameters common to all Olenekian to Anisian simulations 25

Table 5-2 Sedsim input parameters common to all Ladinian to Rhaetian simulations 26

Table 5-3 Sedsim input parameters common to all Hettangian to Pliensbachian simulations 26

Apx Table A.1 Sedsim9 input files 49

Apx Table A.2 Sedsim9 ASCII output files produced by 'graph2dep_100903mac', 'graph2spc2_100617mac ' and 'graph2eclipse' programs. 49

Apx Table A.3 Raw ASCII output files as output directly from 'sedsim9_120427Intelmac' 50

Apx Table A.4 Sedsim9 binary SedView (.cif) output files 51

Acknowledgments

The authors wish to acknowledge financial assistance provided through Australian National Low Emissions Coal Research and Development (ANLEC R&D). ANLEC R&D is supported by Australian Coal Association Low Emissions Technology Limited and the Australian Government through the Clean Energy Initiative.

The outcome and impact of the project would not have been possible without the cooperation and active involvement of many CSIRO geoscientists who gave freely of their experience and knowledge concerning the South Perth Basin area and West Australian Triassic and Early Jurassic depositional systems in general.

We are grateful for all the help we received and the authors of the many publications concerning the system we have modelled, and hope that the outcome justified the involvement and investment in time and effort. Any misunderstandings or misrepresentations of their ideas are entirely our responsibility.

Executive summary

A stratigraphic forward model of the time period from 250 Ma to 182 Ma (Olenekian to Pliensbachian - Base Wonnerup equivalent to top Eneabba equivalent) has been created in that part of the South Perth basin that is a candidate area for geological sequestration of carbon dioxide. We used the CSIRO Sedsim stratigraphic forward modelling software constrained by available well and seismic data and previous published geological studies. The goal was to determine the distribution of grainsize and primary porosity (and permeability via the same transfer function used by Schlumberger) of Triassic and Lower Jurassic sediments below seismic resolution and away from well data across the study area around the Harvey-1 well.

The research targeted the significant current risk involved in applying traditional oil-field reservoir characterisation tools to the construction of static geological models of saline formations. As stated in the latest US DoE document on CCS, "…. The successful characterization of a site is the most important step in ensuring the safe and economic operation of a CO_2 GS site." [2010 DoE Site Screening, Selection, and Initial Characterization for Storage of CO_2 in Deep Geologic Formations. DOE/NETL-401/090808, November 2010].

The project has demonstrated an alternate workflow for producing a static reservoir model for geological sequestration of CO_2. The workflow was based on limited well and seismic data constraints, and used the Sedsim stratigraphic forward modelling software to translate a conceptual geological model into a cellular geological volume. This volume will form the basis of a reservoir flow simulation of CO_2 injection into the Lesueur Sandstone.

Two models have been produced; a 5000 m grid over the 75 km x 40 km area, and within this, a nested 500 m grid over the Collie Hub dynamic model area of 15 km x 10 km.

A blind test of porosity distribution at the Harvey-1 well location suggests that the model may be suitable for use as the basis of a dynamic reservoir simulation.

Output from the model consists of:

- 3D interactive visualisations in SedView format.
- ASCII files in various formats with grain-size, porosity, facies, stratigraphic age, sorting, sand fraction etc. that can be used to generate pseudo-well logs, synthetic seismic sections, permeability and porosity volumes, etc. at the spatial resolution of the grid and the vertical resolution of the depositional events or a fixed vertical scale as required.
- Movies of basin formation from 250 Ma to 182 Ma.

As with any model, it is incomplete at several levels, and will need to be updated as new information become available. However it is hoped that this initial attempt to predictably model facies distribution, porosity and permeability (below seismic resolution and away from well data) will stimulate further use of the stratigraphic forward modelling approach, both at the regional and field scale, for geological sequestration of carbon dioxide, as well as petroleum systems and aquifer-constrained geothermal projects.

1 Introduction

The project described in this report involves the stratigraphic forward modelling by CSIRO of the time period from 250 Ma to 182 Ma (Olenekian to Pliensbachian or Base Wonnerup equivalent to top Eneabba equivalent) in that part of the South Perth basin that is a candidate area for geological sequestration of carbon dioxide (Varma et al (2009), and Causebrook et al (2006)). It is the same area that was the subject of a Schlumberger static and dynamic model. The simulation was constrained by available well and seismic data and built on previous published and restricted studies in the area. The goal was to determine the distribution of grainsize and primary porosity (and permeability via the same transfer function used by Schlumberger) of Triassic and Lower Jurassic sediments below seismic resolution and away from well data across the study area.

The research targeted the significant current risk involved in applying traditional oil-field reservoir characterisation tools to the construction of static geological models of saline formations. As stated in the latest US DoE document on CCS, "…. The successful characterization of a site is the most important step in ensuring the safe and economic operation of a CO_2 GS site." [2010 DoE Site Screening, Selection, and Initial Characterization for Storage of CO_2 in Deep Geologic Formations. DOE/NETL-401/090808, November 2010].

Current geological exploration, appraisal and development costs for geo-sequestration amount to between 5% and 20% of the cost of CO_2 avoided (Allison et al, 2009). The cost of drilling extra wells for monitoring and to replace failed wells has been estimated to increase the cost of geo-sequestration by between 5% and 10%. In the Surat Basin for example, improving the Probability of Success as a function of improved reservoir characterisation (quantified as a greater ratio of successful wells to unsuccessful wells), in A$2009 terms, assuming an injection rate of 50 Mt/year, amounts to a potential improvement of viability of A$500M per year.

Regional background data, plus data derived and processed during the initial CO_2CRC Harvey Ridge assessment, and the subsequent Government of Western Australia Department of Mines and Petroleum (DMP)-funded detailed study by Schlumberger, were used as the basis for a numerical stratigraphic forward model using Sedsim. A three-dimensional process-based reservoir-scale model of the Lower and Upper members of the Lesueur Formation [now Wonnerup and Myalup Formations] was developed in the area of the proposed Collie Hub data well (GSWA Harvey-1) site on Block 1326 Riverdale Rd.

The goal was to demonstrate the feasibility of a novel reservoir characterisation workflow for initial characterisation of saline formation-constrained CCS targets that should increase the probability of success (POS) when compared to conventional workflows. This project can be considered as an opportunity to test the Sedsim stratigraphic forward modelling approach in a region of limited subsurface geological data but with the opportunity to compare and calibrate the model in successive steps as new wells and seismic are obtained. The initial work in this report was completed without the new geological knowledge of the Harvey-1 well, allowing the results to be compared with Harvey-1. Planned new 3D seismic data and potentially subsequent wells will enable further tests and calibrations of this approach. Should this novel approach prove successful at reducing geological uncertainty in advance of well data then this could be a useful workflow for other carbon storage projects in data-poor areas and may enable industry to reduce the time for geological characterisation and enhance risk reduction.

Why is this Research Project needed?

Using the CCS cost evaluations for the Surat Basin case as presented in Allinson et al (2009) and Neal et al (2010), we can recalculate the minimum carbon price for viability of the project as a function of Probability of Success (POS). For variation in POS ranging from 20% to 60% as a result of variation in ability to predict reservoir heterogeneity, for the same NPV/CP relationship the difference in "minimum carbon price required to make the EA&D programme viable" is around ±10 A$/t in each case.

This not only implies that the deep and medium CCS targets are more vulnerable to failure of exploration and appraisal (±30% minimum carbon price for viability) than shallow targets (±10% minimum carbon price for viability), but that the higher the probability of success (due to improved understanding of the reservoir) the greater the improvement in expected value for a given carbon price rise.

So improving the POS (from 20% to 60%) as a function of improved reservoir characterisation (quantified as a greater ratio of successful wells to unsuccessful wells), in A$2009 terms, assuming an injection rate in the Surat of 50 Mt/year amounts to a potential improvement of viability of A$500M per year.

1.1 The technical basis of the Research Project

i. Hypothesis being tested:

Before a site can be approved for the long-term geological sequestration of CO_2 it is necessary (and indeed a statutory obligation in several jurisdictions (see Anonymous, 2010)) to provide a site characterisation. Such characterisation usually proceeds in a series of stages. The initial stage is the provision by a professional geoscientist of a 'static geological reservoir model'. The purpose of this model is to quantitatively predict (beyond our current ability to directly measure) the spatial variation of those properties of the reservoir that can affect CO_2 storage volume, flow rates and flow directions. This is rarely trivial, as sedimentary bodies are normally anisotropic, spatially complex and internally heterogeneous at some scale, and the spatial variation is largely controlled by depositional environment and post-depositional structure and diagenesis.

The initial static model is usually derived using techniques widely applied in the oil industry, namely: interpreting any well data that exist; interpolating between wells; describing the pattern of layering away from wells by interpreting seismic data; converting seismic response (at seismic resolution) to reservoir properties; gridding the properties using a commercial package such as Petrel, RMS, or GoCad. The data on which an initial static model is based are usually sparse, and any wells that exist are often at least an order of magnitude more widely spaced than the required grid cell resolution of the static model. The way this problem is usually approached in the oil industry is to draw on experience with outcrop analogues and 'training' images to fill in the space between wells with hopefully appropriate sediment body shapes. A succession of sedimentological and petrophysical studies from 1988 to 2009, including specific CCS-related work published by Spencer et al (2006), and Dance et al (2009), discuss a variety of interpretations of the Waarre-C depositional system(s) for the CO_2CRC Otway project. The uncertainty involved in deriving an initial static geological model is significant, and impacts on all decisions leading to the engineering success or failure of a CCS project.

This proposal tests the hypothesis that basing a static geological model on a numerical depositional process model rather than a training image or outcrop analogue leads to at least an improved understanding of the uncertainty, and a possible reduction in uncertainty, for the same amount of input data at any given stage of site characterisation.

In the Collie Hub case the sequestration target is a saline formation where no production history or proven "conventional" seal is available, although some exploration companies suspect a shale zone exists at the base of the Eneabba Formation. There are some important differences between an oil-field static geological reservoir model and one designed for CO_2 sequestration in a saline formation. In a saline formation target the reservoir/seal impedance contrast is even less obvious on seismic (due to lack of fluid density contrast), and stratigraphic traps and heterogeneity are thus harder to observe or infer directly.

ii. Why Stratigraphic Forward Modelling ?

When constructing a static geological model, well and outcrop data are commonly interpreted in terms of depositional environment e.g. "braided fluvial system", "tidal fluvial", "abandoned channels", "lower shore-face". This interpretation can be used in a variety of ways. Databases exist of observed characteristics of

sediment bodies deposited in such an environment (both ancient and modern), with spatial variability and typical porosities and permeabilities. Often the environmental interpretation changes as new data become available and the new observations are compared (usually qualitatively) with those deemed to relate to the previous interpretation. If a new observation is incompatible with the previous interpretation of environment then a new model is constructed (e.g. Spencer et al (2006), and Dance et al (2009))

A depositional system is defined largely by the energy of the physical system, the fluid and sediment involved, and the direction, continuity and constraint of the energy gradient and its ability to erode, transport and deposit sediment. Since the 1980's numerical depositional modelling has been steadily developing, in CSIRO and elsewhere, to the state where we can now apply predictive numerical models to most depositional systems, at scales appropriate to reservoir characterisation. This enables us to: test hypotheses concerning the applicability of any given assumed depositional system in a given reservoir; predict the evolution of sediment bodies (reservoir and seal facies) at any location within a prospective area; predict the lateral and vertical variation in reservoir and seal properties at specified scales; constrain predictions with well and seismic data; enable multiple realisations (based not on statistical variation of observations, but on statistical variation of process parameters) and characterise depositional uncertainty in any given model.

2 The Sedsim Program

Sedsim is a three-dimensional stratigraphic forward modelling program developed originally at Stanford University in the 1980's and extensively modified and extended in Australia since 1994 at the University of Adelaide and CSIRO. The basic principles, background to, and operation of, Sedsim is described in Tetzlaff and Harbaugh (1989). Tetzlaff developed the program, with subsequent enhancements by Ramshorn and Wendebourg at Stanford, and Chris Dyt, Fangjun Li, and Tristan Salles-Taing at CSIRO.

Sedsim consists of a series of computer programs that can be linked together or run separately. The core Sedsim flow and sedimentation programs are linked to modules including subsidence, sea level change, wave transport, compaction, slope failure, carbonates, organics and diagenesis. The program models sediment erosion, transport, and deposition, and predicts clastic and carbonate/organic sediment distribution on a given bathymetric/topographic surface. Modules recently added include aeolian deposition, and organic facies distribution.

Sedsim three-dimensional stratigraphic forward modelling software enables a variety of inter-dependent surface and basin-forming processes to be studied at both geological and engineering time scales. The results reflect possible changes in sediment distribution over time as a function of the depositional environment. Past studies that have demonstrated the value of this approach include those by Griffiths et al. (2001), Griffiths and Dyt (2001), Griffiths and Paraschivoiu (1998), Koltermann and Gorelick (1992) and Martinez and Harbaugh (1993). Any computer modelling is only as good as the validity of the input data and the algorithms used in the program. The Sedsim program has been shown to predict sediment distribution in a range of depositional environments and at scales from metres to several kilometres. The derivation of input data for such computer models is no more onerous than that required for a conceptual geological model of an area. However, the need for quantitative data forces the geologist to a greater degree of commitment than may otherwise be the case.

2.1 Stratigraphic Forward Modelling Context

One feature common to exploration, appraisal, and reservoir engineering for hydrocarbons, geological sequestration of CO_2, and geothermal resources is the need to predict rock properties away from limited well data and below seismic resolution. Historically there have evolved many ways of 'filling the gaps', or joining the dots between observations, geological experience and geostatistics being the most common. Modern oil-field workflows use geo-modelling software that requires the user to select training images of depositional systems that have user-selected orientations and properties. These can be selected from libraries, or constructed based on local experience. As the purpose of the exercise is to fill a modelled volume with a grid of cells containing, initially, geological facies (a 'static' model), and subsequently engineering properties for these facies in a 'dynamic' model that can be used to predict fluid volumes, flow patterns and rates of fluid movement, then geological information should be appropriately scaled and relevant to the purpose in hand.

Stratigraphic forward modelling (SFM) is a relatively new approach to performing this geological prediction that explicitly uses, and tests, a quantitative understanding of the processes that deposited the sediments in the palaeogeographical area of interest. Sedsim is the most advanced of the fully 3D hydraulically based stratigraphic forward models.

As in other approaches, the area of study, resolution and scale are primary considerations and should be appropriate for the purpose. For hydrocarbon exploration in an area such as the Perth Basin a 2000 m resolution may be adequate to investigate stratigraphic traps, seal distribution, and areas of potential source rock. Identification of geothermal convective cells would also be possible. Reservoir engineering

grids that require finer resolution must be based on calibrated depositional surfaces of finer resolution, and these were not available for this phase of the study. Although Sedsim allows the nesting of a high-resolution grid within a main coarse-grid simulation there will be no additional information in the fine grid unless there is a high-resolution depositional surface and tectonic history in the high-resolution area. Thus the approach here used a 5 km regional grid within which we nested a 500 m grid over the 'focus' area. For CO_2 sequestration purposes this resolution should be seen as barely adequate for an initial feasibility study. Further discussion of this aspect of modelling is provided in Section 8.1.

2.2 Basic Principles of Sedsim Operation

Hydrodynamics make up the core of the Sedsim program and utilise an approximation to the Navier-Stokes equations (Tetzlaff and Harbaugh, 1989). The approach is described below.

In Sedsim the sediment moves at the same rate as the fluid element, because there is no velocity gradient in the fluid. The boundary between erosion and transportation is determined by the critical shear stress, calculated as a function of particle diameter. Sedsim is typically run using four different siliciclastic grain sizes specified by the user. In addition to this are the options to include two types of carbonate and two types of organic material (e.g. algae or vegetation).

Processes that can now be modelled within Sedsim include: catchment erosion; fluvial processes; wave, tide and storm effects; geostrophic currents; tectonic subsidence and uplift; eustatic and multiple-location lacustrine water level changes; syn-depositional and post-depositional compaction; isostacy; slope failure/slumping; density flows (debris flows to turbidites); carbonates(reef and pelagic) and organics (algae and vegetation); aeolian processes; carbonate diagenetic effects.

In the sections below, only those processes that have been modelled in the Collie Hub simulation are discussed.

2.2.1 FLUID FLOW

Hydrodynamics make up the core of the Sedsim program and utilize an approximation to the Navier-Stokes equations. The full Navier-Stokes equations describing the fluid flow in three dimensions are currently impossible to solve due to limitations in computer speed (it would take longer to simulate a flow than the real event). Sedsim instead simplifies the flow by solving the shallow water equations, utilizing isolated fluid elements to represent continuous flow (Tetzlaff and Harbaugh, 1989, Chapter 2). This Lagrangian approach to the hydrodynamics allows for a significant increase in the speed of computation and the simplification of the fluid flow equations. The downside of this approach is that individual events such as a rapid variation in fluid flows caused by brief downpours and unexpected short-term river meanders cannot be modelled. However, as the timing of these events is impossible to predict, this is a small loss. Simulations over geological periods can at best hope to capture the mean conditions and create a general pattern of sediment distribution, rather than capture the exact timing of each individual pulse of material. With this in mind, the approach utilized by Sedsim will accurately model the 'mean' physics in the simulation.

Modelling of the fluid flow is performed by allowing fluid elements to travel over the grid describing the topographical surface, reacting to the local topography and conditions such as the flow density and the density of the medium through which the element is passing (e.g. air, sea water, or fresh water). The fluid elements are treated as discrete points with a fixed volume, an approach known as "marker-in-cell". As mentioned, several simplifications are made to the Navier Stokes equations, comprehensively described in

Tetzlaff and Harbaugh (1989) with the most important of these being that the flow is expected to be uniform in the vertical direction (i.e. the whole of the fluid element has the same velocity), and that the friction experienced by the fluid element is controlled by Manning coefficients. The net result of these simplifications is that the Navier Stokes equations are modified into non-linear Ordinary Differential Equations (ODEs). These equations are now solved using a modified Cash-Karp Runge Kutta scheme (Press et al., 1992) that ensures stable and accurate 4th order in time solutions.

The resolution of the simulation has an influence on the results. There are two discretisation intervals that must be examined in Sedsim; the temporal and spatial. The spatial resolution is perhaps the most obvious. Because the fluid elements use the grid topography to determine their flow characteristics, features smaller than the grid resolution have no influence upon the flow. The temporal aliasing comes in several forms, which can be controlled by the user:

- The choice of "display interval" in years simulated time (this is equivalent to the temporal resolution in cross-sectional models). This controls how often the data are output from the model. All sediments deposited during a time interval are lumped together in a single layer. Thus multiple events occurring within a display interval are seen as one integrated event (bed).

- The choice of "flow sampling interval". This represents the interval between releases of new fluid elements. For example setting this to 100 years would mean that a new fluid element would be released every one hundred years. That fluid element would then contain the volume of water and sediment as if the original source had flowed for 100 years. As it is moved about the topography it is assumed to flow at each point for 100 years.

- Time step. The time step controls how far the simulation advances in time with each iteration. This variable is automatically calculated by Sedsim, and is chosen to be as large as possible whilst ensuring that the simulation remains numerically stable and accurate. It is also chosen so that no topographical features are by-passed by the fluid elements. It is indirectly controlled by the accuracy factor, which specifies to what precision any change in the flow must be calculated.

- The choice of "extrapolation factor" (ratio of computing time to simulated time). Because of the large geological time scales over which Sedsim must run, a simplification is introduced where the conditions for one time-step are thought of as being representative of the flow over that area for a multiple of that time given by the extrapolation factor. The main purpose of this extrapolation is to allow the fluid elements to interact with other processes (such as sea level movement) which typically occur on much longer time scales by keeping the fluid element in the system for a longer time. It does not affect the number of fluid elements released or the speed of the computations.

- The choice of "parametric sampling interval". This variable affects how often in simulated time other effects such as sea level change, tectonic movement, wave/wind effects and slope instabilities are calculated. These values are generally chosen to be much shorter than the rate at which these events may be observed in the stratigraphic record. For example change in sea level is typically referenced once every 100 years.

2.2.2 SEDIMENT TRANSPORT

Sediment is transported across a bathymetry (bypassed), deposited on its surface, or eroded from the surface, according to the principle of conservation of mass. In other words, for each time interval:

sediment in + sediment eroded = sediment in the fluid + sediment deposited + sediment out

In Sedsim the sediment moves at exactly the same rate as a fluid element, because there is neither a velocity gradient in the fluid, nor any distinction between the rate of transport by the fluid element of the suspended and bed load. Because of the use of the flow-sampling interval (described above), this crude approximation has little effect on the results, as the fluid flow represents a time-averaged response anyway. The boundary between erosion and transportation is determined by the critical shear stress, calculated as a function of particle diameter (threshold shear stress increases linearly with particle diameter above 0.1 mm). The rate of sediment deposition or erosion is proportional to the excess "effective sediment concentration". This is the difference between the actual sediment load within the fluid element and its capacity to hold sediment. This capacity is a function of the water density, the velocity, and average fall rate of the contained sediment and the buoyancy of the flow. Sediment sinks within a fluid element as a function of its excess density over the fluid, its diameter, and the viscosity of water at 15°C. For more detailed consideration of the algorithms used by Sedsim the reader is referred to Tetzlaff and Harbaugh (1989). Sedsim is typically run using four different siliciclastic grain sizes specified by the user. In addition to this is the option to include growth of two types of carbonates (for example coral and forams) and two types of organic material (for example algae and vegetation), and their resultant clastic grains after erosion.

After initial deposition from fluid elements the sediments can still be re-deposited due to slope angle tests in the local environment. The sediment can be diffused over many grid cells until it deposits at a user-defined stable slope angle.

2.2.3 TEMPORAL ALIASING/TIME SAMPLING SENSITIVITY

There are two types of temporal aliasing to consider. The first concerns the relationship between flow time-step and the maximum slope over which sediment will flow. For steep slopes, and irregular bathymetry, the flow needs to be calculated more frequently to ensure realistic sediment geometries. This problem is automatically handled by the code as discussed in the section on fluid flow. A reduction of the flow time-step makes the simulation more stable, and potentially provides marginally higher resolution in the output geometries. A consequence however, is a significant increase in computing time. The second factor influencing temporal aliasing is the display interval. Temporal aliasing is the ability to model a given time event. If it is believed that a fan developed in ten years, its geometry and composition could not be simulated with a time step greater than five years. The consequence of choosing a display interval of 5 ka, therefore, is that the minimum temporal depositional event that can be modelled is one with a duration of 10 ka. If the aim is to model the effect of orbital forcing on high-frequency sedimentation cycles, then a display interval of at most 10 ka would be needed to capture the effects of the 19-21 ka cycle. The "parametric sampling interval" is the time interval at which the sea-level curve is sampled, wave influences calculated, slope stability's checked, compaction calculated etc. The smaller the parametric sampling interval, the higher the resolution of the events that can be modelled, but the penalty is a slightly longer computing time.

2.2.4 TECTONIC SUBSIDENCE

Sedsim can incorporate vertical tectonic movement in a simulation. A subsidence/uplift value is defined for each individual grid node in the initial topography, and these arrays of values can be changed at any time in the simulation, independently of either the display or parametric sampling interval.

2.2.5 COMPACTION

Compaction during the simulation is calculated using a "look-up table" containing porosity values as a function of effective stress and grain size. For each display interval, the lithostatic pressure is calculated from the overburden. This pressure controls compaction and the actual grainsize deposited. Post-depositional burial compaction may be applied either within Sedsim at the end of the simulation, or by an additional program.

2.3 Steps involved in a Sedsim Simulation

The steps involved in building a Sedsim model are:

(1) Pre-modelling data acquisition and evaluation:
   i. Existing literature relating to potential depositional environments and conceptual geological models for the interval and area involved
   ii. In-house studies – regional facies trends
   iii. Paleoclimate information, prevailing winds, rainfall/storm directions/temperatures

(2) Identify underlying topographic surfaces/bathymetry:
   i. Determine seismic coverage
   ii. Extract and identify seismic lines/volumes from which a surface can be extracted
   iii. Understand time-depth relationships and quality of ties using check shot data

(3) Timing and interval of interest:
   i. Choose a time-scale (e.g. Ogg and Gradstein, 2008 IUGS) to use throughout the project and sea level if appropriate (e.g. Haq and Shutter, 2008) – reconcile with earlier boundaries and sea-level curves
   ii. Determine/agree a display interval and check for consequences of temporal aliasing (short term events that have depositional consequences should be captured)
   iii. Choose lower surface – e.g. an unconformity with seismic expression
   iv. Choose flattening surface – e.g. an anhydrite or marine shale or carbonate as proxy
   v. Check availability of biostratigraphic and palynological (pollen) data (look at well-completion-reports and university literature)
   vi. Check availability of ichnofacies/ichnofabric studies and core data
   vii. Check availability of Sr isotope dates

(4) Grid topography at agreed resolution:
   i. Understand and check consequences of aliasing (Nyquist Frequency) at chosen grid resolution – impacts minimum channel and dune sizes that can be modelled; for example, a 100 m model grid spacing will not enable identification or simulation of channels or dunes less than 200 m wide
   ii. Either build or use existing grids for unconformity surfaces
   iii. Review any other intermediate tie-able surfaces/horizons that can be used to validate modelled thicknesses
   iv. Review any available isochron/isochore information for interval of interest.

(5) Determine pre-existing erodible surface – use a subcrop map if available

(6) Decide/determine calibration data to be use – success criteria (which data, which wells, at what resolution?)
   i. Identify wells to use: include both reasonable calibration wells (grain size distributions, grain densities, clay percentages, nature of the surfaces) and blind test wells if available
   ii. Choose key seismic lines for calibration: use dip and strike lines, to constrain surfaces and thickness of layers and as blind test lines

(7) Determine source location and volumes for sediment supply (rivers, beaches, gravity currents etc.)

(8) Determine processes to be included (fluvial, shallow marine, tides, storms, currents, etc. etc.)
(9) Build input files honouring all the above information.
(10) Run Sedsim and check the results against well data.
(11) Modify the input data and re-run the simulation until the match with constraint data is acceptable, and then test against blind-test wells.
(12) Iterate until results converge on agreed measure of success.

The output from Sedsim can be presented as an interactive 3D visualisation (SedView and Paraview options) of the depositional system evolution over time, as Eclipse input files (grdecl output format), as Petrel/RMS/GoCad input files, pseudo wells, and synthetic seismic volumes.

3 Conceptual Model of the Triassic and Lower Jurassic deposition in the South Perth Basin

"The Perth Basin is a north to north-northwest trending, onshore and offshore sedimentary basin extending about 1300 km along the south-western margin of the Australian continent. This is a large (172 300km2), structurally complex basin that formed during the separation of Australia and Greater India in the Permian to Early Cretaceous. It includes a significant onshore component and extends offshore to the edge of continental crust in water depths of up to 4500m.

The structural architecture of the Perth Basin is the product of oblique rifting during the Permian, Late Triassic to Early Jurassic and Middle Jurassic to Early Cretaceous, superimposed over pre-existing basement terrains. Extension during the Permian produced a series of deep (up to 15km), north-south trending rift basins (Bunbury Trough and Dandaragan Trough) along the western margin of the Yilgarn Craton. The Abrolhos Sub-basin represents a north-western branch of the Permian rift system formed along the south-western margin of the Northampton Complex, which is separated from the Dandaragan Trough by an intra-basin high represented by the Beagle Ridge, Dongara Terrace and Greenough Shelf. The Houtman Sub-basin is a major depocentre for Triassic and Jurassic sedimentary rocks that formed as a westward thickening sag basin across a hinge zone during the Middle Triassic to Middle Jurassic, and was extensively faulted during Late Jurassic to Early Cretaceous rifting. The Vlaming Sub-basin is the major Middle Jurassic to Early Cretaceous rift basin in the Perth Basin and is characterised along its northern extent by a very large and deep half graben that dips to the west. The footwall block of this half graben consists of a series of shallow tilted fault blocks containing mainly Permian and older strata from the Edward's Island Block.

Breakup during the Early Cretaceous (Valanginian) was associated with widespread inversion, erosion, strike-slip tectonics and volcanism, which significantly modified the structural architecture of the Perth Basin. Major structural elements associated with breakup tectonism include an area of inverted Permian half graben in the Turtle Dove Ridge and the Zeewyck Sub-basin that formed in a zone of strike-slip faulting along the Turtle Dove Transfer.

The stratigraphy and petroleum system elements of the Perth Basin developed during the tectonic evolution of the basin and vary significantly from north to south. Initial rifting established a series of Permian to Early Triassic depocentres for fluvial and marine siliciclastics with minor carbonates and coals in the north, while in the south fluvial siliciclastics and coals dominated. These Permian- and Early Triassic-age rift-sag deposits are associated with the major petroleum system in the north Perth Basin, particularly the Kockatea Shale, which forms an important oil source rock and regional seal to underlying reservoirs.

A second phase of rifting in the Late Triassic and Early Jurassic was associated with widespread fluvial and deltaic deposits, including a thick succession of siliciclastics and coals (Cattamarra Coal Measures), which are overlain by Middle Jurassic marine shales (Cadda Formation) in the north Perth Basin. These Early to Middle Jurassic strata form a second proven petroleum system in the north Perth Basin. The final rift and breakup phase in the Middle Jurassic to Early Cretaceous was associated with deposition of fluvial and marine siliciclastics (Yarragadee Formation, Parmelia Group and Warnbro Group), which form the main petroleum system in the Vlaming Sub-basin." [Geoscience Australia. http://www.ga.gov.au/energy/province-sedimentary-basin-geology/petroleum/offshore-southwest-australia/perth-basin.html#overview]

The following descriptions are from Crostella and Backhouse (2000).

Note that the lithostratigraphic unit formerly informally known as Myalup now has a provisional informal name of Yalgorup (GSWA communication, 2012)

"Lesueur Sandstone

The term Lesueur Sandstone was introduced by Willmott, Johnstone, and Burdett (Willmott, 1964) for the medium to very coarse grained sandstone of Middle – Late Triassic age. The type section is the interval 264–1008 m in Woolmulla 1 in the northern Perth Basin (Mory and Iasky, 1996). The Lesueur Sandstone in the Vasse Shelf and Bunbury Trough ranges in thickness from 331 m in Alexandra Bridge 1, where it is eroded, up to 1995 m in Whicher Range 3. The isopach map of the unit shows depositional thinning to both the west and south....., whereas to the north, on the Harvey Ridge, the unit is 2292 m thick in Lake Preston 1.

In the southern Perth Basin, and in the southernmost part of the central Perth Basin, the fluvial Lesueur Sandstone may be differentiated into two members ....., which is consistent with the description of the Lesueur Sandstone in Lake Preston 1 by Young and Johanson (1973). These members are here named the Wonnerup Member and the Myalup Member. The Wonnerup Member comprises homogeneous sandstone, whereas the Myalup Member includes sandstone with subordinate interbeds of finer clastic rocks. In the Wonnerup Member, the sandstone is feldspathic, poorly sorted, coarse to very coarse grained, generally unconsolidated, and light grey to colourless, in contrast to the Myalup Member, which is dark grey. The fine-grained clastic rocks are mostly siltstone beds up to 20 m thick.

The interval from 2640 m (8661.42 ft) to 3644 m (11955.38 ft) in Wonnerup 1 (latitude 33°37'59", longitude 115°28'24") is nominated as the type section of the Wonnerup Member. The type section of the Myalup Member is nominated as the interval between 1219 m (3999.34 ft) and 2045 m (6709.32 ft) in Lake Preston 1 (latitude 32°55'13", longitude 115°39'39"). The boundary between the two members is a good regional seismic marker. On wireline logs, the Myalup Member shows a similar character to the overlying Jurassic units.

The Lesueur Sandstone has not been penetrated in the central Perth Basin. The formation conformably overlies the Lower Triassic Sabina Sandstone in the southern part of the basin and the Early – Middle Triassic Woodada Formation in the northern Perth Basin. No stratigraphic hiatus, however, is implied, because Dolby and Williams (1973) have correlated the palynological assemblage between 3078 and 3094 m in Lake Preston 1 with assemblages typical of the Woodada Formation in the northern Perth Basin. In the southern Perth Basin, therefore, the lower part of the Lesueur Sandstone is approximately coeval with the Woodada Formation of the northern Perth Basin, whereas the upper part passes upwards into the Cattamarra Coal Measures. In the central part of the basin, the unit passes upwards into the Eneabba Formation ..... In the northern Perth Basin, the Woodada Formation represents a depositional environment transitional between the underlying fine- grained marine Kockatea Shale and the overlying, predominantly sandstone, fluviatile Lesueur Sandstone. In the southern Perth Basin, the Wonnerup Member is lithologically closer to the Lesueur Sandstone, and the Myalup Member represents a transitional environment between the underlying Wonnerup Member and the overlying Cattamarra Coal Measures. On a wider scale, the Myalup Member appears to correlate with the uppermost part of the Mungaroo Formation of the Barrow–Dampier Sub-basin of the Northern Carnarvon Basin.

Balme (1966) suggested a Middle – Late Triassic age, on the basis of a poorly diversified palynological assemblage from the Lesueur Sandstone in Pinjarra 1. A similar age is indicated for the unit in Wonnerup 1 (Union Oil Development Company, 1972), Lake Preston 1 (Dolby and

Williams, 1973), Sabina River 1 (Ingram, 1982), and in the northern part of the basin (Mory and Iasky, 1996).

Eneabba Formation

The Eneabba Formation was elevated to formation status by Mory (1994). The type section is the interval 2320–2978 m (7612 ft to 9770 ft) in Eneabba 1 in the northern Perth Basin. This Lower Jurassic unit is characterized by the presence of multicoloured siltstone and shale interbedded within dominantly sandstone lithologies. In unpublished WAPET reports, the Eneabba Formation was originally referred to as the 'Multicoloured Member' of the Cockleshell Gully Formation, but this definition has been abandoned. The Eneabba Formation is widespread in the northern Perth Basin, and is also recognized in Lake Preston 1 and Pinjarra 1 within the central Perth Basin. However, this unit has not been identified in the southern Perth Basin, where the Cattamarra Coal Measures directly overlies the Lesueur Sandstone ..... Based on the presence of the Corollina torosa Zone, Discovery Petroleum NL (1992a) interpreted the presence of the Eneabba Formation in Chapman Hill 1 and other wells in the Bunbury Trough. Although that interpretation is not followed here, it shows that there is a section in the Bunbury Trough that is a time equivalent to the Eneabba Formation. In this Report, that section is included within the Cattamarra Coal Measures because the multicoloured fine-grained clastic rocks characteristic of the Eneabba Formation are absent.

Lithologically, the Eneabba Formation consists of feldspathic, coarse to very coarse-grained sandstone interbedded with local minor conglomerate, and multi- coloured claystone and siltstone (Mory and Iasky, 1996). In the type section, the ratio between the multicoloured fine clastic rocks and the sandstones is approximately 1:5. This is assuming that the lower and upper boundaries are present at the first appearance and disappearance respectively of the very distinctive multicoloured sediments. The Eneabba Formation is conformably overlain by the Cattamarra Coal Measures.

A fluviatile environment is envisaged for the formation. The sandstone intervals probably represent channel-fill deposits. The multicoloured clastic rocks indicate an oxidizing environment and suggest episodes of subaerial exposure, and are interpreted as overbank floodplain deposits. In the northern Perth Basin, the Eneabba Formation contains assemblages assigned to the Corollina torosa Zone of Early Jurassic age (Mory and Iasky, 1996). Sparse palynological data in Lake Preston 1 and Pinjarra 1 indicate a similar age."

On the basis of the few palynoforms from wells Lake Preston-1 and Pinjarra-1 the successions modelled were:

1. Wonnerup Equivalent [Olenekian to Anisian 250 Ma to 237 Ma *(Nicoll et al 2009)*]

2. ~~Myalup~~ [Yalgorup] Equivalent [Ladinian to Rhaetian 237 Ma to 198 Ma *(Nicoll et al 2009)*]

3. Eneabba Equivalent [Hettangian to Pliensbachian 198 Ma to 182 Ma *(Nicoll et al 2009)*)]

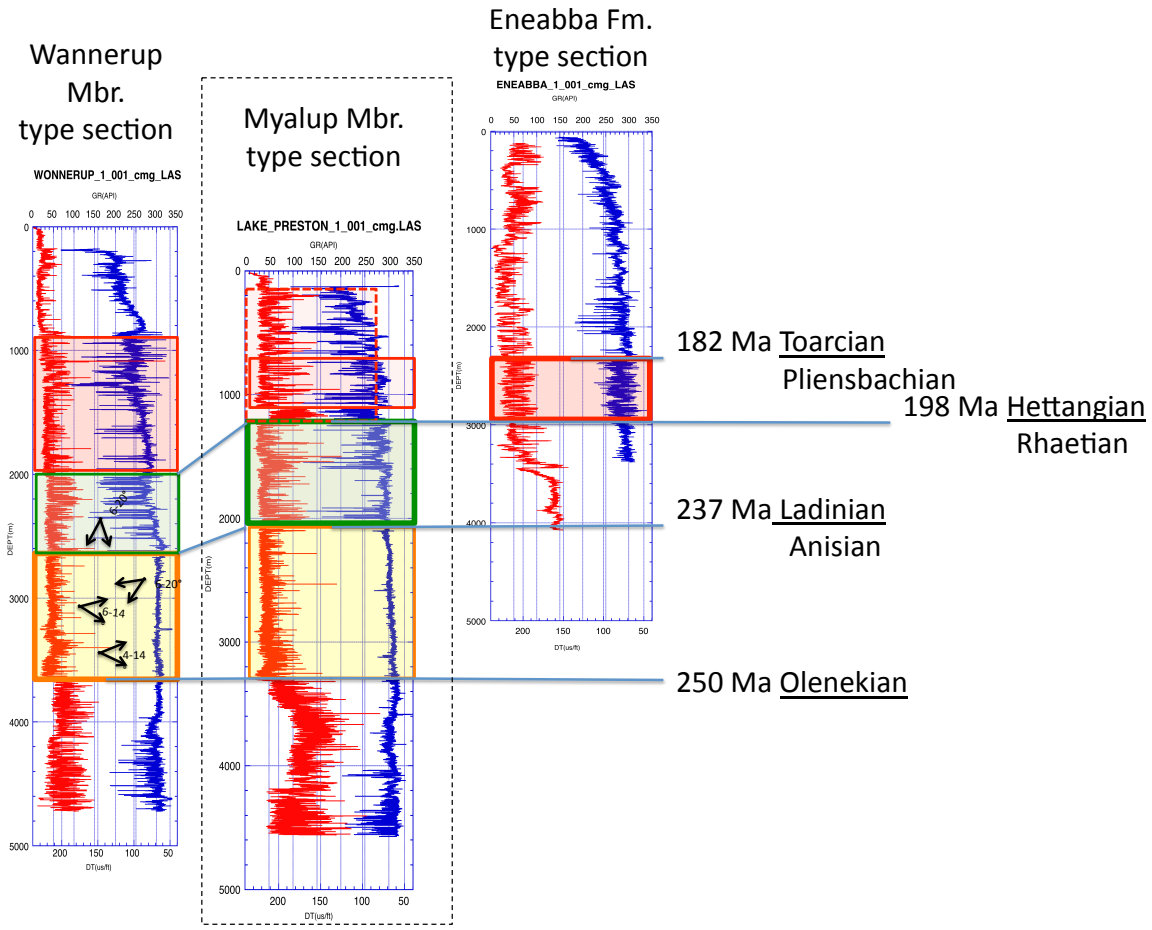

Figure 1 **The stratigraphic succession that has been modelled is from 250 Ma to 182 Ma Early Triassic to Early Jurassic. The Lake Preston-1 well is within the simulation area. The orange stratigraphic unit is the Wonnerup Member and equivalent, the type section for which is the interval shown in the Wonnerup-1 well 75 km south west of the simulation area. The green stratigraphic unit is the Yalgorup [previously known as the Myalup] Member and equivalent, the type section for which is in the Lake Preston-1 well in the simulation area. The red stratigraphic unit is the Eneabba Formation and equivalent, the type section for which is in the Eneabba-1 well, 300 km north north west of the simulation area.**

4 Method

The Sedsim computer program was used to explore conceptual depositional models by producing numerical stratigraphic forward models based on the current understanding of the stratigraphy and depositional systems within the Southern Perth Basin. Three-dimensional stratigraphic forward modelling enables us to study, at geological time scales, the combined influence of a variety of inter-dependent basin processes and factors on basin fill. The results reflect possible changes in sediment distribution over time as a function of changes to the depositional environment.

Input data included a range of initial surface bathymetries, grain-size distributions and sediment supply rates linked to climate proxies provided from palynology and global sea level curves. All other input parameters were iteratively tested.

An initial understanding of the depositional environment and facies distributions in the area away from existing well data is necessary. Sedsim results, when matched only to well data, can create a defendable representation of the expected lithofacies to be encountered. Using seismic data as an additional constraint enable a much closer match with stratal geometries, and therefore with stratigraphy.

The Sedsim program is now capable of displaying over a thousand layers during a single simulation (for example 10 Ma with a temporal resolution of 10 ka). Spatially, the program is capable of simulating an area of up to 1000 by 1000 grid cells with grid resolutions from a few centimetres to several kilometres.

Sedsim code will run on any fast computer, and the simulation results can be displayed on any computer running OpenGL. The speed of simulation depends very heavily on the number of fluid elements being modelled at any given time, the number of options included (such as compaction, isostasy, tectonics etc.), and the spatial and temporal resolution required.

This particular set of simulations was carried out on a 64 bit CSIRO MacBookPro computer in Perth.

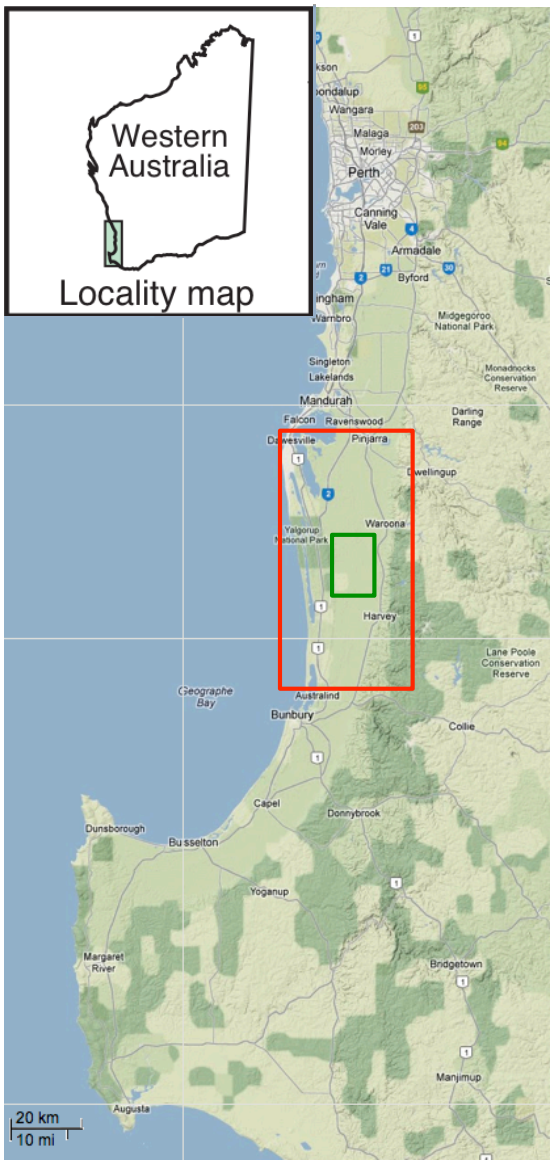

Figure 2 Present day regional location of the South Perth Basin in south-western Australia, with the 5 km grid simulation area marked by the red rectangle. The higher resolution (500 m grid) area is outlined in green.

4.1 Area and Scope of Investigation

The simulation area chosen includes most of the locally significant structural elements and regional sediment supply areas (Figures 2 and 3) and is defined by the following corner-point coordinates:

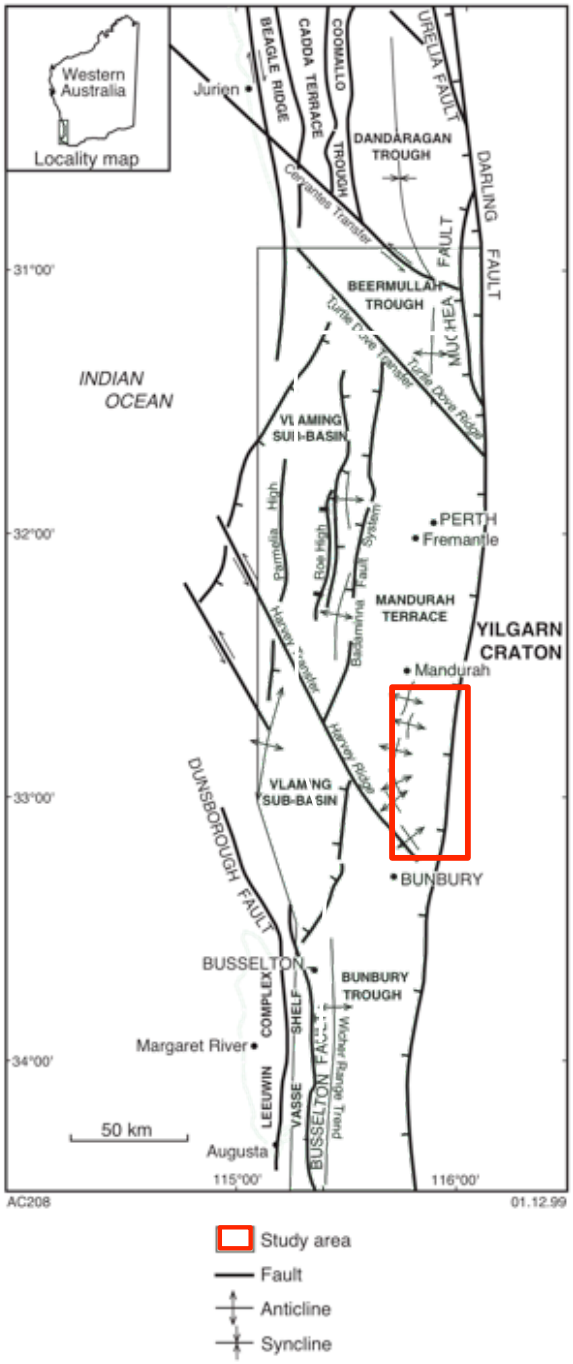

Figure 3 **South Perth Basin and main structural features. The red rectangle marks the 15x8, 5000 m resolution simulation area. (adapted from Crostella and Backhouse (2000))**

SW corner
GDA-MGA: (UTM with GRS80 ellipsoid)
Zone: 50 H
Easting: 370000.0 Northing: 6320000.0
Latitude: -33 ° 15 ' 3.98 " S Longitude: 115 ° 36 ' 17.03 " E

NE corner
GDA-MGA: (UTM with GRS80 ellipsoid)
Zone: 50 H
Easting: 405000.0 Northing: 6390000.0
Latitude: -32 ° 37 ' 12.4 " Longitude: 115 ° 59 ' 19.48 " E

The simulation area was chosen to include most of the significant structural elements and regional sediment supply areas. The higher resolution focus area includes inshore areas of interest for geological carbon sequestration.

4.1.1 TIME PERIOD OF INTEREST

The time period simulated in the model begins at the Early Triassic (250 Ma) and runs to mid Early Jurassic (182 Ma). In lithostratigraphic terms this corresponds to the Wonnerup Member, described as a "homogeneous sandstone, feldspathic, poorly sorted, coarse to very coarse-grained, unconsolidated and light grey to colourless", the overlying Yalgorup Member, described as "fine, dark grey clastic sediments interbedded with sandstone", and the uppermost Eneabba Formation, described as "feldspathic sandstone interbedded with local minor conglomerate and multicoloured claystone and siltstone; rare coal".

"*The Upper Triassic to Lower Jurassic sequence of the Perth Basin is composed of barren quartz sandstones and redbeds and as a consequence is poorly dated. An unconformity, approximating the "mid-Hettangian break" (Helby et al., 1987) is believed to separate the Triassic Lesueur Sandstone from the overlying Eneabba Member of the Cockleshell Gully Formation (Playford et al., 1976). The Eneabba Member was shed from highlands on the Yilgarn Block and accumulated in alluvial fan to flood plain environments, within a rift valley setting." (Bradshaw and Yeung, 1990)*

Biostratigraphically the intervals involved include Early Triassic to Early Jurassic palynozones (well completion reports from Lake Preston-1, Wonnerup-1 and Pinjarra-1). No evidence of marine biota was identified by the biostratigraphers involved.

The ages employed in the model were derived from the ICS Chart (2009) and the radiometric ages of Ogg et al. (2008) (Figure 4). Eustatic sea level values are derived from Haq and Al-Qahtani (2005). Although the simulations were run at a display resolution of 75 ka, the sea level curve and tectonic subsidence files were sampled at 10 ka.

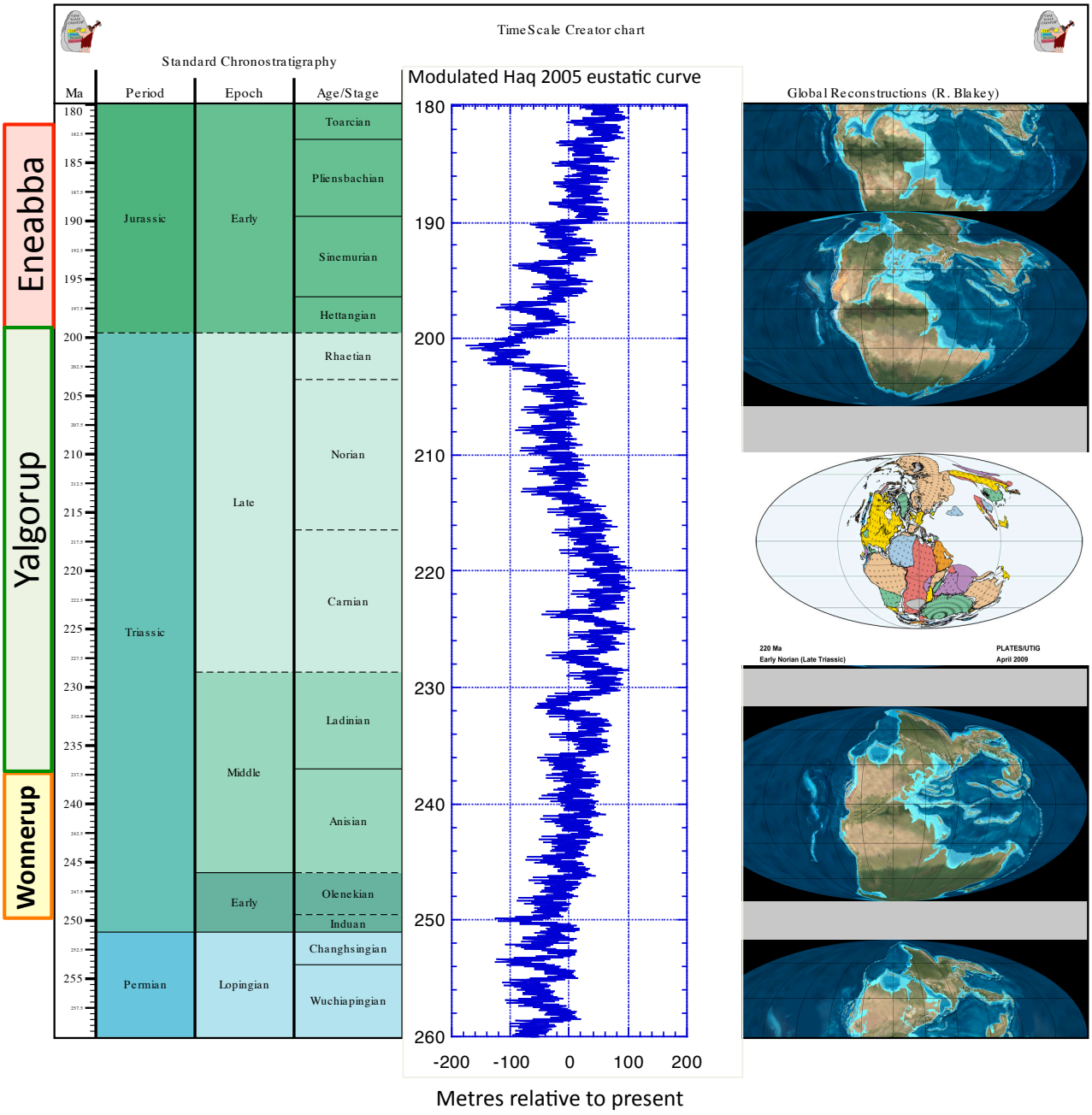

Figure 4 Stratigraphic intervals with the **Haq and Al-Qahtani (2005) sea level curve. Ages on the left of the diagram from Ogg, et al. (2008) and the ICS Chart (2009). The blue curve is the Haq and Al-Qahtani sea level curve, modulated by the Quaternary Milanković frequencies and phase relationships and sampled at 5 ka as used for the Sedsim simulation. Background chart from TimeScale Creator (TSCreator visualization of enhanced Geologic Time Scale 2004 database (Version 5.3; 2012) James Ogg (database coordinator) and Adam Lugowski (software developer) http://www.tscreator.org. P**late reconstructions from Blakey (2008).

4.2 Data sources

Data inputs for the simulations were derived from published literature and access to the Petrel Collie Hub Project and associated reports. The sections below detail the data required for input into Sedsim and the individual sources involved. All the input data types discussed below are of course subject to uncertainty. The uncertainty in the initial surface is constrained by additional information (where available) from dipmeter and core data concerning overall flow directions and thus regional stream/river flow directions. In the present case the location of rivers draining the Yilgarn Craton were identified from literature studies on Perth Basin palaeo-river channels. The choice of gradient of the major river from the Antarctic land mass is discussed below and, although there is uncertainty in this, published sedimentological observations and the well established relationship between channel type, flow rate and gradient suggests that the overall channel belt geometry selected is defensible. Uncertainties in river flow characteristics are constrained by the resultant deposition and preservation patterns seen on seismic, and core data where available. Uncertainty in input grain sizes and their initial depositional slopes affects the location and area of sediment facies. Using established relationships for these, constrained by observations where available, minimises the risk associated with incorrect selection. Forward seismic modelling based on the Sedsim results will help towards further reducing this risk.

4.2.1 TOPOGRAPHIC/BATHYMETRIC SURFACE

The seismically identifiable horizon 'Top Sabina', was used as the initial 250 Ma depositional time for the Sedsim model. This assumes that the first deposition event on this surface is Olenekian in age. However, there has been significant fault movement of this surface since deposition and the surface as it is today does not represent the early Triassic palaeogeography. The depositional environment of the Wonnerup Member has been identified as fluvial with possible lacustrine intervals from core and cuttings in well intersections in the South Perth Basin. Given this, and based on Smith (1983), the initial 5000 m resolution surface test (Figure 5) had an average gradient of 0.0002 to the north which, with a channel-full flow rate of 25 m^3s^{-1} would be appropriate for the deposition of a belt of anastomosing channels. The surface rose to the east representing the Darling Fault scarp through which several rivers flowed depositing alluvial fans.

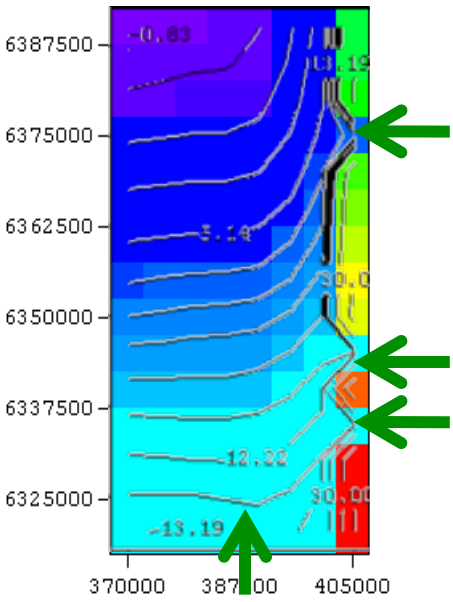

Figure 5 Initial 5000 m resolution depositional surface with a gradient of 0.0002. Sediment sources are shown as green arrows. Contours in metres.

The absolute altitude of the surface is unknown, apart from the fact that it must have been above the height of any eustatic excursion during the time period of deposition. From Figure 4 it can be seen that the absolute height of the depositional surface above sea level must have been greater than 60 m from 250 Ma to 237 Ma in order to remain non-marine.

Initial simulations were based on the coarse grid alone to test the nature of the sediment distribution.

4.2.2 TECTONIC HISTORY

Published descriptions of the environment of deposition for the Wonnerup Member suggest that there was no identified trend in flow gradient with time, or period of inundation. It seems reasonable therefore, to test the hypothesis that the surface gradients remained stationary throughout the depositional period, and the preserved thickness was accommodated by subsidence that kept pace with deposition. If this is the case then a seismic-derived isochore for the Top Sabina to Top Wonnerup interval can be used as a subsidence control. Without higher resolution seismic surface interpretations or biostratigraphic control it is necessary to assume that the subsidence rates at each grid node are constant

throughout the interval, although subsidence rates vary from one grid node to the next. Allowing for compaction, and providing the seismic surfaces have been tied to wells where available, this produces thickness and lithofacies matches at well locations, provided the above mentioned assumptions are valid.

Higher resolution (500 m grid size) isochores derived from the original seismic surfaces are nested within the coarse grid in the focus area to provide higher-resolution facies distributions.

4.2.3 SEISMIC

Six 2D seismic lines were available from a 2011 survey over part of the simulation area at 3km to 8km line spacing and 12 ms TWT vertical resolution.

In order to provide consistency between the Schlumberger static model intervals and the Sedsim model, the same seismic-derived surfaces in depth used by the Schlumberger Project were made available for the Sedsim simulation.

These were:

horiz-EarlyCret_uc-144Ma.xyz

horiz-UNIQ1-topEneabbaShale-196Ma.xyz

horiz-UNIQ2-BaseEneabbaShale-206Ma topTriassic_uc.xyz

horiz-UNIQ3-topMyalup-220Ma.xyz

horiz-UNIQ4-topWannerup-235Ma.xyz

horiz-UNIQ5-TopSabina-245Ma-LowerTriassic.xyz

horiz-UNIQ6-Base Sabina-248Ma topPermian_uc.xyz

These point-data sets were interpolated to give initial orthogonal grids with 500 m resolution (Appendix I)

An example of the 500 m grids for Top Sabina and Top Wonnerup together with the derived isochore is shown below.

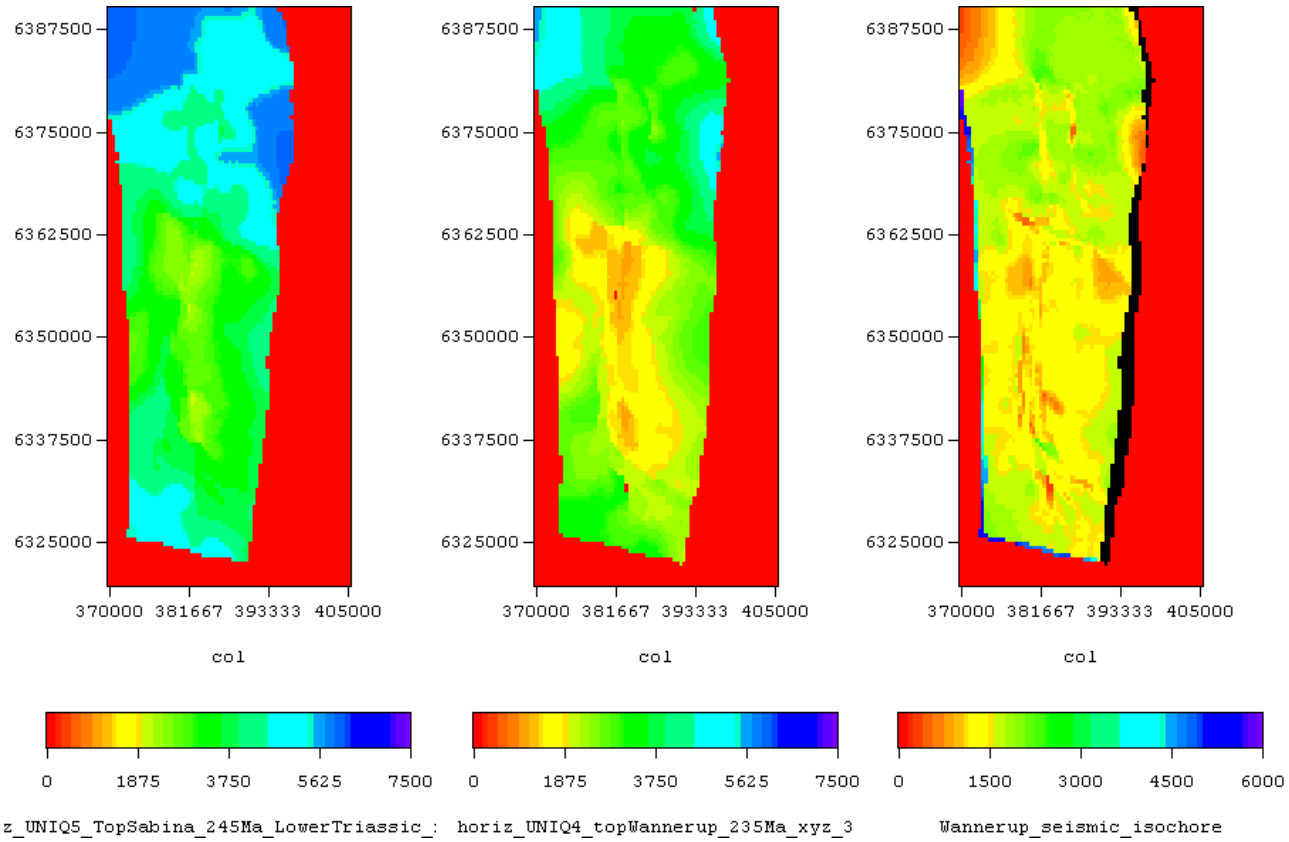

Figure 6 Top Sabina horizon gridded at 500 m (left), Top Wonnerup horizon gridded at 500 m) (centre), Wonnerup isochore gridded at 500 m (right). All values in metres.

This suggests variable amounts of syn-depositional fault movement during Wonnerup deposition.

4.2.4 SEA LEVEL CURVE

The low-frequency component of the eustatic sea level curve used in the simulation is based on that published by Haq and Al-Qahtani (2005) (Figure 4). The low frequency curve is then modulated for the simulation by the Quaternary Milanković frequencies and phase relationships. This assumes that the components of orbital eccentricity, obliquity, and precession extend beyond the currently observed limits of around 6 Ma. The amplitudes of sea-level fluctuation associated with the frequency of change are difficult to determine without running trial experiments. The constraining criteria in shallow marine environments are the rate of movements of facies belts over the particular bathymetric slopes, which are a function mostly of residual slopes associated with sediment grain sizes. However these are criteria are not available (or relevant) in fluvial systems. The observed Quaternary amplitudes (Hays et al, 1976) decay from the present day to 5.5 Ma, but in this Triassic to Early Jurassic (greenhouse conditions) simulation the high-frequency amplitudes have been held constant throughout the simulation at 25 m times the Milanković z-score giving a modulation centred on zero and ranging up to ±50m around the low-frequency component. The modulated curve is available at 5 ka resolution, but this simulation used a 40 ka version, aliasing all but the 100 ka and longer cycles.

Although there are no recorded marine deposits in the South Perth basin over the period of the simulation it is possible to use the eustatic sea level curve as a proxy for rate of global climate change in turn affecting rates of erosion, transport and deposition within fluvial environments.

The model can be used to test the hypothesis that siliciclastic sediment supply is a function of climate change rather than being constant over time. We make the explicit and controversial assumption that

Milanković cycles, together with the low-frequency eustatic curve, are an indicator (however remote or indirect) of the cause of changing pattern of hinterland erosion, transport and sediment deposition through the medium of rainfall.

Siliciclastic source velocities, flow rates and sediment concentrations in the simulation are treated as a function of the ***rate*** of eustatic change rather than the sea level value itself. In other words we make the explicit assumption that ***high rates of sea-level rise*** are associated, through warmer wetter conditions, with increased rates of rainfall, weathering, and sediment supply to the basin. Likewise ***high rates of sea-level fall*** are associated, through cooler drier conditions, with reduced rates of rainfall, weathering, and sediment supply to the basin. At 45°S a dry intra-continental location may have only experienced periodic flood events from the Darling Scarp, while the flow in the main Antarctic river, sourced from the high latitudes in greenhouse conditions, may have had a more even flow regime along the floor of the basin. The onset of varigated clays with some features of evaporitic conditions around 198 Ma reinforces the predominently dry regime conceptual model, especially in the upper section.

Note that all ages used in this modelling study are from GTS2004 (Gradstein et al, 2004), modified by Ogg et al. (2008) and the ICS Chart (2009).

4.2.5 CLIMATE

The palaeogeographical location of the South Perth Basin in the Early Triassic (250 Ma) was very close to the Antarctic continental mass between 60°S and 70°S (Figure 7).

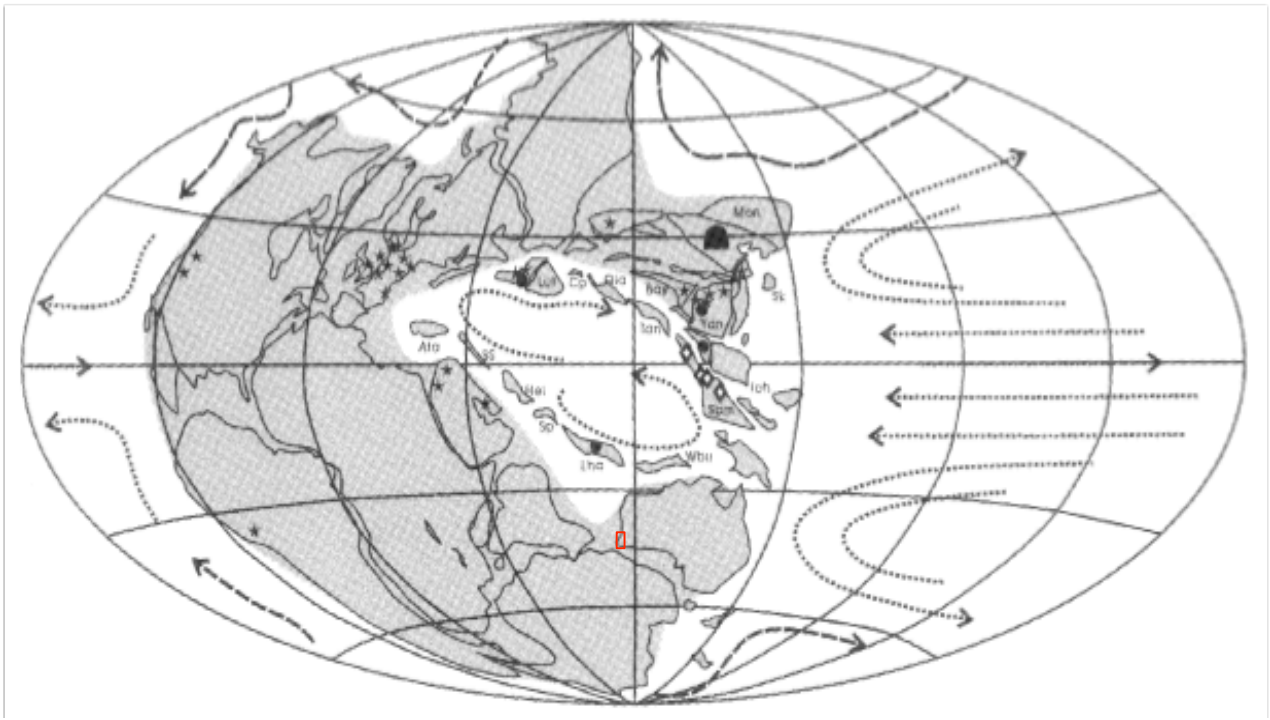

Figure 7 Anisian (245 Ma) palaeogeography and the simulation area marked in red (modified after Yan and Zhao, 2001, Figure 3).

4.2.6 DEPOSITIONAL SYSTEMS

The simulation was split into three depositional periods:

a) 250 Ma to 237 Ma, corresponding to the Wonnerup Member (Olenekian to top Anisian); The Lesueur Sandstone is composed of coarse-grained sandstone with minor siltstone and conglomerate and was deposited in a non-marine, probably fluvial, environment (Mory & Iasky, 1996).

b) 237 Ma to 198 Ma, corresponding to the Yalgorup Member (earlier named Myalup), Carnian to Hettangian; From Norvik (2003), "*Towards the end of the Early Triassic, there was regression to fluvial facies (Woodada Formation). This was followed after a localised disconformity by further Early to end Triassic, long-lived fluvial systems (Lesueur Sandstone) (Fig. 4c). In this study, the Lesueur rivers are assumed to have flowed from the south or SW and covered both the Perth Basin and much of the Yilgarn Craton. Palaeo-current data in the northern Perth Basin support a SW to NE river direction in this area (Mory & Iasky, 1996) and the local isopachs suggest a degree of syn-depositional thickening into the Urella Fault.*"

c) 198 Ma to 182 Ma, corresponding to the deposition of the Eneabba Formation (Sinemurian to top Pliensbachian); *"Around the beginning of the Jurassic, there was a slightly diachronous change to non-marine red bed sedimentation (Eneabba Formation), including multi-coloured silts and clays, with some channel sands. These sediments may have been laid down in playa lakes and high sinuosity rivers. Minor extensional syn-depositional faulting is indicated in some parts of the northern Perth Basin at this time. This mild tectonism apparently ceased in the Pliensbachian at a localised disconformity, and was followed by deposition of delta-top swamp deposits, the Cattamarra Coal Measures (Fig. 4d). Overall, this Eneabba–Cattamarra succession suggests gradual slowing of sedimentation and/or growth of accommodation space, perhaps accompanied by slow transgression*", Norvik (2003).

The main depositional processes involved in the simulation are shown below:

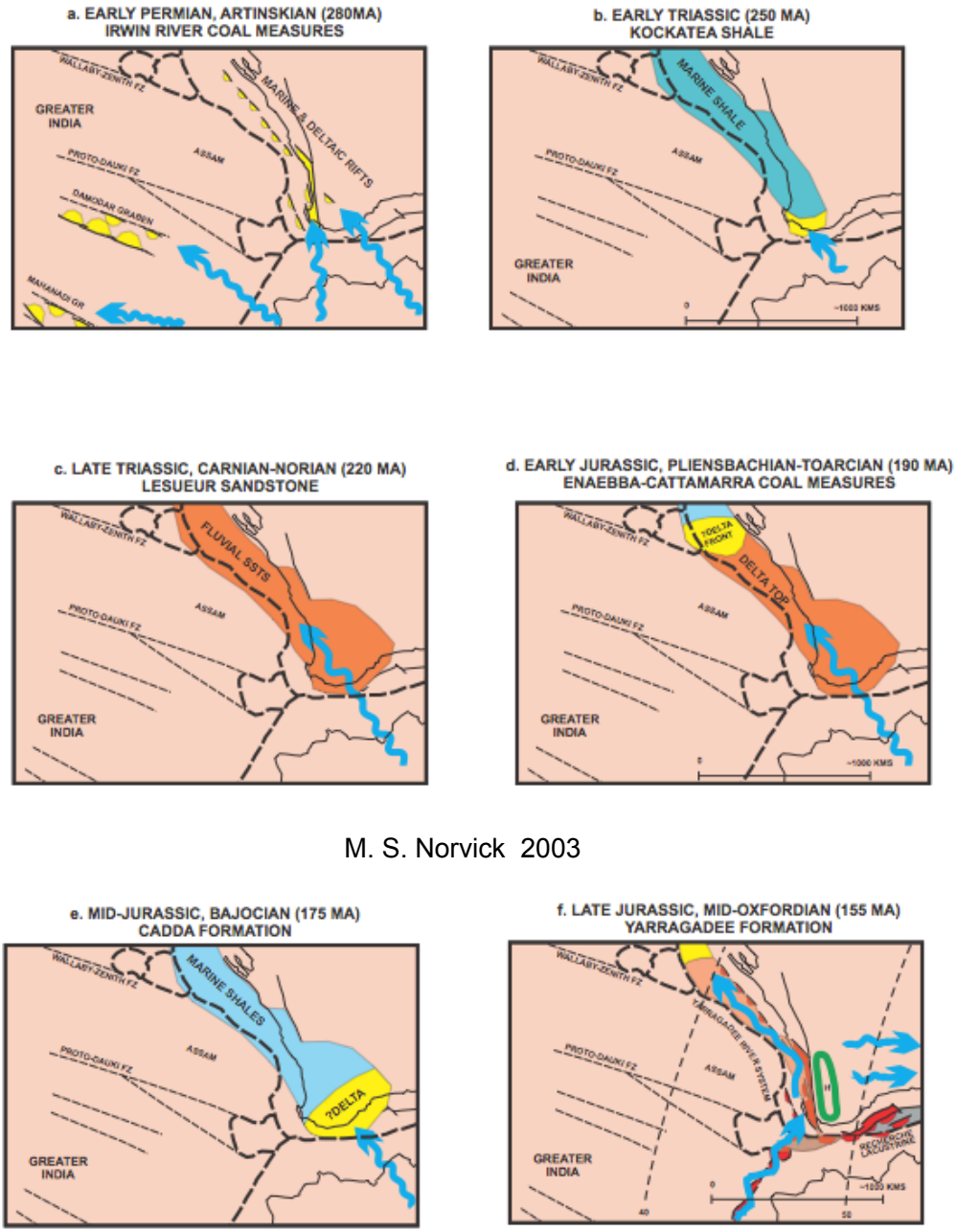

Figure 8 Palaeogeographic reconstructions and major river directions for the Perth Basin (Norvik, 2003)

4.2.7 PETROGRAPHIC DATA

Well completion reports are the main source of petrographic studies of cores from within the Perth Basin and, together with cuttings data from mud-logs, have provided a useful overview of the grain-size distributions of the preserved sediments at various stratigraphic intervals. For each complete simulation Sedsim needs to maintain the same siliciclastic grain sizes and densities. This means that a broad enough range needs to be selected to cover deposition anywhere in the basin throughout time.

Table P3. Summary of Petrographic Results (Samples PJ1:D1-D4)

Sample ID	PJ1-D1	PJ1-D2	PJ1-D3	PJ1-D4
Sample Depth (ft)	7306.7	9494.9	7965.0	14098.8
Lithology	sandy mudstone	argillaceous mudstone	sandstone	sandstone
Max Grain Size	f sand (~200 microns)	m sand (~350 microns)	c sand (~650 microns)	c sand (~800 microns)
Detrital Grain Types	Q, PF, KF, chert	Q, PF, KF, chert	Q, KF, PF, chert	Q, KF, chert
Dominant Matrix Composition	argillaceous	argillaceous	grain-supported	grain-supported
Detrital Clays	IL>I/S>Sm	I/S > IL > Kao > Chl	I/S = Kao = Chl > Sm	IL > Chl
Biotic Grains	none observed	none observed	none observed	none observed
Accessory Grains	chlorite, mica, glauconite, zircon	chlorite, mica	chlorite, mica, rare zircon	mica, rare chlorite and zircon
Organic Type	discrete particles, partially replaced with pyrite	discrete particles	rare discrete particles	rare discrete particles
Authigenic Minerals	pyrite	pyrite	chert cement, replacive pyrite	chert cement, rare replacive pyrite
Pore Types	matrix microporosity, fracture porosity (fractured grains),	matrix microporosity	intergranular pores	intergranular pores, pseudomatrix porosity, fracture porosity (fractured grains), dissolution porosity (degraded feldspars)
Petrographic Comments	moderately well laminated, common elongate chlorite flakes (up to 70 microns long), abundant silt and sand-sized detrital grains, micas are smaller in size than chlorite, chert likely detrital in origin	poorly laminated, abundant clays, matrix darkened by chlorite (green hue), visible chlorite flakes and micas are smaller than within PJ1-D1	non-laminated, sample dominated by detrital quart sand, degraded feldspars, chert both detrital in origin and in the form of cement	non-laminated, dominated by quartz sand, degraded feldspars, chert both detrital in origin and in the form of cement, pseudomatrix material

Abbreviations: c = course, chl = chlorite, f = fine, IL = illite, I/S = mixed-layer illite-smectite, Kao = kaolinite, KF = potassium feldspar, m = medium, PF = plagioclase feldspar, Q = quartz, Sm = smectite

TerraTek
A Schlumberger company
1935 S. Fremont Drive • Salt Lake City, Utah 84104
Telephone (801) 584-2400
FAX (801) 584-2406

Figure 9 Core petrographic data from Wonnerup Member (PJ1-D4), Yalgorup Member (earlier named Myalup) (PJ1-D2 and PJ1-D3) and Eneabba Fm. (PJ1-D1) in Pinjarra-1. From Schlumberger-TerraTek, 2010.

Given the observed grain-size distributions, the input siliciclastic grain-sizes for the Sedsim runs were chosen as 0.3 mm (medium sand), 0.15 mm (fn sand), 0.07 mm (v fn sand), and 0.0004 mm (clay). A grain density of 2650 kg m^{-3} was selected for each of the four grainsizes.

4.2.8 BIOSTRATIGRAPHIC DATA

Although biostratigraphic data are somewhat sparse in these largely terrestrial deposits, well completion reports and studies by McLoughlin & Hill (1996) and others have in the past been used both for biostratigraphic zonation and for an indication of the regional climate during the modelled period. The biozones were linked to the radiometric time scale of Ogg and Gradstein (2008). The available data support a predominantly non-marine environment of deposition.

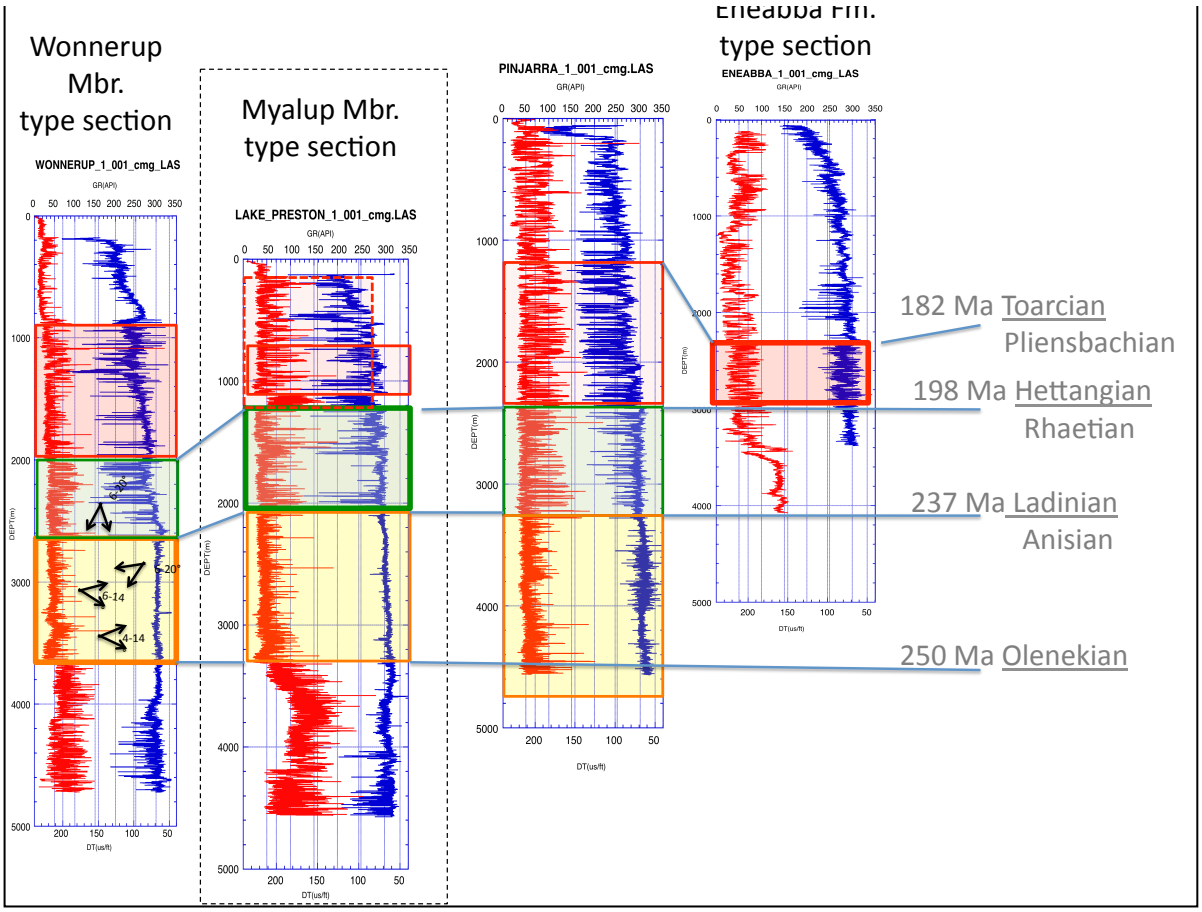

Figure 10 Wells in the simulation area and type wells for Wonnerup Member, Yalgorup (Myalup) member and Eneabba Fm.. Red wireline traces are gamma, and blue wireline traces are sonic logs. Orange boxes are Wonnerup intervals, green boxes demarcate Yalgorup intervals and red boxes mark Eneabba intervals. Depths are mRKB.

4.2.9 WELL DATA (INCLUDING WIRELINE, CUTTINGS AND CORE)

Wireline data were used to provide information concerning depositional directions via dipmeter studies, and to provide constraint data for the simulations. Three wells (Pinjarra-1, Lake Preston-1 and Preston-1) were initially available in the area of the simulation. Harvey-1 data were made available after the initial simulations were completed. Wireline logs, cuttings and core descriptions were available from published sources.

Table 4-1 Selected wells with unit tops (mRKB).

[Note * = base not reached/not recognised.]

Xutm	Yutm	Well	Top Eneabba	Top Yalgorup	Top Wonnerup	Top Sabina
374918	6356907	Lake_Preston_1	650	1219	2046.6	3250
384964	6383888	Pinjarra_1	1095	2371	3279.3	*
379524	6353611	Preston_1	204.8	*	*	*
385510	6348840	Harvey-1	250	704	1380	2895

5 Construction of the depositional model

5.1 Conceptual models

The conceptual models used for each of the three major depositional periods

1. Wonnerup Equivalent [Olenekian to Anisian 250 Ma to 237 Ma *(Nicoll et al 2009)*]

2. ~~Myalup~~ [Yalgorup] Equivalent [Ladinian to Rhaetian 237 Ma to 198 Ma *(Nicoll et al 2009)*]

3. Eneabba Equivalent [Hettangian to Pliensbachian 198 Ma to 182 Ma *(Nicoll et al 2009)*)]

are described in Section 3 of this document.

5.2 Computer model

Sedsim is one of the few programs able to construct a regional-scale 3D model by simulating most of the major geological processes and factors that affect clastic sediment deposition, including basement erosion, sediment supply, in-situ carbonate and organic growth, vertical tectonic movement, compaction, isostasy, sea level movement, sand dune formation, river flow and waves. The initial test models for the South Perth Basin were run at 5 km resolution. Once we were satisfied with the results at 5 km resolution the simulation was re-run at with a 500 m nested grid around the location of the Schlumberger Petrel static model.

5.2.1 OLENEKIAN TO ANISIAN (250 MA TO 237 MA) [WONNERUP EQUIVALENT]

Table 5-1 Sedsim input parameters common to all Olenekian to Anisian simulations

Sedsim COMMAND	INPUT DATA
TIME	From 250 Ma to 237 Ma with 75 ka display resolution, 10 ka flow resolution
GRID	15 by 8 nodes with a grid spacing of 5000 m, 0 degrees rotated from UTM north. SW Corner coordinates (UTM zone 50 H) E 370000 S 6320000
SEDIMENTS	Medium sand (0.3 mm), fine sand (0.15 mm), v fine (0.07 mm), clay (0.0004 mm), density of all grains 2650 kg/m^3 .
SLOPE	Maximum subaerial slopes for the four grain sizes: 0.007 0.0055 0.005 0.003, minimum slope, 0.0001 (0.0057°), calling interval 20000 years
SEA LEVEL	**Haq_plus_dnag_5ka.sl** modulated from Haq and Al-Qahtani (2005)
FLUID SOURCES	Variable sources over time. Bankfull discharge rate 10 to 43 m^3/s sediment concentrations 0.7 to 3 kg/m^3 , 1 to 5 m flow height, initial grain-size distributions of 5-50% coarsest, 10-25% medium, 12-35% fine, 22-50% finest. Initial velocities 1 to 3 ms^{-1}

Several different simulations were run testing different hydraulic conditions, source locations and topography, however, all simulations had common elements. These are summarized in Tables 5.1 to 5.3. A list of input files is appended in Appendix I and the actual text files are available on the associated DVD.

5.2.2 LADINIAN TO RHAETIAN (237 MA TO 198 MA) [YALGORUP EQUIVALENT]

Table 5-2 Sedsim input parameters common to all Ladinian to Rhaetian simulations

Sedsim COMMAND	INPUT DATA
TIME	From 237 Ma to 198 Ma with 75 ka display resolution, 10 ka flow resolution
GRID	15 by 8 nodes with a grid spacing of 5000 m, 0 degrees rotated from UTM north. SW Corner coordinates (UTM zone 50 H) E 370000 S 6320000
SEDIMENTS	Medium sand (0.3 mm), fine sand (0.15 mm), v fine (0.07 mm), clay (0.0004 mm), density of all grains 2650 kg/m^3 .
SLOPE	Maximum subaerial slopes for the four grain sizes: 0.007 0.0055 0.005 0.003, minimum slope, 0.0001 (0.0057°), calling interval 20000 years
SEA LEVEL	**Haq_plus_dnag_5ka.sl** modulated from Haq and Al-Qahtani (2005)
FLUID SOURCES	Variable sources over time. Bankfull discharge rate 1 to 43 m^3/s sediment concentrations 0.1 to 3 kg/m^3 , 1 to 5 m flow height, initial grain-size distributions of 5-50% coarsest, 3-25% medium, 2-35% fine, 22-85% finest. Initial velocities 1 to 3 ms^{-1}

5.2.3 HETTANGIAN TO PLIENSBACHIAN (198 MA TO 182 MA) [ENEABBA EQUIVALENT]

Table 5-3 Sedsim input parameters common to all Hettangian to Pliensbachian simulations

Sedsim COMMAND	INPUT DATA
TIME	From 250 Ma to 237 Ma with 75 ka display resolution, 10 ka flow resolution
GRID	15 by 8 nodes with a grid spacing of 5000 m, 0 degrees rotated from UTM north. SW Corner coordinates (UTM zone 50 H) E 370000 S 6320000
SEDIMENTS	Medium sand (0.3 mm), fine sand (0.15 mm), v fine (0.07 mm), clay (0.0004 mm), density of all grains 2650 kg/m^3 .
SLOPE	Maximum subaerial slopes for the four grain sizes: 0.007 0.0055 0.005 0.003, minimum slope, 0.0001 (0.0057°), calling interval 20000 years
SEA LEVEL	**Haq_plus_dnag_5ka.sl** modulated from Haq and Al-Qahtani (2005)
FLUID SOURCES	Variable sources over time. Bankfull discharge rate 10 to 43 m^3/s sediment concentrations 0.7 to 3 kg/m^3 , 1 to 5 m flow height, initial grain-size distributions of 5-50% coarsest, 3-25% medium, 0-35% fine, 25-87% finest. Initial velocities 1 to 3 ms^{-1}

5.3 Initial altitude and Sea level curves

As discussed in the preceding sections, although the simulations all used the published eustatic sea level curve modulated from Haq and Al-Qahtani (2005) modulated with a high frequency Milankovic signal, the simulation area is considered to have been above sea level by an undetermined amount. The initial topographic values were chosen to descend 13 m from south to north with the northern edge 62 m above sea level given the published eustatic sea level height of -62 mrp at 250 Ma. This gives a mean initial topographic gradient of 0.00017 equivalent to that of a typical anastomosing-to-meandering channel system (Smith, 1983) given the bankfull discharge rate used. The absolute height above sea level of the

river system is not known, although there are no published observations of alpine palynoforms in the section, and there are Norvik's (2003) observations that the marine Kockatea Shale shoreline was close to the southern end of the simulation area (Figure 8) at around 250 Ma. This suggests that an altitude at the southern end of the simulation area of 75 mrp may not be unreasonable.

The variation in eustatic level was considered to be a climate proxy and the *rates* of change of eustatic sea level (rather than the absolute value) have been used as indicators of process change. A high RATE of rising eustatic level is taken as indicating wetter climatic conditions, and conversely a high rate of falling eustatic level was taken as indicating cooling/drying conditions. These assumptions seem defendable in the depositional systems experienced by the Southern Perth Basin at 40° to 45°S from 250 Ma to 182 Ma.

5.4 Tectonic movement

In these simulations the tectonic movement (subsidence rate and location) was controlled by the available seismically derived isochores for each of the four time intervals. This was justified by the overall continuity of depositional system (fluvial with occasional lacustrine periods), which suggest that the local gradients and position above sea level were maintained throughout the simulation.

5.5 Manning Coefficients and Porosity Table

The Manning Coefficients were set to the default values of Sedsim, with the coefficient set to 0.02 for open channel flow.

The table defining the loss of porosity due to burial compaction (porosity response to effective stress) was developed using published porosity-depth curves and the wireline porosity logs from Lake Preston-1 and Pinjarra-1. The table used is listed below:

```
POROSITY TABLE
# rows: constant fine-to-coarse ratio   0.0   0.05  0.50  0.85  1.0
# columns: constant effective pressure (MPa)   0  5.5  11  22   33  44  55  90
# 0    250m  500m  1000m  1500m    2000m  2500m  4000m
 0.35  0.27   0.24  0.18   0.15   0.10   0.08   0.05
 0.32  0.28   0.25  0.18   0.15   0.10   0.08   0.05
 0.40  0.36   0.30  0.22   0.20   0.16   0.10   0.08
 0.58  0.43   0.40  0.35   0.25   0.20   0.16   0.12
 0.60  0.55   0.50  0.40   0.30   0.25   0.18   0.15
```

The following input sediment data are used in conjunction with the above table:

Coarsest	Medium	Fine	Finest
0.3 (mm)	0.15 (mm)	0.07 (mm)	0.0004 (mm)
2650.00 (gm/cc)	2650.00 (gm/cc)	2650.00 (gm/cc)	2650.00 (gm/cc)

Thus, a sediment composed of 100%, 0.3 mm mean diameter quartz (density 2.65 gm/cc) has an initial depositional porosity of 35% which reduces by compaction to 5% on being buried to 4000 metres (effective stress of 90 MPa). A sediment composed of 100%, 0.0004 mm mean grain size sediment (i.e. clay) will have an initial porosity of 60%, which reduces by compaction to 15% (total porosity, not effective porosity) on being buried to 4000 metres (effective stress of 90 MPa). Intermediate percentages of relatively fine and coarse sediment will have the porosity reductions shown by intermediate rows.

6 Experimental runs

6.1 Initial round of simulations at 5 km resolution

The initial experiments tested the conceptual models from published literature and discussions for each of the three time periods .

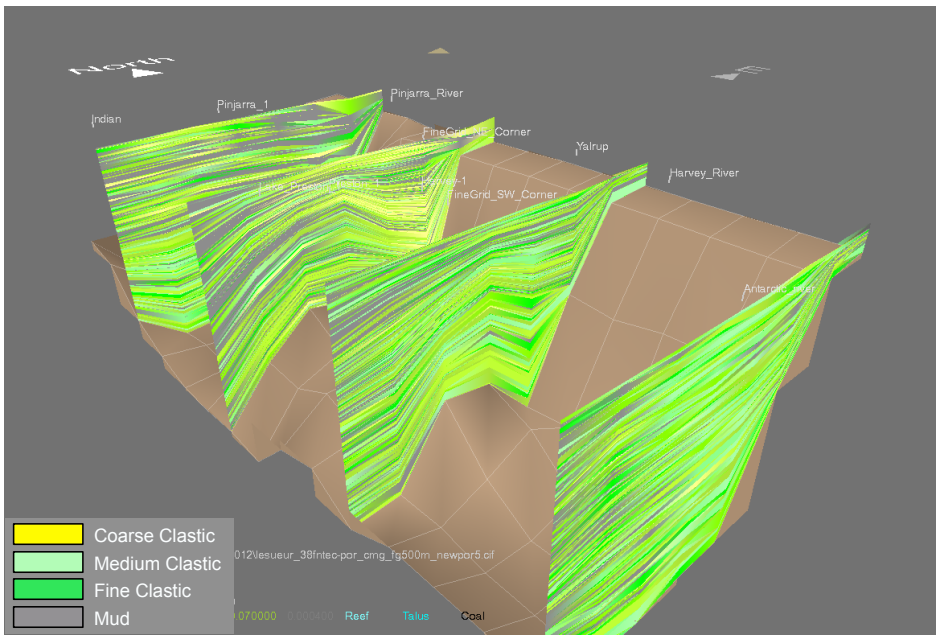

Figure 11 East-West lithology sections across the simulated area. Grain sizes as shown in the legend.

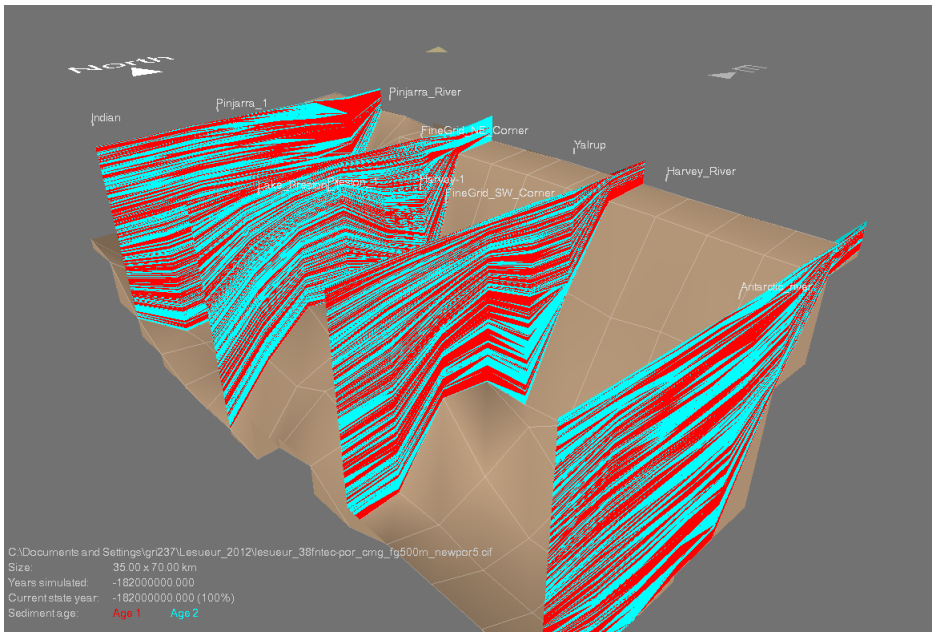

Figure 12 East-West 'pseudo seismic' sections across the simulated area. Alternate time layers are code red and blue.

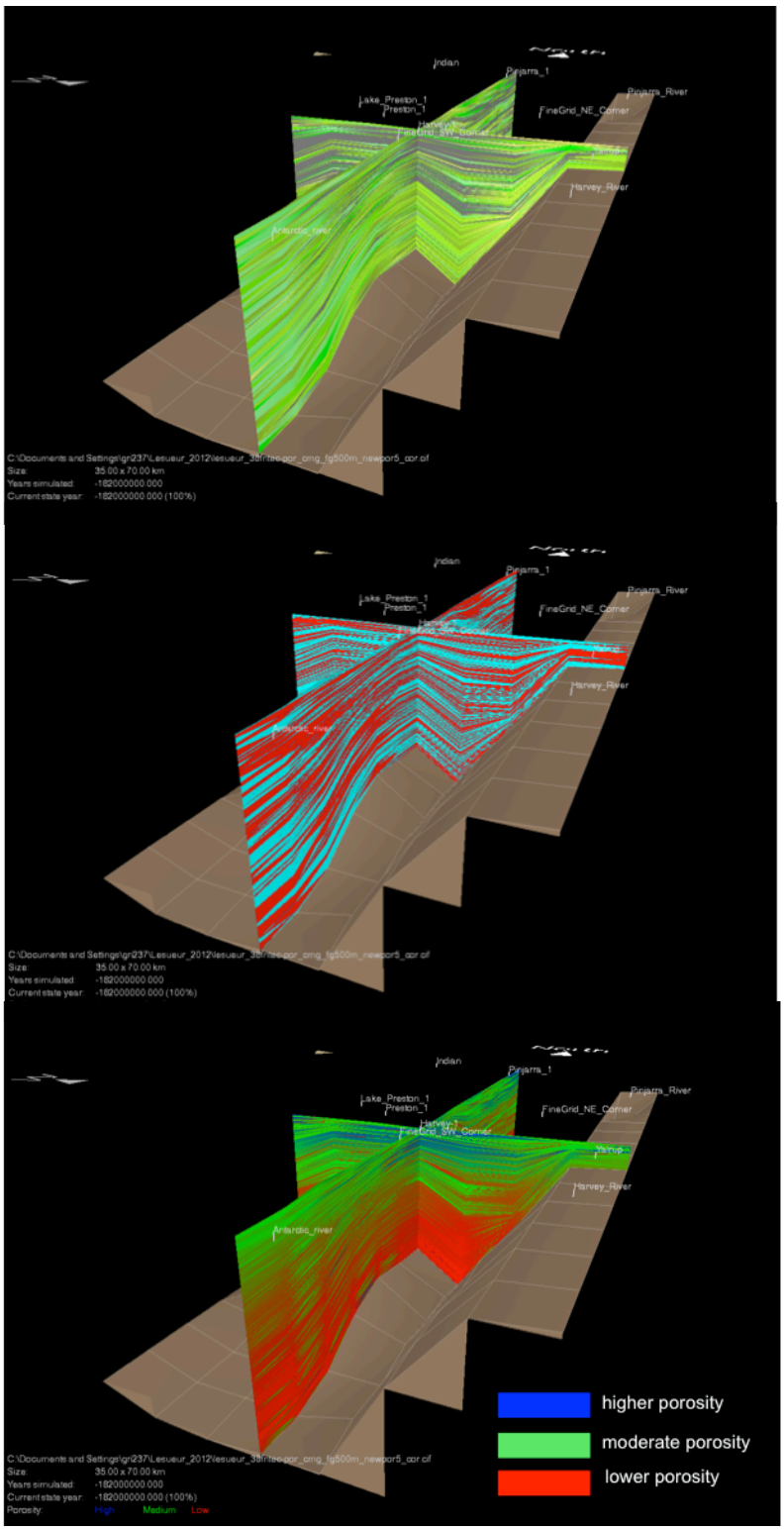

Figure 13 Sections from the 5 km resolution model, crossing at the Harvey-1 well position, showing Sedsim predicted lithology, pseudo-seismic and porosity distributions.

Maps of the 5 km resolution model results are shown below (Figures 14 to 17 inclusive) for each of the three depositional periods simulated.

6.1.1 OLENEKIAN TO ANISIAN (250 MA TO 237 MA) [WONNERUP EQUIVALENT]

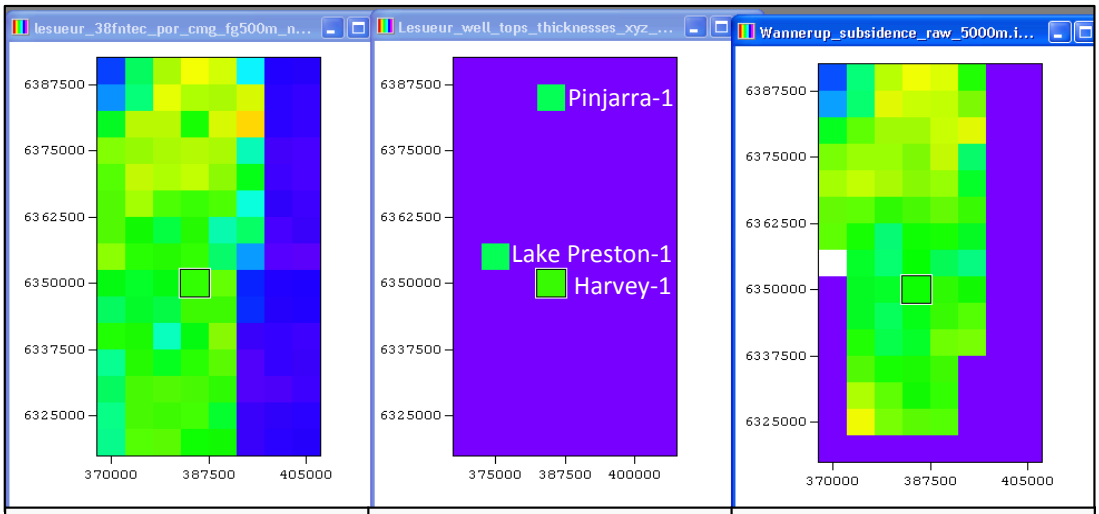

Sedsim predicted thickness (m)	Observed well thickness (m)	Seismic isochore (m)
1501	1515	1421

Figure 14 Wonnerup equivalent thickness comparisons with the seismic isochore at 5 km resolution and the well data set. Left-hand image is the Sedsim predicted thickness distribution. The centre image shows the observed well thicknesses. The right-hand image is the seismic isochore. The legend for all maps is shown below. The actual values in metres at the location of the Harvey-1 well are shown in the table.

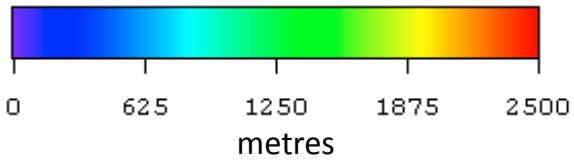

The colour bar above applies to all thickness maps.

6.1.2 LADINIAN TO RHAETIAN (237 MA TO 198 MA) [YALGORUP EQUIVALENT]

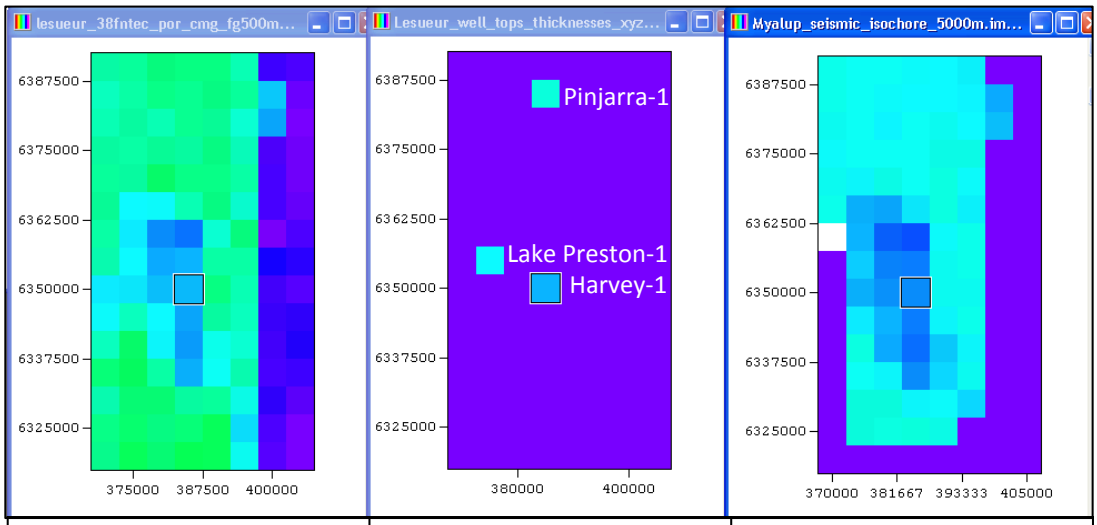

Sedsim predicted thickness (m)	Observed Well Thickness (m)	Seismic Isochore (m)
680	676	584

Figure 15 Yalgorup equivalent thickness comparisons with the seismic isochore at 5 km resolution and the well data set. The explanation of columns and legend is otherwise as in Figure 11.

6.1.3 HETTANGIAN TO PLIENSBACHIAN (198 MA TO 182 MA) [ENEABBA EQUIVALENT]

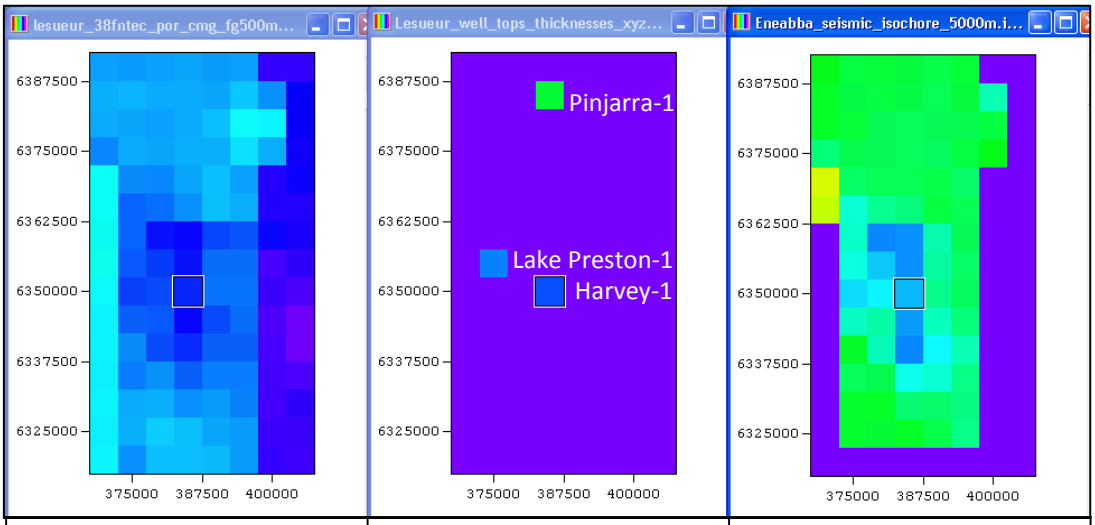

Sedsim predicted thickness (m)	Observed Well Thickness (m)	Seismic Isochore (m)
365	454	688

Figure 16 Eneabba equivalent thickness comparisons with the seismic isochore at 5 km resolution and the well data set. The explanation of columns and legend is otherwise as in Figure 11.

6.1.4 OLENEKIAN TO PLIENSBACHIAN (250 MA TO 182 MA) [LESUEUR AND ENEABBA FM.] SAND FRACTION.

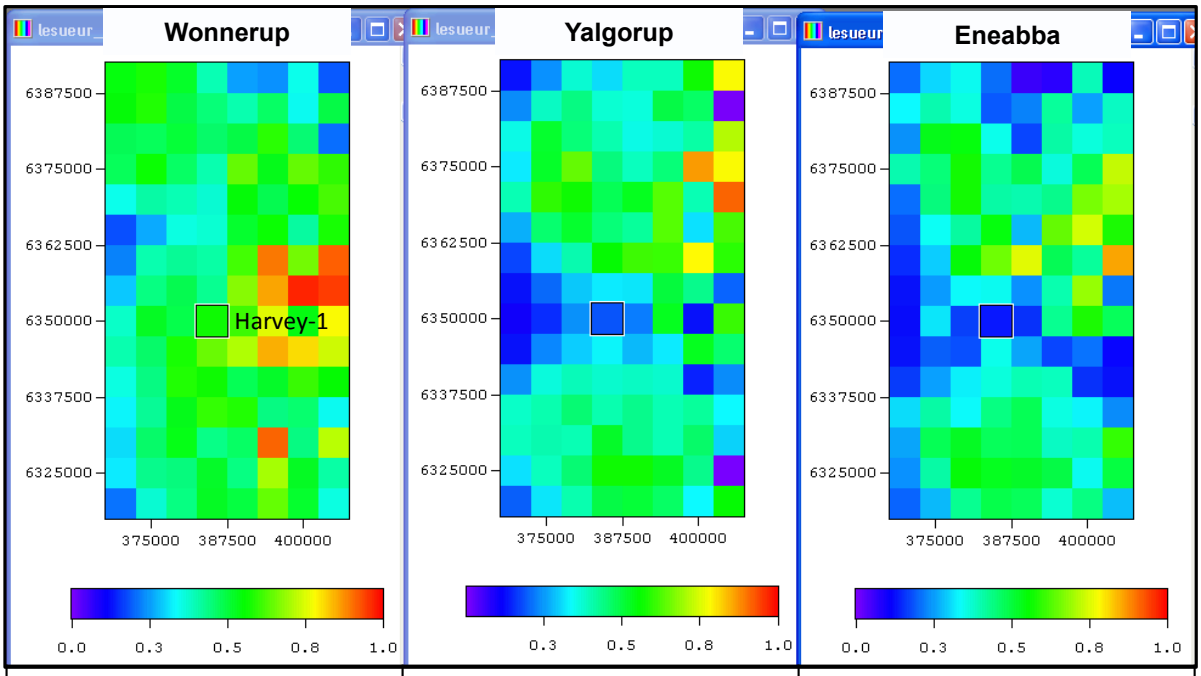

Sedsim predicted sand fraction Wonnerup Member at Harvey-1	Sedsim predicted sand fraction Yalgorup Member at Harvey-1	Sedsim predicted sand fraction Eneabba Fm. at Harvey-1
0.56	0.19	0.l13

Figure 17 Sedsim sand fraction predictions at 5 km resolution for each of the lithostratigraphic units modelled. The predicted values at the location of the Harvey-1 well are shown in the table.

6.2 Nested 500 m grid simulations

Following the completion of the 5000 m grid model (15 x 8 cells) and constraint against formation thicknesses at the Lake Preston-1 and Pinjarra-1 wells, higher resolution surfaces were derived from the available seismic data. Both the corresponding grid nodes at the 5000 m depositional surface, and the subsidence grids were reconciled with the higher resolution nodes. The nested grid location (Figure 18) was adjusted from the original Schlumberger dynamic model grid to include the Harvey-1 location.

The simulation was then run again using the higher-resolution surfaces in the nested grid location while the coarser grid provided the flow boundary conditions for the higher resolution area.

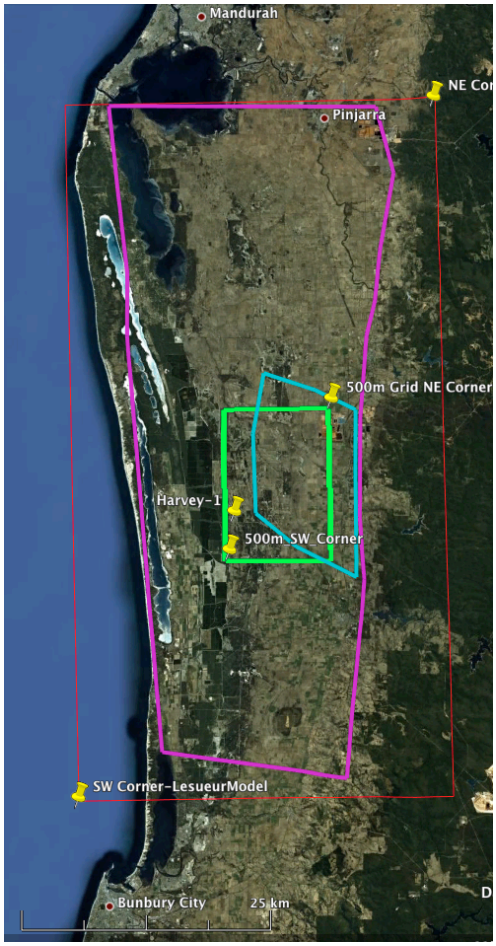

Nested 500 m grid coordinates (31 x 21 cells)

NE corner
GDA-MGA: (UTM with GRS80 ellipsoid)
Zone: 50 H
Easting: 395000.0 Northing: 6360000.0
Latitude: -32 ° 53 ' 27.39 '' Longitude: 115 ° 52 ' 43.19 '' E

SW corner
GDA-MGA: (UTM with GRS80 ellipsoid)
Zone: 50 H
Easting: 385000.0 Northing: 6345000.0
Latitude: -33 ° 015 ' 38.67 '' S Longitude: 115 ° 46 ' 09.14 '' E

Figure 18 Green rectangle marks the location of the nested Sedsim 500 m grid within the 5000 m Sedsim simulation (fine red rectangle). The pink and blue polygons mark the boundaries of the Schlumberger static and dynamic models respectively.

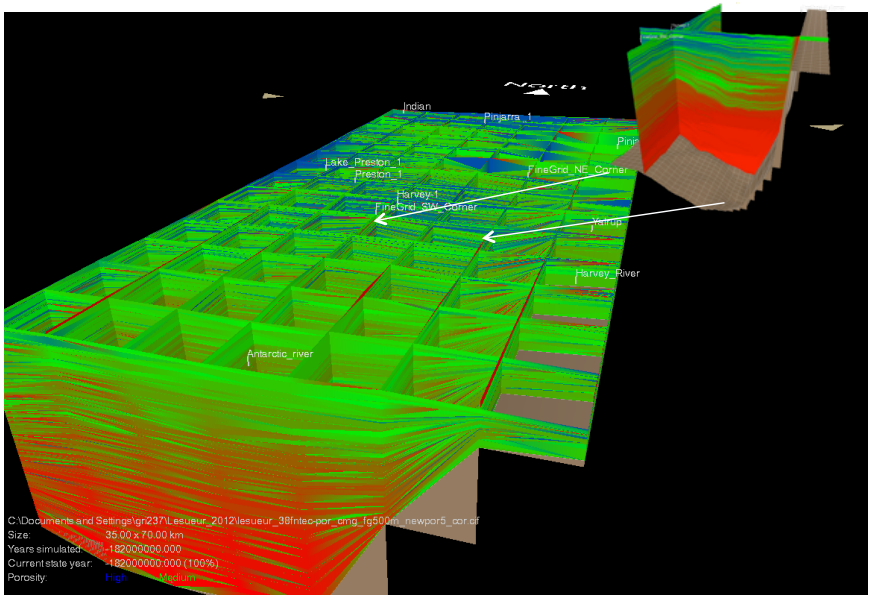

Figure 19 Coarse and fine grid porosity volumes showing the location of the 500 m nested grid.

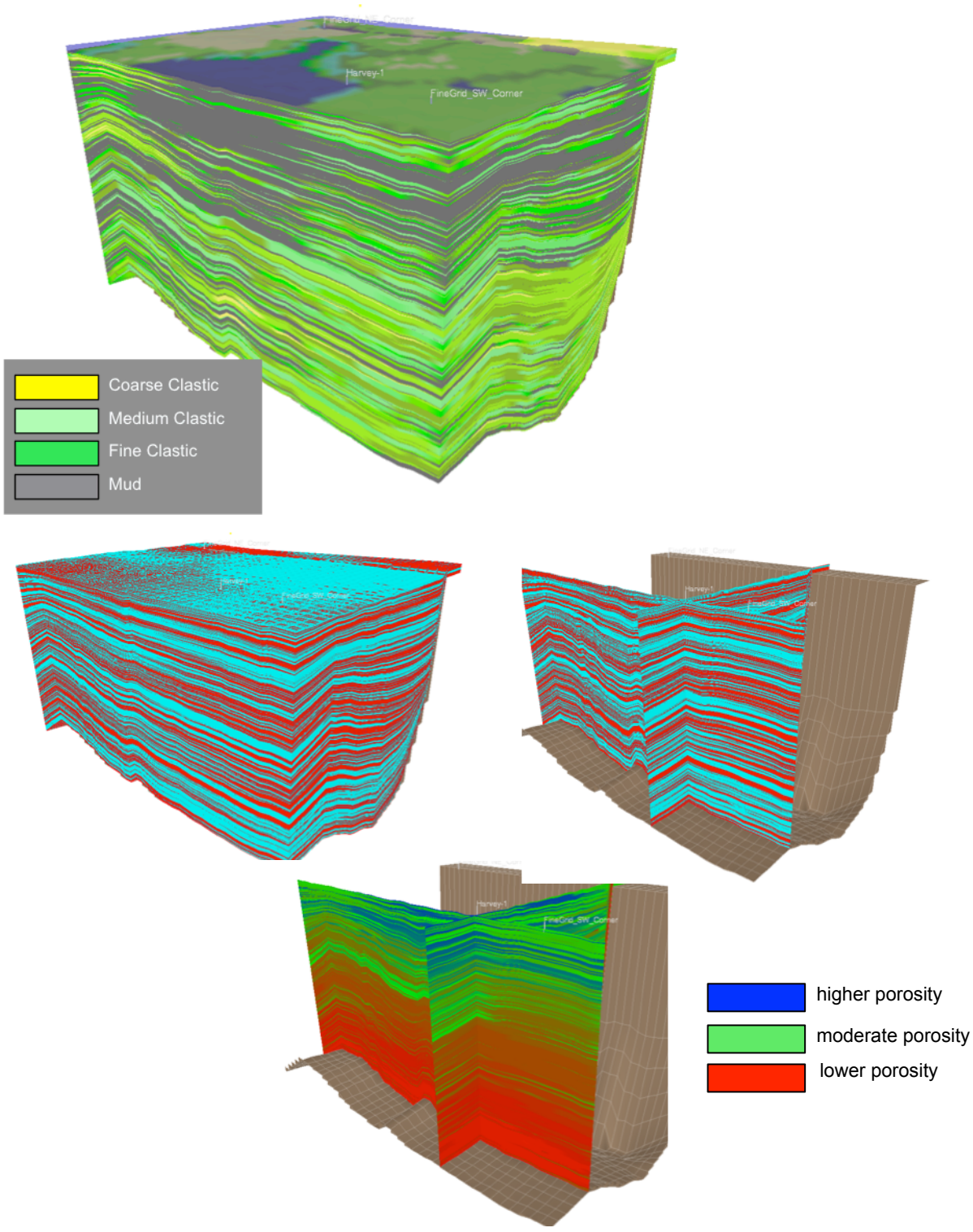

Figure 20 Sedsim predicted 500 m grid volume. Lithology, pseudo-seismic and porosity sections

6.2.1 OLENEKIAN TO ANISIAN (250 MA TO 237 MA) [WONNERUP EQUIVALENT] THICKNESSES.

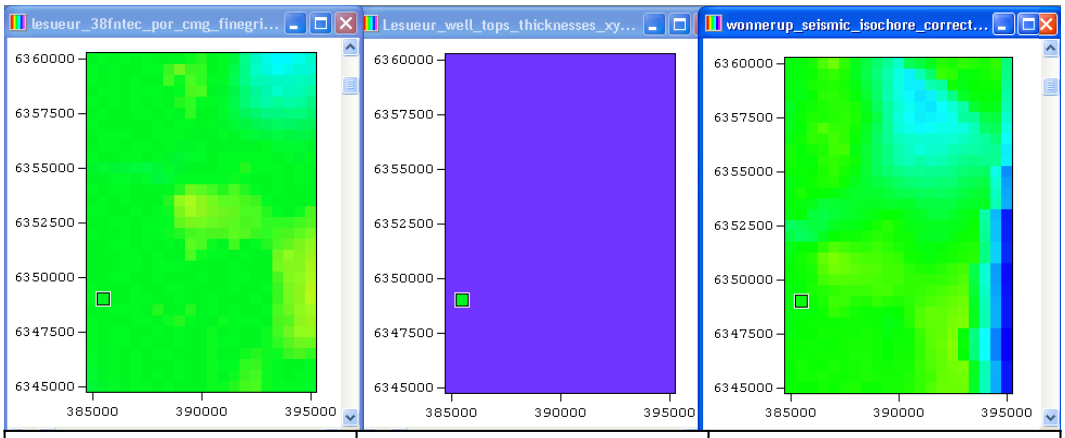

Sedsim predicted thickness (m)	Observed Well Thickness (m)	Seismic Isochore (m)
1449	1515	1371

Figure 21 Wonnerup equivalent thickness comparisons with the seismic isochore at 500 m resolution and the Harvey-1 well data set. The explanation of columns and legend is otherwise as in Figure 14.

6.2.2 LADINIAN TO RHAETIAN (237 MA TO 198 MA) [YALGORUP EQUIVALENT]

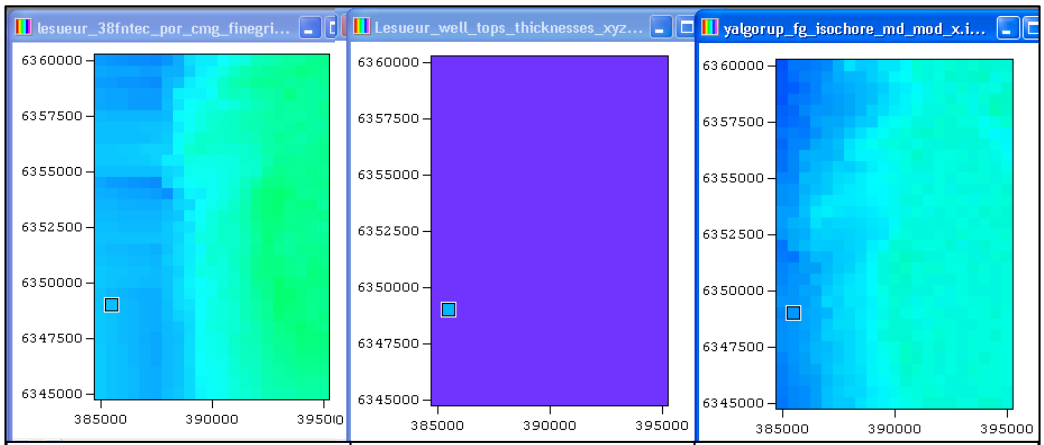

Sedsim predicted thickness (m)	Observed Well Thickness (m)	Seismic Isochore (m)
691	676	599

Figure 22 Yalgorup equivalent thickness comparisons with the seismic isochore at 500 m resolution and the Harvey-1 well data set. The explanation of columns and legend is otherwise as in Figure 14.

6.2.3 HETTANGIAN TO PLIENSBACHIAN (198 MA TO 182 MA) [ENEABBA EQUIVALENT]

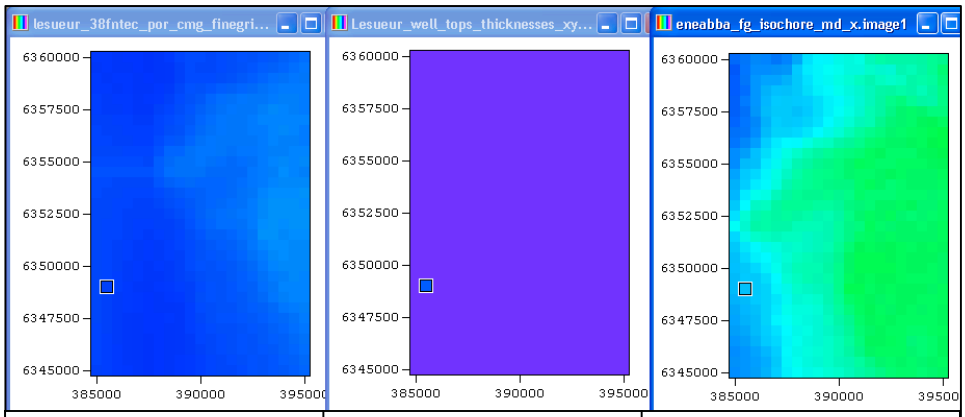

Sedsim predicted thickness (m)	Observed Well Thickness (m)	Seismic Isochore (m)
373	454	706

Figure 23 Eneabba equivalent thickness comparisons with the seismic isochore at 500 m resolution and the Harvey-1 well data set. The explanation of columns and legend is otherwise as in Figure 14.

7 Verification

Verification of stratigraphic forward models is always challenging. The choice of comparator depends on the purpose of the simulation, and needs to take into consideration the relative resolutions of the model and observations.

The reason for carrying out this particular study was to examine the possible advantages of using stratigraphic forward modelling for constructing a carbon sequestration static model. If we are looking for carbon storage in a saline aquifer we often have very limited subsurface data in the area of interest. We therefore need appropriate technology to decrease the time to characterisation and reduce geological uncertainty when selecting sites and drilling wells to prove up a selected site.

What are the critical components in a saline aquifer carbon sequestration case ?

- Do we have a competent seal? i.e. can stratigraphic forward modelling help predict the likelihood of fine grained strata being present and geographically continuous within the area. In the present case the most important comparison as a calibration point is the extent of the Yalgorup silty-shaley zones at the Harvey-1 location that were not predicted by interpolating between offset wells.
- Do we have storage capacity and injectivity? Here the likely distribution of higher permeability sands is important. The Harvey-1 well showed higher permeability than anticipated in the Wonnerup section from neighbouring wells. Can stratigraphic forward modelling improve predictability ?

In the present case we made blind predictions about Harvey-1 sediment distribution. However, we can also use the present study as part of a continuing 'data assimilation' programme with progressive prediction and validation as new data become available, using the Harvey-1 well as an initial calibration and then re-predicting and re-validating against new 3D seismic and the next Harvey 2 and 3 wells to be drilled in a year.

In the coarse regional grid case, the horizontal cell dimensions were 5000 m x 5000 m. The vertical resolution was 75000 years geological time giving a depth resolution varying from 1 mm to 10 m depending on grain size and sedimentation rate. In the fine grid, over the area of the static model, the horizontal cell dimensions were 500 m x 500 m with the same vertical resolution.

If we are comparing these results at a well intersection with a diameter of influence of the wireline logging tool of at most 5 m then we should not expect 1:1 correlation of every sand body recorded on the wireline logs. Indeed it may be worth considering to what degree the wireline or core-plug values observed at the well may be extrapolated away from the well location.

Comparing SFM results with seismic isochores is another possibility, and here the horizontal resolution is comparable. Unfortunately the vertical seismic resolution at 2000 m depth is of the order of 10 m. The isochore comparisons in Figures 14 to 23 illustrate this typical issue of poor agreement between observed seismic and observed well thicknesses and between model predicted thickness results and both seismic and well data. The error between seismic and well thicknesses is typically of the same order as the error between simulation results and either well or seismic observations. This is partly due to the difference between a lithostratigraphic formation top pick and a time/biostratigraphic top. Sedsim tops are time horizons more equivalent to seismic horizons than lithostratigraphic formation tops as defined in the type sections (Figure 10).

A comparison of wireline porosity log values from the wells and those from Sedsim simulation results at the nodes closest to Pinjarra-1 and Lake Preston-1 (Figure 24) shows that the shale and sand values from the

Sedsim results match that from the wells reasonably well given the volume sampled by the simulation and the distance of the simulation nodes from the well locations. The effect of bad hole conditions on the log values can also be seen. The comparison with the Pinjarra-1 and Lake Preston-1 wells was completed before the Harvey-1 well was considered and the porosity-depth relationships from the two wells were used to constrain the Sedsim porosity matrix (Figure 24, B). Note that the Pinjarra-1 values track the observations reasonably well in good hole sections. In the Lake Preston-1 location the sand porosity values are up to 5 porosity units (i.e. 0.05) too high.

The Harvey-1 result shown in Figure 25 represents a blind test. Reasonable agreement is shown with core plug values and the modal wireline log porosities derived from neutron, density and sonic logs. Note that above 850 mRKB the Sedsim porosities are the only values available due to the bad hole effects on neutron and sonic wireline porosities.

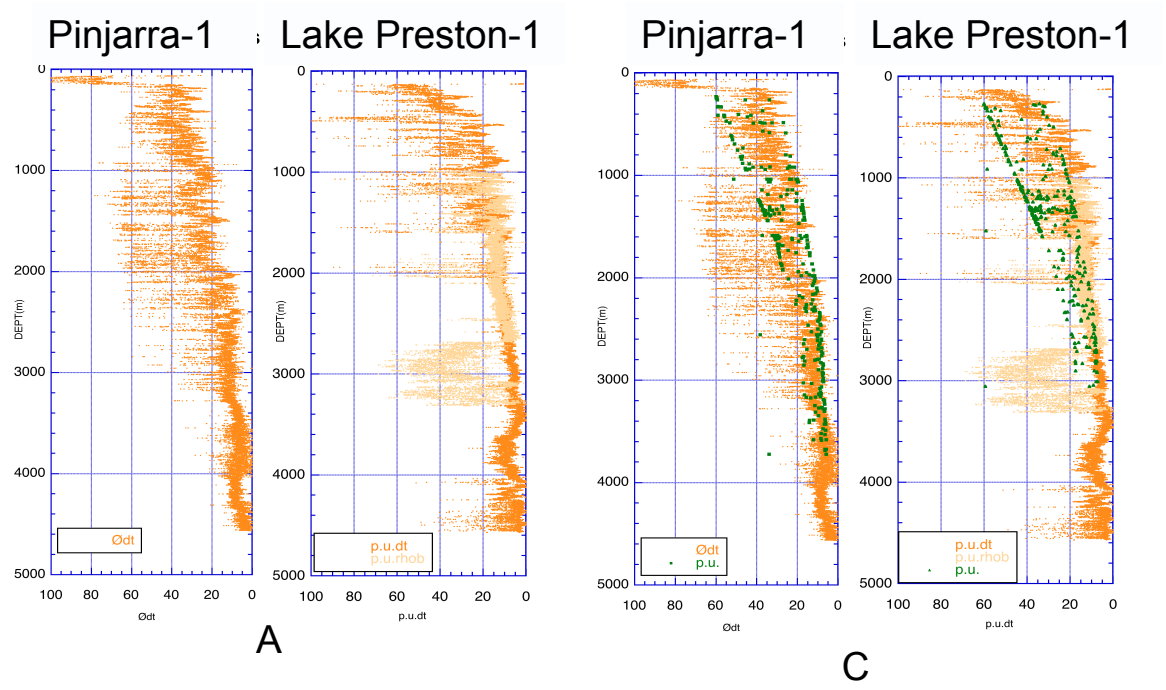

B

Porosity table

m:s	burial depth (m) 0	250	500	1000	1500	2000	2500	4000
0.00	0.35	0.27	0.24	0.18	0.15	0.10	0.08	0.05
0.05	0.32	0.28	0.25	0.18	0.15	0.10	0.08	0.05
0.50	0.40	0.36	0.30	0.22	0.20	0.16	0.10	0.08
0.85	0.58	0.43	0.40	0.35	0.25	0.20	0.16	0.12
1.00	0.60	0.55	0.50	0.40	0.30	0.25	0.18	0.15

Figure 24 Constraint well porosity distribution with lithology and depth. (A) Pinjarra-1 sonic porosity values, Lake Preston-1 sonic porosity (dark orange) and density porosity (light orange) distribution with depth. (B) Sedsim porosity table calibrated against these wells. Rows show the effect of different mud: sand ratios on fractional porosity response to pressure (burial depth). (C) The application of this table to Sedsim prediction of porosity at 5 km grid resolution at these two well locations.

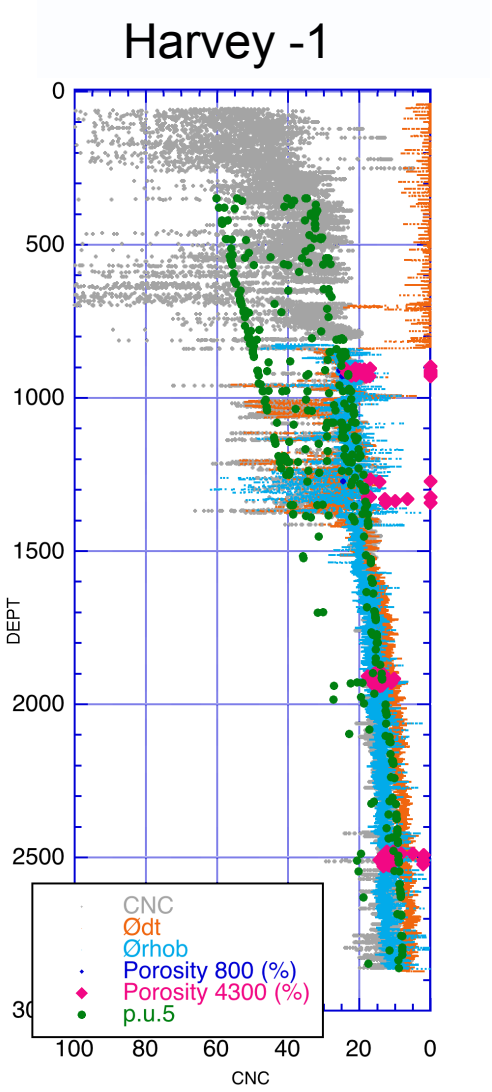

Figure 25 Observed and predicted porosity distribution with depth in the Harvey-1 well. The Sedsim porosity values were derived as described above (Section 5.5) from a porosity matrix calibrated against Pinjarra-1 and Lake Preston-1 well data. The observed porosity values in the well were CNC (Neutron porosity), Ødt (sonic porosity), Ørhob (density porosity), Porosity 4300 and Porosity 800 (core plug values), and the Sedsim predicted values (p.u.5).

Validation against seismic sections is also carried out. In the case of the Collie Hub area there were recent 2D seismic lines (Figures 26 and 27). Although it is possible to produce a true synthetic seismic section or volume from Secdsim output, in this case we have simply shown a 'pseudo-seismic' section consisting of alternate red-blue colours for the display time intervals (75000 years for each interval). The Sedsim stratal geometries produced using this approach are usually comparable to those from seismic sections and act as a simple check on subsidence or uplift rates. In this case the seismic imaging of the Darling Fault zone is problematic, with a possible low angle discontinuity that is being investigated. The comparison in

Figure 26 Location of seismic lines . Line '11GA_LL2-mig-final' is shown in red in relation to the Lake Preston-1 well location.

this case between the Sedsim stratal geometries and the seismic suggests that there is more complexity in the eastern third of the succession than has been included in the present Sedsim model. This will be investigated further in the next phase of modelling.

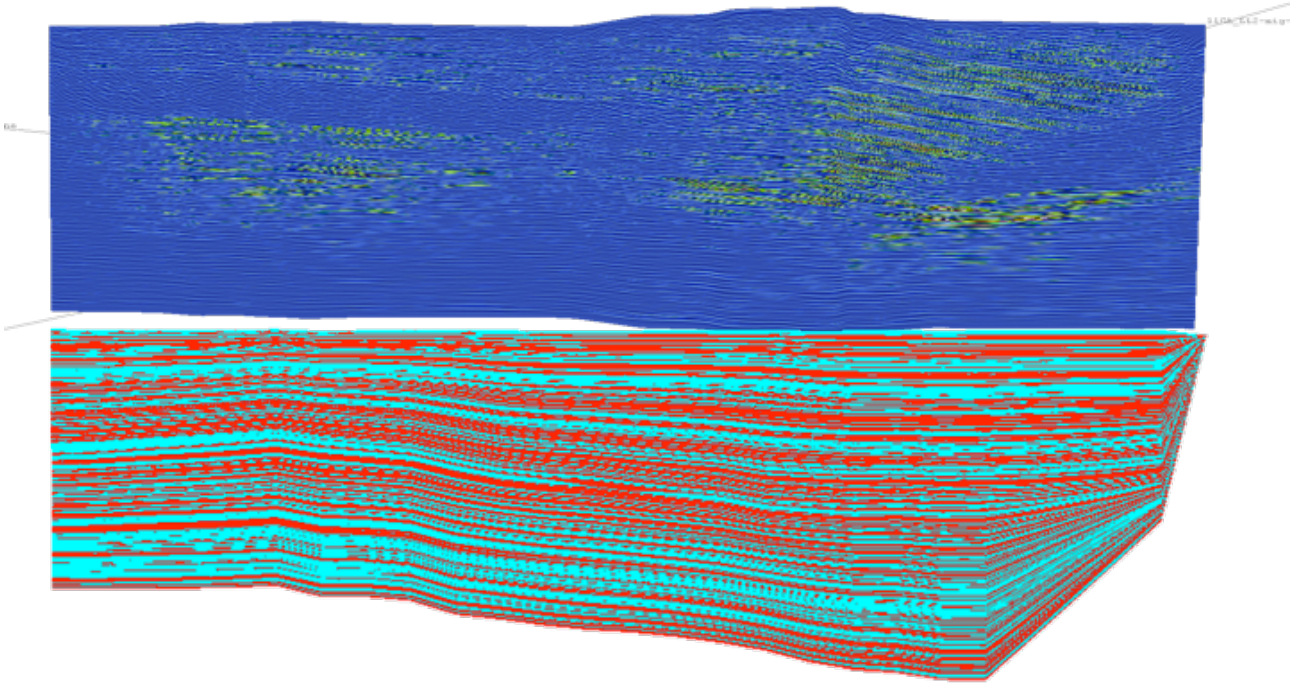

Figure 27 Seismic line '11GA_LL2-mig-final' (upper), at the location shown in Figure 26 compared with a 'pseudo-seismic' section (lower) from the Sedsim simulation at approximately the same location.

8 Static Model

A 'static reservoir model' is a numerical, layered, geological volume in which the main stratigraphic units are represented as lithofacies, each of which is associated with a porosity and permeability, or a statistical distribution of porosities and permeabilities. The concept has evolved to allow a sedimentological and/or stratigraphic conceptual representation, that is geologically defensible, to form the framework around which a numerical model of fluid flow in the reservoir volume (the 'dynamic' model) can be built.

"A model of a specific volume of the subsurface that incorporates all the geologic characteristics of the reservoir. Such models are used to quantify characteristics within the subsurface volume that are relatively stable over long periods of time and can, therefore, be considered static. These attributes include the structural shape and thicknesses of the formations within the subsurface volume being modeled, their lithologies, and the porosity and permeability distributions. These last two characteristics often vary significantly from location to location within the volume, resulting in heterogeneity. However, porosity and permeability are stable in the near-geologic timeframe and do not change due to the movement of fluids or gases through any of the formations pore spaces. The result of reservoir characterization is a reservoir characterization model (also known as a static model and sometimes referred to as a geologic model)."
Schlumberger Glossary © 2012 Schlumberger Limited.

The primary objective of this phase of the project was to demonstrate an alternative workflow based on stratigraphic forward modelling, to building a static geological model of the Collie Hub CO_2 injection site.

The goal was to develop a model with sufficient detail to represent vertical and lateral heterogeneity at the appropriate scale, which could be used as a tool for reservoir management. This required that the model be appropriately layered (850 layers, 2.3 m average thickness), and have appropriate XY cell dimensions (500x500m; 4 cells per km^2). These criteria resulted in the development, at the fine grid resolution, of a 500000 cell model for the 150 km^2 area modelled. The nature of the static reservoir model can be seen in Figures 19 and 20. The cell values are exported in the form of a corner-point 'grdecl' format file that can be input into a variety of reservoir engineering tools such as Schlumberger's 'Eclipse', Roxar's 'VIP', or reactive transport models such as LBNL's 'ToughReact'.

The Sedsim generated static model provides an alternative to the existing Schlumberger model that is based on a stochastic generation of properties based on natural analogues. The alternative Sedsim model can be subsequently used to see how uncertainty in the static model may result in uncertainty in the Hub CO_2 plume evolution. This can serve to reduce risk for the SW Hub project (or at least better quantify risk).

9 Discussion

A Sedsim stratigraphic forward model of the South Perth Basin has been constructed from 250 Ma to 182 Ma at spatial resolutions of 5 km and 500 m. The area of the 8 km resolution study was 75 km by 40 km, while the 500 m nested grid covered an area of 15 km by 10 km within the 5 km model. Fluvial to paralic sedimentation of siliciclastics has been simulated at a temporal resolution of 250 ka. Extensive literature studies have provided the essential background information for determining the succession of environmental controls on sediment supply and deposition throughout the basin.

River source locations and flow regimes have been identified and quantified. The resultant figures displayed in this brief report are only a minor part of the output from the study. Together with the associated files that allow interactive 3D interogation of the output at the various scales in SedView and Paraview, there are the ascii numerical output files that have been downloaded to ANLEC R&D. The input files for the various simulations have been transferred to ANLEC R&D to enable ANLEC R&D to re-run the simulations if necessary, or to experiment with changed parameters provided a licensed copy of the Sedsim program is available.

The numerical results of the simulations are provided as ascii files that can be input to any spreadsheet or statistical program, Petrel, RMS or Eclipse.

We consider the overall simulation, as the first attempt to create a stratigraphic forward model of the Triassic to Early Jurassic of the South Perth Basin in 3D at high resolution, to have been successful in that it has provided a test of the various depositional system hypotheses expressed in several papers and PhD studies by Willmott (1964), Balme (1966), Young and Johanson (1973), Dolby and Williams (1973), Playford et al. (1976), Ingram (1982), Helby et al. (1987), Bradshaw and Yeung (1990), Mory (1994), Mory & Iasky (1996), Crostella and Backhouse (2000), Norvik (2003) and others. We started by investigating the origin of the sediment brought into the basin in the Olenekian. A dominant Antarctic source was compared with local Yilgarn sources. The best agreement with seismic stratal geometries and well data was achieved with a balance of around 70% flow from the south with the rest from valleys in the Yilgarn at the location of present day river systems. A river to the east of Pinjarra-1 (possibly the present day location of South Dandalup River valley) seems to have provided a significant volume of sediment into the northern part of the modelled area throughout the period 237 Ma to 182 Ma.

The model predicted an increase in lacustrine deposition between the Pinjarra-1 location and Lake Preston-1 location during the Yalgorup and Eneabba equivalent periods (237 Ma to 182 Ma). If verified by observation this could be an area of improved seal quality since lacustrine deposition often represents fine grain material that could form a seal to CO_2 storage, and its geographic distribution has a direct relation to containment security and thus storage capacity (Figure 17). Prior to drilling Harvey-1 the previous geological characterisation did NOT predict seal lithologies in the Yalgorup.

Prior to Harvey-1 there was a large risk of getting tight rock with little injectivity or capacity in the Wonnerup. The Harvey -1 showed that this was not the case, and this was also predicted by the Sedsim model (Figure 25) although there is a diagenetic component to the preserved porosity that Sedsim only indirectly incorporated (via the porosity matrix calibrated against Pinjarra-1 and Lake Preston-1 wells).

This project has demonstrated an alternate workflow for producing a static reservoir model for geological sequestration of CO_2. The workflow was based on limited well and seismic data constraints, and used the Sedsim stratigraphic forward modelling software to translate a conceptual geological model into a cellular geological volume. This volume will form the basis of a reservoir flow simulation of CO_2 injection into the Lesueur Sandstone. The validity of this Sedsim 'static' model was examined by a blind comparison of Sedsim predicted porosity distribution with depth against the Harvey-1 well data. The results (Figure 25) are promising. The next phase of the project will use this static volume as the basis of a fluid flow 'Eclipse' simulation of CO_2 injection. These results will be compared with the Schlumberger Eclipse results using the

same fluid flow properties and boundary conditions. When the real injection of CO_2 is carried out at the Collie Hub site it will be possible to compare the predicted break-through times from the two models. This will be the first time such a comparative experiment has been conducted and we expect to gain insights into the relative merits of the two workflows for planning future sequestration projects.

The model has 850 layers at 250000 year intervals. This translates into varying thicknesses depending on grain size and rate of sedimentation at any given location. Upscaling can be achieved by increasing the layer time intervals. In phase II of the project it is planned to vary the layer durations (reduce the number of layers) and test the effect on the predicted break-through times.

The model as presented here is deterministic, and the end result of a series of over fifty trial simulations. In stratigraphic forward modelling the well and seismic data are used as constraints to predictions rather than the basis of an interpolation or inverse scheme. Convergence of results on the constraint wells and seismic stratal geometries is at present carried out manually. We have plans to automate this process.

It is possible to create an uncertainty model by running many forward models with a stochastic variation of input parameters. This has not been done in this phase of the project but would be a possible extension. Other areas of possible future improvement are thickness calibration (Figures 14 to 17) against well data, although the use of lithostratigraphic formations rather than ages or biozones in the wells will always influence Sedsim-Formation thickness comparisons.

Given that the key concerns for any Geological Carbon Storage site evaluation are **injectivity, capacity** and **containment**, we need to reduce geological uncertainty in these components early in the characterisation of a selected storage site. Any technological approach to prospectivity must therefore:

(1) define the likelihood of reservoir quality sands and their distribution (reduce injectivity and capacity risk).
(2) define the likelihood of seal quality strata and its distribution (reduce containment risk).

We have demonstrated in this project that stratigraphic forward modelling, and Sedsim in particular, is a potentially useful tool in this respect.

There will be future calibration opportunities at this site as new 3D seismic is acquired and additional wells drilled. The Sedsim static model will be used to predict the strata to be encountered at the next wells and then the model will be re-calibrated post-drill.

10 Conclusions

The first ever three-dimensional numerical stratigraphic forward model of the Triassic and Early Jurassic succession, from 250 Ma to 182 Ma, in the South Perth Basin has been constructed using published palaeogeographical and palaeoclimate data, constrained by sedimentation process observations from three wells. Two models have been produced; a 5000 m grid over the 75 km x 40 km area, and within this a nested 500 m grid over the Collie Hub dynamic model area of 15 km x 10 km.

A blind test of porosity distribution at the Harvey-1 well location suggests that the model may be suitable for use as the basis of a dynamic reservoir simulation.

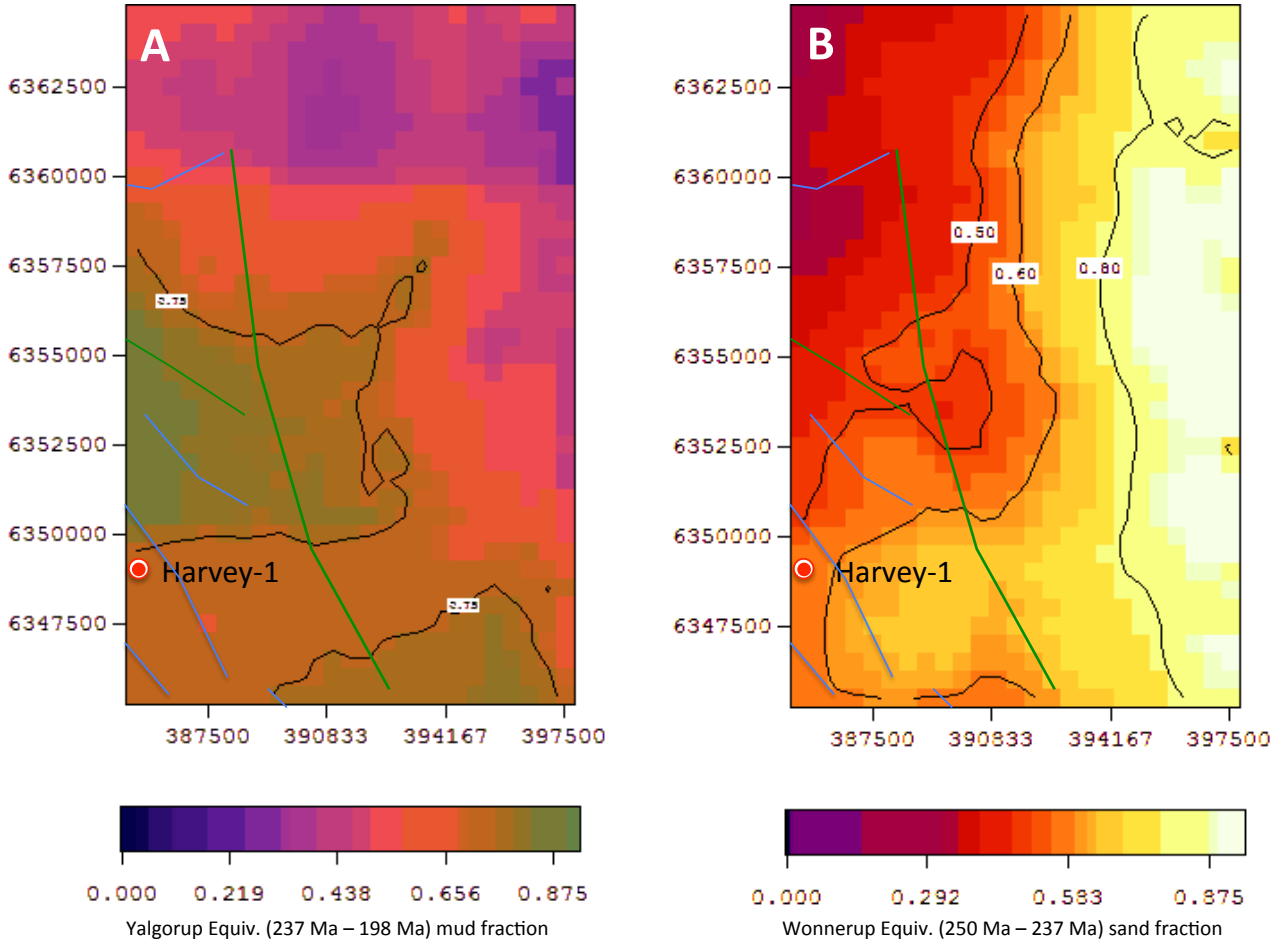

Figure 28 The area shown is the 500 m resolution static model grid around Harvey-1 well location. A) Sedsim predicted seal potential in the Yalgorup equivalent (75% mud contour shown). B) Sedsim predicted sand fraction in the Wonnerup equivalent. Faults interpreted from the 2011 2D seismic lines are overlain on the Sedsim facies maps. Green lines represent faults with unspecified downthrow to the West and SW, while blue lines represent faults with unspecified downthrow to the North and NE (Langhi et al, 2013).

There are areas within the 500 m resolution static model area of Sedsim-predicted seal potential in the Yalgorup (Figure 28, A), and areas of reservoir potential in the Wonnerup (Figure 28, B), that may be of use in selecting future well locations. These features may be combined in a predictive Common Risk Segment (CRS) map for the area (Figure 29).

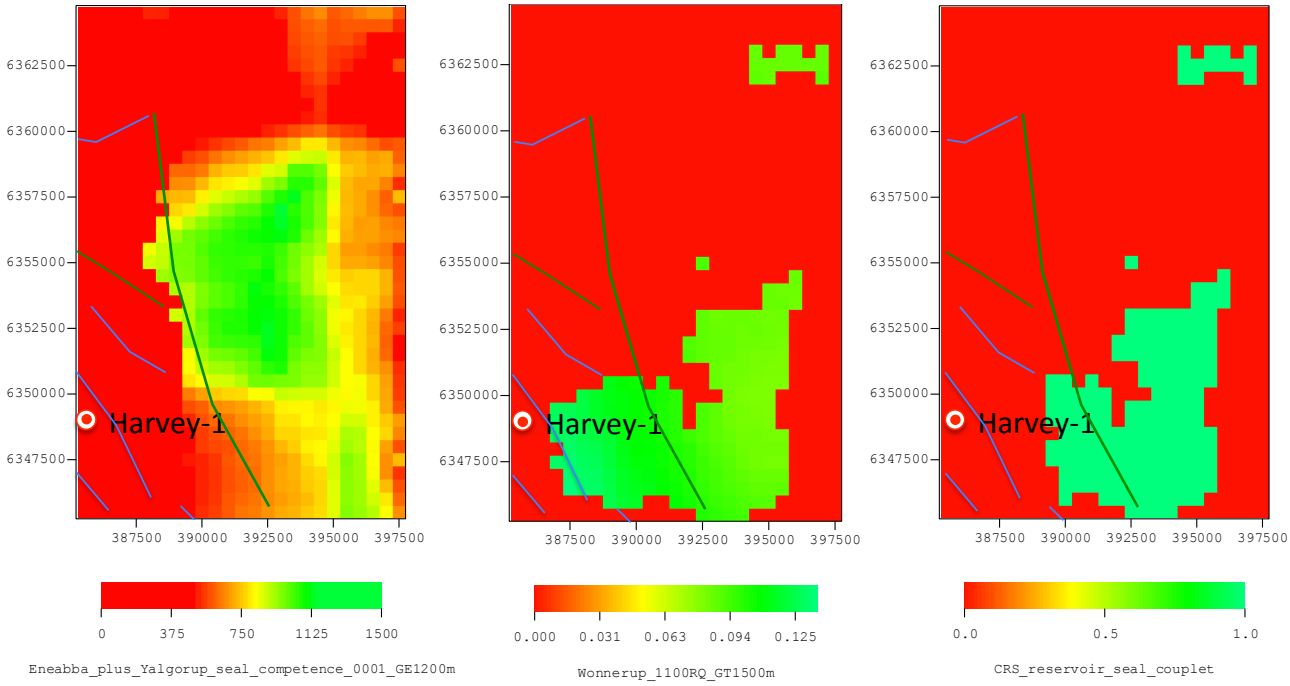

Seal competence defined as Effective mud thickness for Eneabba and Yalgorup ischore > 1200m

Reservoir quality defined as weighted mean porosity over 8% for locations with net:gross >60%, and gross thickness > 1500m

CRS = locations where the seal and reservoir criteria coincide.

Figure 29 Sedsim predicted risk maps for seal and reservoir for the 500 m grid area (red higher risk, green lower risk). The Common Risk Segment (CRS) map combines the seal and reservoir risk in a simplistic (unweighted) fashion. The green CRS areas are those where the optimum seal and reservoir conditions coincide at the same Sedsim node. Note that this is a conservative case. Faults interpreted from the 2011 2D seismic lines are overlain on the Sedsim CRS maps. Green lines represent faults with unspecified downthrow to the West and SW, while blue lines represent faults with unspecified downthrow to the North and NE (Langhi et al, 2013).

While it is too early to say if this proposed approach will lead to the desired increase in Probability of Success (page 1 of this report) over earlier approaches to reservoir characterisation, the next phase of the project will use these stratigraphic forward modelling results in a comparative dynamic model which will provide a testable predicted break-through time for CO_2 injection.

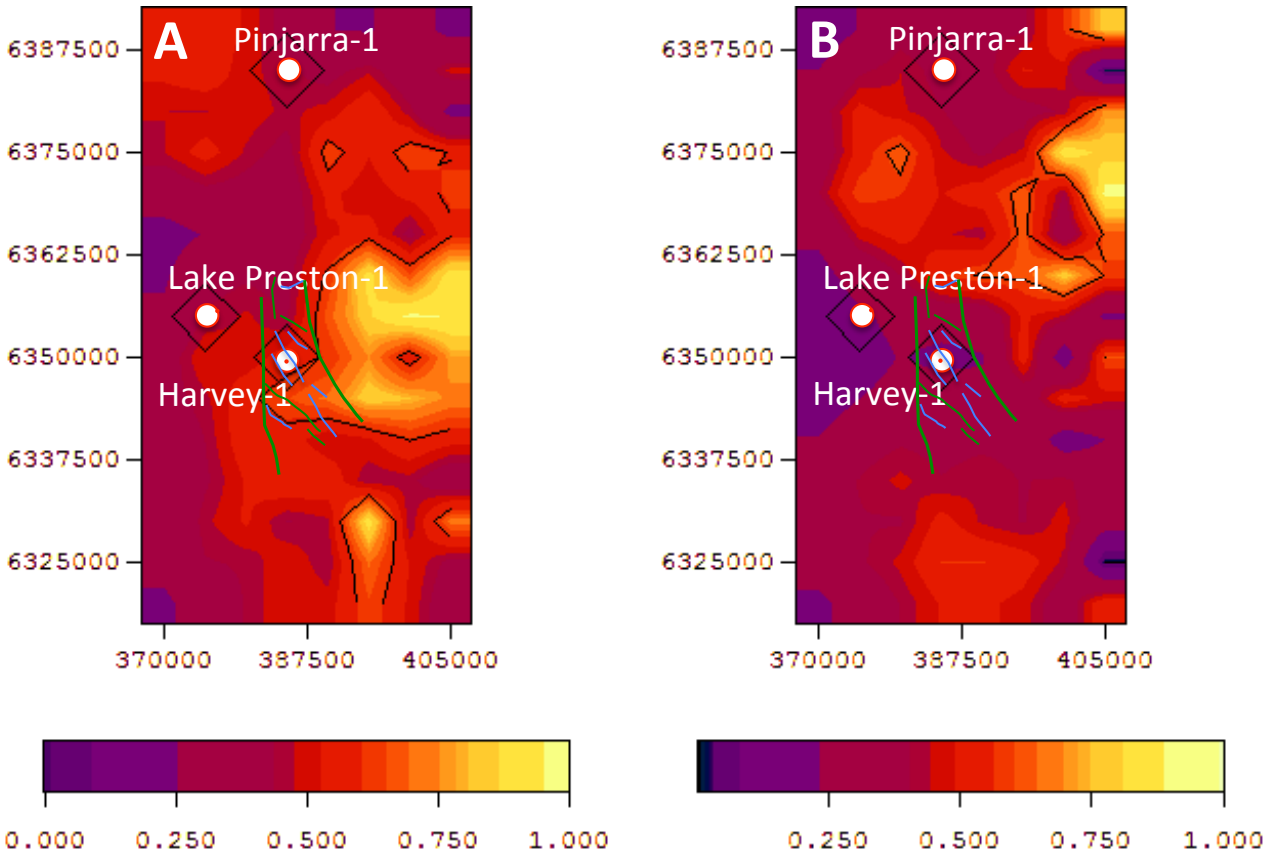

Wonnerup Equiv. (250 Ma – 237 Ma) sand fraction (0.6 contour)

Yalgorup Equiv. (237 Ma – 198 Ma) sand fraction (0.6 contour)

Figure 30 The area shown is the 5000 m resolution regional model grid. A) Sedsim predicted sand fraction in the Wonnerup equivalent (60% sand fraction contour shown). B) Sedsim predicted sand fraction in the Yalgorup equivalent (60% sand fraction contour shown). Faults interpreted from the 2011 2D seismic lines are overlain on the Sedsim facies maps. Green lines represent faults with unspecified downthrow to the West and SW, while blue lines represent faults with unspecified downthrow to the North and NE (Langhi et al, 2013).

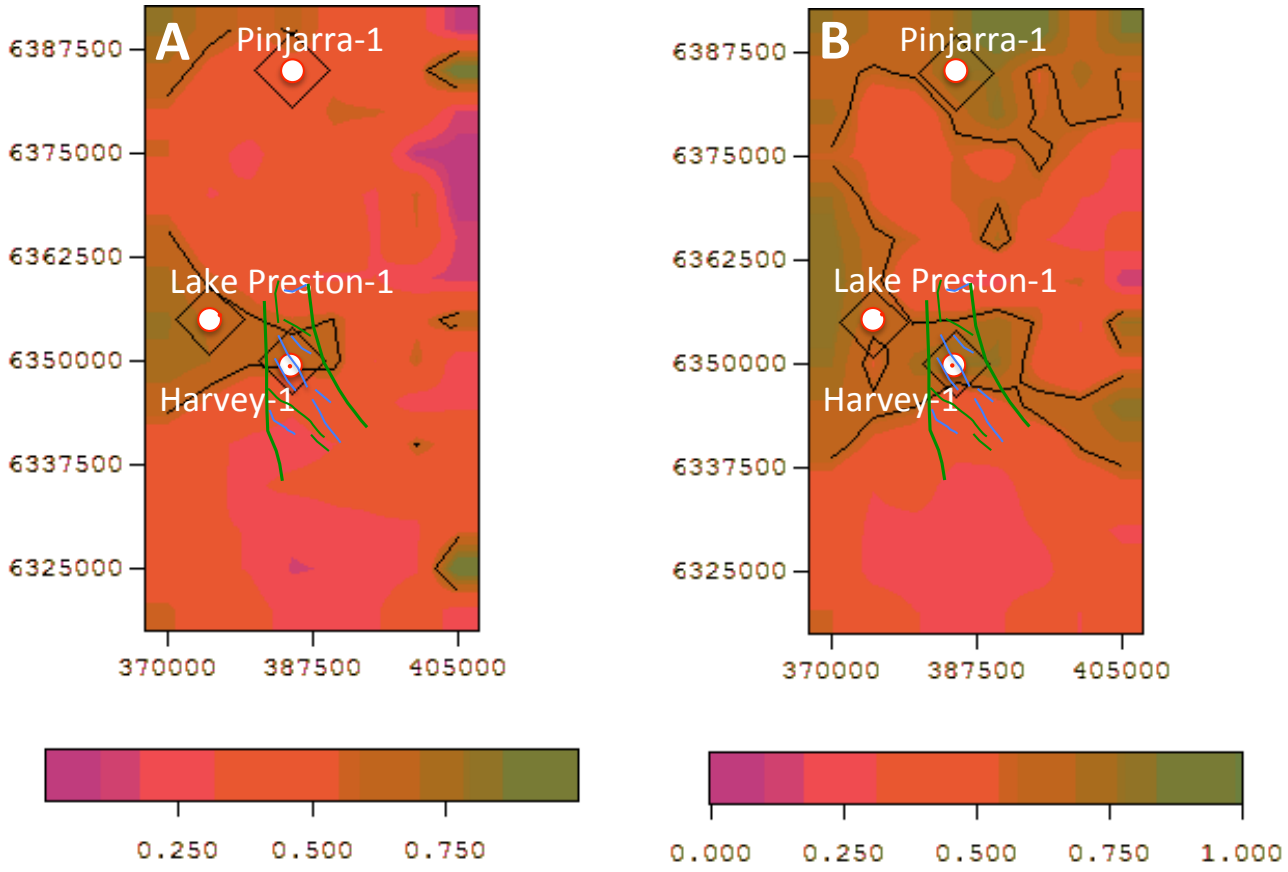

Yalgorup Equiv. (237 Ma – 198 Ma) mud fraction (0.6 contour)

Eneabba Equiv. (198 Ma – 182 Ma) mud fraction (0.6 contour)

Figure 31 The area shown is the 5000 m resolution regional model grid. A) Sedsim predicted mud fraction in the Yalgorup equivalent (60% mud fraction contour shown). B) Sedsim predicted mud fraction in the Eneabba equivalent (60% mud fraction contour shown). Faults interpreted from the 2011 2D seismic lines are overlain on the Sedsim facies maps. Green lines represent faults with unspecified downthrow to the West and SW, while blue lines represent faults with unspecified downthrow to the North and NE (Langhi et al, 2013).

Output from the model consists of:

- 3D interactive visualisations in SedView format.
- ASCII files in various formats with grain-size, porosity, facies, stratigraphic age, sorting, sand fraction etc. that can be used to generate pseudo-well logs, synthetic seismic sections, permeability and porosity volumes, etc. at the spatial resolution of the grid and the vertical resolution of the depositional events or a fixed vertical scale as required.
- Movies of basin formation from 250 Ma to 182 Ma.

As with any model, it is incomplete at several levels, and will need to be updated as new information become available. However it is hoped that this initial attempt to predictably model facies distribution, porosity and permeability (below seismic resolution and away from well data) will stimulate further use of the stratigraphic forward modelling approach, both at the regional and field scale, for geological sequestration of carbon dioxide, as well as petroleum systems and aquifer-constrained geothermal projects.

Appendix A E-Documents provided in the data base

A.1 Sedsim9 simulation input files

A.1.1 COMMAND, TOPOGRAPHY, SEALEVEL, TECTONIC FILES

The following files enable a Sedsim run using the unix binary 'sedsim9_120427Intelmac' or Windows equivalent 2012 sedsim9 binary.

Apx Table A.1 Sedsim9 input files

FILE PURPOSE	FOLDER	FILE NAME
ASCII simulation command file	ANLEC_LesueurSFM_Phase1_input	lesueur_38fntec-por_cmg_fg500m_newpor5.sif
ASCII initial surface (5000 m grid)	ANLEC_LesueurSFM_Phase1_input	lesueur_toptest05.top
ASCII subsidence/uplift files (5000 m and 500 m grid)	ANLEC_LesueurSFM_Phase1_input	lesueur_subsidence_17reconto17fg.tec lesueur_subsidence_17fg500m.tec
ASCII sea level file	ANLEC_LesueurSFM_Phase1_input	Haq_plus_dnag_5ka.sl

A.2 Sedsim9 simulation output files

A.2.1 ASCII PROCESSED OUTPUT FILES

The following files can be opened in any text reader or spreadsheet

Apx Table A.2 Sedsim9 ASCII output files produced by 'graph2dep_100903mac', 'graph2spc2_100617mac ' and 'graph2eclipse' programs.

FILE CONTENT	FOLDER	FILE NAME
ASCII simulation result volume in xyz format for the entire 5000 m grid volume	ANLEC_LesueurSFM_Phase1_dep_output	lesueur_38fntec-por_cmg_fg500m_newpor5 _cor_dep _all.xyz
ASCII simulation result volume in xyz format for the entire 500 m grid volume	ANLEC_LesueurSFM_Phase1_dep_output	lesueur_38fntec-por_cmg_finegrid_newpor5_cor_dep_all.xyz
ASCII simulation result volume in xyz format for the Lake Preston-1, Pinjarra-1 and Harvey-1 well locations from the 5000 m grid volume	ANLEC_LesueurSFM_Phase1_dep_output	lesueur_38fntec-por_cmg_fg500m_newpor5_cor_dep_LP1 _PJ1_H1.xyz
ASCII simulation result volume in xyz format for the Harvey-1 well location from the 500 m grid volume	ANLEC_LesueurSFM_Phase1_dep_output	lesueur_38fntec-por_cmg_fg500m_newpor5_cor_dep_H1.xyz

ASCII simulation result isochore in xyz format for the entire 5000 m grid Wonnerup Member (250 Ma to 237 Ma)	ANLEC_LesueurSFM_Phase1_spc_grdecl_output	lesueur_38fntec-por_cmg_fg500m_newpor5_Won_cor_spc.xyz
ASCII simulation result isochore in xyz format for the entire 5000 m grid Yalgorup Member (237 Ma to 198 Ma)	ANLEC_LesueurSFM_Phase1_spc_grdecl_output	lesueur_38fntec-por_cmg_fg500m_newpor5_Yalg_cor_spc.xyz
ASCII simulation result isochore in xyz format for the entire 5000 m grid Eneabba Formation (198 Ma to 182 Ma)	ANLEC_LesueurSFM_Phase1_spc_grdecl_output	lesueur_38fntec-por_cmg_fg500m_newpor5_Won_cor_spc.xyz
ASCII simulation result isochore in xyz format for the entire 500 m grid Wonnerup Member (250 Ma to 237 Ma)	ANLEC_LesueurSFM_Phase1_spc_grdecl_output	lesueur_38fntec-por_cmg_finegrid_newpor5_Won_cor_spc.xyz
ASCII simulation result isochore in xyz format for the entire 5000 m grid Yalgorup Member (237 Ma to 198 Ma)	ANLEC_LesueurSFM_Phase1_spc_grdecl_output	lesueur_38fntec-por_cmg_finegrid_newpor5_Yalg_cor_spc.xyz
ASCII simulation result isochore in xyz format for the entire 5000 m grid Eneabba Formation (198 Ma to 182 Ma)	ANLEC_LesueurSFM_Phase1_spc_grdecl_output	lesueur_38fntec-por_cmg_finegrid_newpor5_Eneab_cor_spc.xyz
ASCII simulation result in grdecl format for the entire 500 m grid volume. Note that only grain sizes and porosity are included in this file.	ANLEC_LesueurSFM_Phase1_spc_grdecl_output	lesueur_38fntec-por_cmg_finegrid_newpor5_cor.grdecl

A.2.2 ASCII RAW OUTPUT FILES

The following files can be opened in any text reader or spreadsheet

Apx Table A.3 Raw ASCII output files as output directly from 'sedsim9_120427Intelmac'

FILE CONTENT	FOLDER	FILE NAME
ASCII uncompacted simulation results for the entire 5000 m grid volume	ANLEC_LesueurSFM_Phase1_raw_5000m_output	lesueur_38fntec-por_cmg_fg500m_newpor5.GRAPH, TOT,FLO,SED,BAS,CMP,TEC,INFO,TIME
ASCII compacted simulation results for the entire 5000 m grid volume	ANLEC_LesueurSFM_Phase1_raw_5000m_output	lesueur_38fntec-por_cmg_fg500m_newpor5.GRAPC, TOC
ASCII uncompacted simulation results for the entire nested 500 m grid volume	ANLEC_LesueurSFM_Phase1_raw_500m_output	lesueur_38fntec-por_cmg_finegrid_newpor5.GRAPH, TOT ,SED,BAS,CMP
ASCII compacted simulation results for the entire nested 500 m grid volume	ANLEC_LesueurSFM_Phase1_raw_500m_output	lesueur_38fntec-por_cmg_finegrid_newpor5. GRAPC, TOC

A.2.3 BINARY OUTPUT FILES

The following files can be opened in the SedView 3D viewer

Apx Table A.4 Sedsim9 binary SedView (.cif) output files

FILE CONTENT	FOLDER	FILE NAME
SedView file for the compacted 5000 m grid volume	ANLEC_LesueurSFM_Phase1_cif_output	lesueur_38fntec-por_cmg_fg500m_newpor5_cor.cif
SedView file for the compacted 500 m grid volume	ANLEC_LesueurSFM_Phase1_cif_output	lesueur_38fntec-por_cmg_finegrid_newpor5_cor.cif
SedView file for the uncompacted 5000 m grid volume	ANLEC_LesueurSFM_Phase1_cif_output	lesueur_38fntec-por_cmg_fg500m_newpor5.cif
SedView file for the uncompacted 500 m grid volume	ANLEC_LesueurSFM_Phase1_cif_output	lesueur_38fntec-por_cmg_finegrid_newpor5.cif

References and Bibliography

Abeysinghe, P.B. 2003 Silica resources of Western Australia Geological Survey of Western Australia. Mineral Resources Bulletin 21 228p

Al-Khadhrawi, M.R., Cantrell, D.L., Griffiths, C.M., Franks, S.G., 2011: Quantitative Prediction of Reservoir Quality: A Permo-Carboniferous Reservoir, Saudi Arabia.

Allinson, W.G., Cinar, Y., Hou, W., Neal, P.R., 2009: The Costs of CO_2 Transport and Injection in Australia, School of Petroleum Engineering, The University of New South Wales, Sydney, Australia. CO_2TECH Report Number RPT09-1536. Prepared for the Carbon Storage Taskforce, Department of Resources, Energy and Tourism, Canberra.

Anonymous, 2010: Site Screening, Selection, and Initial Characterization for Storage of CO_2 in Deep Geologic Formations DOE/NETL-401/090808, November 2010

Appleyard, S.J. , Commander, D.P. , Allen, A.D. 1993 Groundwater Vulnerability to Contamination - northern part of Perth Basin, 1:500 000 map. Geological Survey of Western Australia 1v map

Appleyard, S.J. , Commander, D.P. , Allen, A.D. 1993 Groundwater Vulnerability to Contamination - southern part of Perth Basin, 1:500 000 map. Geological Survey of Western Australia 1v map

Appleyard, S.J. 1991. The geology and hydrogeology of the Cowaramup borehole line Perth Basin, Western Australia. Geological Survey of Western Australia. Report 30 p1-12

Appleyard, S.J., Commander, D.P., Allen, A.D., 1993, Groundwater Vulnerability to Contamination - southern part of Perth Basin, 1:500 000 map., Geological Survey of Western Australia, 1v, map

Appleyard, S.J., Commander, D.P., Allen, A.D., 1993, Groundwater Vulnerability to Contamination - northern part of Perth Basin, 1:500 000 map., Geological Survey of Western Australia, 1v, map

Backhouse, J. 1993 Palynology and correlation of Permian sediments in the Perth, Collie, and Officer Basins, Western Australia. Geological Survey of Western Australia. Report 34 p111-128

Balme, B.E. 1969 The Triassic System in Western Australia. APEA Journal 9(2) p67-78

Banks, M.R. 1969 Correlation chart for the Triassic System in Australia. IN Gondwana stratigraphy. Unesco, France 1v p478-481

Baxter, J.L. 1977 Heavy mineral sand deposits of Western Australia. Geological Survey of Western Australia. Mineral Resources Bulletin 10

Beddoes, L. R. Jr. 1973 Oil and gas fields of Australia, Papua New Guinea and New Zealand. Tracer Petroleum & Mining Publications Pty Ltd, Sydney 1v

Bergmark, S.L. , Evans, P.R. 1987 Geological controls on reservoir quality of the northern Perth Basin. APEA Journal 27(1) p318-330

Blakey, R.C., 2008. Gondwana paleogeography from assembly to breakup- A 500 m.y. odyssey. *In* Fielding, C.R., Frank, T.D., and Isbell, J.L., eds., Resolving the Late Paleozoic Ice Age in Time and Space: Geological Society of America Special Paper 441. p. 1-28.

Blyth, C.I. 1994 Beagle seismic survey interpretation report WA-22-P (North). Woodside Offshore Petroleum, PSLA 92/30 (unpublished)

Bradshaw, B.E. , Rollet, N. , Totterdell, J.M. , Borissova, I. 2003 A Revised Structural Framework for Frontier Basins on the Southern and Southwestern Australian Continental Margin Geoscience Australia. Record 1v. 44p

Bradshaw, B.E. , Rollet, N. , Totterdell, J.M. , Borissova, I. 2003 A Revised Structural Framework for Frontier Basins on the Southern and Southwestern Australian Continental Margin Geoscience Australia. Record 1v. 44p

Bradshaw, B.E., Rollet, N., Totterdell, J.M., Borissova, I., 2003, A revised structural framework for frontier basins on the southern and south-western Australian continental margin., Geoscience Australia. Record, 2003/03, 44. (Refid: 13490)

Bradshaw, M., & Yeung, M., 1990, The Jurassic Palaeogeography Of Australia. BMR Record 1990/76 Palaeogeography 26, Bureau Of Mineral Resources, Geology And Geophysics Australian Petroleum Industries Research Association, Palaeogeographic Maps Project 1990

Briese, E.H. 1979 The geology and hydrogeology of the Moora Borehole Line. Western Australia. Department of Mines. Annual Report 1978 p60-66

Cadman, S.J. , Pain, L. , Vuckovic, V. 1994 Perth Basin, Western Australia. Australian Petroleum Accumulations. Report 10 103pp

Cadman, S.J., Pain, L. and Vuclovic, V. 1994 Perth Basin, WA. Australian Petroleum Accumulations Report 10, Bureau of Resources Sciences, Canberra

Cadman, S.J., Pain, L., Vuckovic, V., 1994, Perth Basin, Western Australia., Australian Petroleum Accumulations. Report, 10, 103pp. (Refid: 43031)

Cantrell, D.L., Griffiths, C.M., Franks, S.G., Al-Khadhrawi, M.R., 2010: Prediction of Unayzah Reservoir Quality Ahead-of-the-Bit. AAPG Search and Discovery Article #90105, AAPG GEO Middle East Conference & Exhibition, Manama, Bahrain, 7-10 March 2010

Causebrook, R., Dance, T., and Bale, K., 2006. Southern Perth Basin: Site Investigation and Geological Model for Storage of Carbon Dioxide. Research Program 1.1- Technologies for Assessing Sites for CO_2 Storage. December 2006, CO_2CRC Report No: RPT06-0162

Cockbain, A.E. , Lowry, D.C. , Cope, R.N. , Low, G.H. , Playford, P.E. 1975 Phanerozoic. Geological Survey of Western Australia. Memoir 2 p223-433

Cockbain, A.E. 1986 Phanerozoic sedimentary basins of Western Australia and their petroleum potential. Geological Survey of Western Australia. Record 1986/6

Cockbain, A.E., Lowry, D.C., Cope, R.N., Low, G.H., Playford, P.E., 1975, Phanerozoic., Geological Survey of Western Australia. Memoir, 2, p223-433. (Refid: 36890)

Commander, D.P. 1978 Hydrogeology of the Eneabba borehole line. Geological Survey of Western Australia. Annual Report 1977 p13-18

Commander, D.P. 1989 Hydrogeological map of Western Australia, 1:2 500 000. Geological Survey of Western Australia 1v Map

Commander, D.P., 1989, Hydrogeological map of Western Australia, 1:2 500 000., Geological Survey of Western Australia, 1v, Map

Cope, R.W. , Playford, P.E. 1971 The Phanerozoic stratigraphy of Western Australia: a correlation chart in two parts. Geological Survey of Western Australia. Report 1970 p32-33

Cowley, R., 2001, MkII Airborne Laser Fluorosensor survey reprocessing and interpretation report: Perth Basin, Western Australia, AGSO Record 2001/19, 2001/19, 32. (Refid: 12756)

Crostella, A. 1995 An evaluation of the hydrocarbon potential of the onshore northern Perth Basin, Western Australia. Western Australia Geological Survey, Report 43, 67p

Crostella, A. 2001 Geology and petroleum potential of the Abrolhos Sub-basin, Western Australia. Western Australia Geological Survey, Report 75, 57p

Crostella, A. , Backhouse, J. 1999 South-North Log Correlation: Sue 1 to Woodada 3 IN Crostella, A. and Backhouse, J. "Geology and petroleum exploration in the central and southern Perth Basin" Geological Survey of Western Australia. Report 57 Map

Crostella, A. , Backhouse, J. 2000 Geology and petroleum exploration of the central and southern Perth Basin, Western Australia Geological Survey of Western Australia. Report 57, 85

Crostella, A. , Backhouse, J. 2000 Geology and petroleum exploration of the central and southern Perth Basin, Western Australia Geological Survey of Western Australia. Report 57 85

Crostella, A. 2001 Geology and petroleum potential of the Abrolhos Sub-basin, Western Australia Geological Survey of Western Australia. Report 75 57p

Crostella, A. and Backhouse, J. 2000 Geology and petroleum exploration of the central and southern Perth Basin, Western Australia. Western Australia Geological Survey, Report 57, 85p

Crostella, A., 1995, An evaluation of the hydrocarbon potential of the onshore northern Perth Basin, Western Australia, Geological Survey of Western Australia. Report, 43, 67. (Refid: 12757)

Crostella, A., Backhouse, J., 1999, South-North Log Correlation: Sue 1 to Woodada 3 IN Crostella, A. and Backhouse, J. "Geology and petroleum exploration in the central and southern Perth Basin", Geological Survey of Western Australia. Report, 57

Crostella, A., Backhouse, J., 1999, South-North Log Correlation: Sue 1 to Woodada 3 IN Crostella, A. and Backhouse, J. "Geology and petroleum exploration in the central and southern Perth Basin", Geological Survey of Western Australia. Report, 57, Map

Crostella, A., Backhouse, J., 2000, Geology and petroleum exploration of the central and southern Perth Basin, Western Australia, Geological Survey of Western Australia. Report, 57, 85. (Refid: 12758)

Dance, T., Spencer, L., and Xua, J.-Q.,, 2009: Geological Characterisation of the Otway Project Pilot Site: What a Difference a Well Makes. Energy Procedia, 1, (2009), p2871-2878

Davidson, W.A., 1995, Hydrogeology and groundwater resources of the Perth region, Western Australia, Geological Survey of Western Australia. Bulletin, 142, 257p. (Refid: 12759)

Dolby, J.H. , Balme, B.E. 1976 Triassic palynology of the Carnarvon Basin, Western Australia. Review of Palaeobotany and Palynology 22(2) p105-168

Dyt, C., Griffiths, C. M., and Paraschivoiu, E., 1999: Clastic depositional modelling with Sedsim. In SIAM - Mathematical and Computational Issues in the Geosciences, San Antonio

Dyt, C., Johnson L., Griffiths C. Paraschivoiu E., Li F., 2008. Depositional scenario modelling of Io-Jansz Oxfordian siliciclastic deposits, North West Shelf, Australia", APPEA Journal, Vol 48, extended abstract

Evans, B.J. , Paterson, G.A. , Frey, S.E. 1987 Fault plane resolution using the low-fold 3D seismic technique over Woodada Gas Field, Perth Basin, Western Australia. APEA Journal 27(1) p298-301

Falvey, D.A. , Symonds, P.A. , Colwell, J.B. , Willcox, J.B. , Marshall, J.F. , Stagg, H.M.J. 1990 Australia's deepwater frontier petroleum basins and play types. APEA Journal 30(1) p239-262

Geological Survey of Western Australia , Petroleum Division 2003 Summary of petroleum prospectivity, onshore Western Australia: Bonaparte, Canning, Officer, Perth, Southern Carnarvon and Northern Carnarvon Basins Department of Industry & Resources WA 1v 28p

Geological Survey of Western Australia , Petroleum Division 2004 Summary of Petroleum Prospectivity, Onshore Western Australia and State Waters 2004: Bonaparte, Canning, Officer, Perth, Southern Carnarvon, and Northern Carnarvon Basins Department of Industry & Resources WA 1v 28p

Geological Survey of Western Australia 1973 Dongara-Hill River, Western Australia, 1:250 000 geological series map. Sheets SH/50-05 & SH/50-09, 1st edition. Geological Survey of Western Australia 1v

Geological Survey of Western Australia 2005 Summary of petroleum prospectivity, Western Australia 2005: Bonaparte, Bight, Canning, Officer, Perth, Northern Carnarvon and Southern Carnarvon Basins Geological Survey of Western Australia 2005 36p

Geological Survey of Western Australia, 1973, Dongara-Hill River, Western Australia, 1:250 000 geological series map. Sheets SH/50-05 & SH/50-09, 1st edition., Geological Survey of Western Australia, 1v

Gorter, J.D. , Hearty, D.J. , Bond, A.J. 2004 Jurassic petroleum systems in the Houtman Sub-basin, Northwestern Offshore Perth Basin, Western Australia: A Frontier Petroleum Province on the Doorstep? APPEA Journal 44(1) p13-57

Griffiths C. M., Paraschivoiu E., Dyt, C., Lotfpour, M., 2006. Dezful Embayment, Asmari Equivalent (34 - 18 Ma) Sedsim modelling of depositional systems – regional study. Contribution to Phase 2 of IOR-JSP project. February 2006. CSIRO Petroleum Confidential report to NIOC. Confidential Report No: 06-013

Griffiths, C. M., 2006, CSIRO Submission to the Australian Senate Rural and Regional Affairs and Transport References Committee – "Inquiry into Australia's future oil supply and alternative transport fuels." February 2006.

Griffiths, C. M., 2007. Lake Qinghai, China: Using 3D stratigraphic forward modelling to predict organic carbon content of a non-marine basin system. International conference on Non-Marine Basin Systems: Depositional Processes And Products, Stratigraphy, and Petroleum Reservoir Exploration. May 10-12, 2007. Mengxi Hotel, Beijing. Extended Abstract and Poster

Griffiths, C. M., 2010. Recent advances in stratigraphy – a commentary. First Break, 28, January 2010, 53-55.

Griffiths, C. M., and Dyt, C., 2001: Six Years of Sedsim Exploration Applications (Abstract Only), AAPG Bulletin, 85 (2001), pg 13.

Griffiths, C. M., And Paraschivoiu, E., 1998: Three-Dimensional Forward Stratigraphic Modelling of Early Cretaceous Sedimentation on The Leveque and Yampi Shelves, Browse Basin. The APPEA Journal, V. 38, No.1, P.147-158.

Griffiths, C. M., Dyt, C. P., Li, F., 2006, Stratigraphic Forward Modelling for the Past, Present and Future. Invited keynote presentation at the EAGE Grenoble Workshop "From Seismic Interpretation to Basin Modelling", September 2006.

Griffiths, C. M., Dyt, C., Huang, X., 2011. Sedsim simulation of the Late Jurassic Yarragadee Fm. in the Perth Basin. Confidential CSIRO Report for WA Geothermal Centre of Excellence.

Griffiths, C. M., Dyt, C., Paraschivoiu, E., and Liu, K., 2001: Sedsim in Hydrocarbon Exploration. In Merriam, D., Davis, J. C. (Eds) Geologic Modeling and Simulation. Kluwer Academic, New York.

Griffiths, C. M., Salles, T., Dyt, C., 2009. Hawtah Trend – Predicting Unayzah facies distribution using Sedsim. CSIRO Confidential report # 09-xxx for Saudi Aramco.

Griffiths, C. M., Salles, T., Dyt, C., 2011. Stratigraphic Forward Modelling of the Gippsland Basin from

Gurevich, B., Gerhardt, A., Lambert G., Griffiths, D.M., and Dyt, C. 2006, Numerical modelling of seismic character of depositional sequences, EAGE Internat. Geophys. Conf. Exhib., Saint-Petersburg, Russia, 16-19 October 2006, Expanded Abstracts, paper 1092.

Hall, P.B. 1989 The future prospectivity of the Perth Basin. APEA Journal 29(1) p440-449

Hall, P.B., 1989, The future prospectivity of the Perth Basin., APEA Journal, 29(1), p440-449. (Refid: 41728)

Harley, A.S. 1975 Earth tide influence on ground water levels, Hill River area, Perth Basin. Western Australia. Department of Mines. Report 1974 p21-24

Harley, A.S. 1975 The geohydrology of the Watheroo-Jurien Bay drillhole line, Perth Basin. Western Australia. Department of Mines. Report 1974 p24-29

Harris, L.B., 1994, Structural and tectonic synthesis for the Perth Basin, Western Australia., Journal of Petroleum Geology, 17, 129-156. (Refid: 14253)

Hirschberg, K-J.B. 1989 Busselton shallow-drilling groundwater investigation, Perth Basin. Geological Survey of Western Australia. Report 25 p17-37

Hocking, R.M. , Preston, W.A. 1998 Western Australia: Phanerozoic geology and mineral resources. AGSO Journal of Australian Geology and Geophysics 17(3) 245-260

Hocking, R.M., 1994, Subdivisions of Western Australian Neoproterozoic and Phanerozoic sedimentary basins., Geological Survey of Western Australia. Record, 1994/4, p1-84. (Refid: 43442)

Iasky, R.P. 1993 A structural study of the southern Perth basin, Western Australia. Geological Survey of Western Australia. Report 31 56pp

Iasky, R.P., 1993, A structural study of the southern Perth basin, Western Australia., Geological Survey of Western Australia. Report, 31, 56pp. (Refid: 43096)

Johnstone, M.H. , Jones, D.K. , Pearson, G.R. , Smith, D.N. , Thomas, B.M. 1976 The Phanerozoic of the Perth and Carnarvon Basins, Western Australia. 25th International Geological Congress. Excursion Guide 39C

Johnstone, M.H. , Lowry, D.C. , Quilty, P.G. 1973 The geology of south-western Australia - a review. Royal Society of Western Australia. Journal 56 5-15

Jones, D.K. , Pearson, G.R. 1972. The tectonic elements of the Perth Basin. APEA Journal 12(1) p17-22

Jones, D.K. 1976 Perth Basin IN Economic Geology of Australia and Papua New Guinea 3. Petroleum. Leslie, R.B., Evans, H.J. & Knight, C.L. (Editors) AusIMM. Monograph Series 7 p108-126

Jones, D.K., Pearson, G.R., 1972, The tectonic elements of the Perth Basin., APEA Journal, 12(1), p17-22. (Refid: 31568)

Jones, N.T. and Hall, A.D. 2002 The Cliff Head Oil Discovery - Offshore Perth Basin. The Sedimentary Basins of Western Australia. Proceedings PESA Symposium, Perth, 901-909

Jutson, J.T., 1914, An outline of the physiographical geology (physiography) of Western Australia, Geological Survey of Western Australia. Bulletin, 61, 22. (Refid: 2063)

Kantsler, A.J. , Cook, A.C. 1979 Maturation patterns in the Perth Basin. 1979 Apea Conference Perth 11-14 March, 1979. APEA Journal 19(1) p94-107

Kantsler, A.J., Cook, A.C., 1979, Maturation Pathways in the Perth Basin, APEA Journal, 19, 94-107. (Refid: 12762)

Kempton, R.H., Liu, K., Boreham, C., Bradshaw, B.E., Eadington, P.J. and Passmore, V. 2002 Oil migration and accumulation in the offshore Perth Basin, Western Australia. CSIRO Confidential Report 02-005 to Geoscience Australia, 71p

Kern, A.M. 1993 The geology and hydrogeology of the superficial formations between Cervantes and Lancelin, Western Australia. Geological Survey of Western Australia. Report 34 p11-36

Koltermann, C E., and Gorelick, S.M., 1992: Palaeoclimatic Signature in Terrestrial Flood Deposits. Science, 256, pp 1775-1782.

Langhi, L., Ciftci, B., Strand, J. (2013). Fault seal first-order analysis –SW Hub. CSIRO, Australia. CSIRO Report EP13879

CheersLau, J.E. , Commander, D.P. , Jacobson, G. 1987 Hydrogeology of Australia. Bureau of Mineral Resources, Australia. Bulletin 227

Li, F., Dyt, C.P., and Griffiths, C.M., 2003: A coastal morphodynamic model for cross-shore sediment transport. Coastal Engineering, pages 335–344

Li, F., Dyt, C.P., and Griffiths, C.M., and McInnes, K., 2007: Predicting seabed change as a function of climate change over the next fifty years in the Australian southeast. Coastline Changes: Interrelation of Climate and Geological Processes. Special Paper 426, Chapter 4, The Geological Society of America. Eds. Harff, J., Hay, W.W., and Tetzlaff, D.M. 43-64

Lockwood, A.M. , D'Ercole, C. 2003 Geophysical investigation of the Bernier Ridge and surrounding area, Southern Carnarvon Basin, Western Australia Geological Survey of Western Australia. Report 89 53p

Lord, J.H. 1975 Perth Basin - Permian W.A. In Traves D.M. and King D.(Eds) - Economic geology of Australia and Papua New Guinea - 2.Coal AusIMM. Monograph Series 6 p269-272

Lord, J.H. 1979 Mineral deposits of Western Australia - Mineral fuels - Coal IN Prider, R.T. (ed.) "Mining in Western Australia" University of Western Australia Press 1v p131-144

Lowry, D.C. 1974 Dongara-Hill River, Western Australia, 1:250 000 geological series explanatory notes. Sheet SH/50-05. Bureau of Mineral Resources, Australia 1v 33pp

Magus, D.J. , Bratrud, T.F. , Molnar, E.L. , Wiltshire, M.J. 1980 Low permeability sandstones in Australia can be fracture stimulated. APEA Journal 20(1) p176-190

Markl, R.G., 1974, Evidence for the breakup of eastern Gondwanaland by the Early Cretaceous, Nature, 251, 196-200. (Refid: 12764)

Marshall, J.F. , Lee, C.S. , Ramsay, D.C. , Moore, A.M.G. 1989 Tectonic controls on sedimentation and maturation in the offshore North Perth Basin. APEA Journal 29(1) p450-465

Marshall, J.F., Lee, C.S., Ramsay, D.C., Moore, A.M.G., 1989, Tectonic controls on sedimentation and maturation in the offshore North Perth Basin., APEA Journal, 29(1), p450-465. (Refid: 41729)

Marshall, J.F., Lee, C.S., Ramsey, D.C. and Moore, A.M.G. 1989 Tectonic controls on sedimentation and maturation in the offshore north Perth Basin. The Australian Petroleum Production & Exploration Association (APEA) Journal, 29 (1), 450-465

Martinez, P. and Harbaugh, J.W., 1993: Simulating Nearshore Environments. Pergamon Press, New York.

McLoughlin, S. & Hill, R.S. 1996. The succession of Western Australian Phanerozoic floras. In, Hopper, S.D. et al. (eds) Gondwanan Heritage: Past, Present and Future of the Western Australian Biota (Proceedings of the Conference on Systematics, Evolution and Conservation of the Western Australian Biota, Perth, 1993), Surrey Beatty, Sydney, pp. 61–80

McTavish, R.A. , Dickins, J.M. 1974 The age of the Kockatea Shale (Lower Triassic), Perth Basin - A reassessment. Geological Society of Australia. Journal 21(2) p195-201

Moncrieff, J.S. 1989 Hydrogeology of the Gillingarra Borehole Line, Perth Basin. Geological Survey of Western Australia. Report 26 p105-126

Mory, A.J. , Commander, D.P. 1994 Geology of the Arrowsmith-Beagle Islands 1:100 000 Sheet Geological Survey of Western Australia. Explanatory Notes 1v 26p

Mory, A.J. , Commander, D.P. 1994 Geology of the Hill River - Green Head 1:100 000 Sheets. Geological Survey of Western Australia. Explanatory Notes 1v 29p

Mory, A.J. , Iasky, R.P. 1995 Geology of the Irwin River Coalfield Area, W.A. (1:100 000 map sheet area) Geological Survey of Western Australia. Report 44 Plate 1 (map)

Mory, A.J. , Iasky, R.P. 1995 Wedge Island, W.A. 1:100 000 geological sheet. Geological Survey of Western Australia 1v map

Mory, A.J. , Iasky, R.P. 1996 Stratigraphy and structure of the onshore northern Perth Basin Western Australia Geological Survey of Western Australia. Report 46 102pp

Mory, A.J. , Lasky, R.P. , Preston, W. 1994 Arrowsmith-Beagle Islands 1:100 000 Sheet. 1st Edition. Geological Survey of Western Australia 1v Map Legend

Mory, A.J. , Lasky, R.P. 1995 Mingenew-Dongara 1:100 000 geological sheet. Geological Survey of Western Australia 1v Map Legend

Mory, A.J. 1994 Hill River-Green Head 1:100 000 Sheet. 1st Edition. Geological Survey of Western Australia 1v

Mory, A.J. 1995 Geology of the Mingenew-Dongara 1:100 000 Sheet Geological Survey of Western Australia. Explanatory Notes 1v 39p

Mory, A.J. 1995 Geology of the Wedge Island 1:100 000 Sheet Geological Survey of Western Australia. Explanatory Notes 1v 19p

Mory, A.J. and Iasky, R.P. 1996 Stratigraphy and structure of the onshore northern Perth Basin. Western Australia Geological Survey, Report 46

Mory, A.J., 1994, Hill River-Green Head 1:100 000 Sheet. 1st Edition., Geological Survey of Western Australia, 1v, Map Legend

Mory, A.J., Iasky, R.P., 1995, Geology of the Irwin River Coalfield Area, W.A. (1:100 000 map sheet area), Geological Survey of Western Australia. Report, 44, Plate 1 (map)

Mory, A.J., Iasky, R.P., 1995, Wedge Island,W.A. 1:100 000 geological sheet., Geological Survey of Western Australia, 1v, map

Mory, A.J., Iasky, R.P., 1996, Stratigraphy and structure of the onshore northern Perth Basin Western Australia, Geological Survey of Western Australia. Report, 46, 102pp. (Refid: 23279)

Mory, A.J., Lasky, R.P., 1995, Mingenew-Dongara 1:100 000 geological sheet., Geological Survey of Western Australia, 1v, Map Legend

Mory, A.J., Lasky, R.P., Preston, W., 1994, Arrowsmith-Beagle Islands 1:100 000 Sheet. 1st Edition., Geological Survey of Western Australia, 1v, Map Legend

Myers, J.S. 1995 Geology of the Albany 1:1 000 000 sheet. Geological Survey of Western Australia 1v 9p

Myers, J.S., Hocking, R.M., 1998, Geological map of Western Australia 1:2 500 000. 13th Edition., Geological Survey of Western Australia, Map, Map Legend. (Refid: 44867)

Neal, P.R. , Hou, W., Allinson, W.G., and Cinar, Y., 2010: Costs of CO_2 Transport and Injection in Australia. SPE 133900. SPE Asia Pacific Oil & Gas Conference and Exhibition, Brisbane, Queensland, Australia, 18–20 October 2010.

Nicoll, R.S., Laurie, J.R., Kelman, A.P., Mantle, D.J., Haines, P.W., Mory, A.J., Hocking, R.M., 2009. Canning Basin Biozonation and Stratigraphy, 2009. Chart 31.

Norlin, W.K. 1981 Woodada 1 - A discovery in the Perth Basin. APEA Journal 21(1) p55-59

Norvick, M.S., 2003. Tectonic and Stratigraphic History of the Perth Basin. Geoscience Australia, Record 2004/16. 18p

Norvick, M.S. 2004 Tectonic and stratigraphic history of the Perth Basin Geoscience Australia. Record 2004/16 18p + unnumb. pages of figures,chart

Norvick, M.S., 2004, Tectonic and stratigraphic history of the Perth Basin, Geoscience Australia. Record, 2004/16, 18p + unnumbered pages of figures, chart. (Refid: 14227)

Owad-Jones, D. and Ellis, G. 2000 Western Australia atlas of petroleum fields, onshore Perth Basin. Petroleum Division, Department of Minerals and Energy Western Australia, Volume 1, 114p

Owad-Jones, D., Ellis, G., 2000, Western Australia atlas of petroleum fields, onshore Perth Basin, Petroleum Division, Department of Minerals and Energy Western Australia, Volume, 1, 114. (Refid: 12766)

Petkovic, P., Brett, J., Morse, M.P., Hatch, L., Webster, M.A., Roche, P., 1999a, Gravity, magnetic and bathymetry grids from levelled data for southwest Australia - Southwest region, Australian Geological Survey Organisation. Record, 1999/47, . (Refid: 12767)

Playford, P.E. , Cockbain, A.E. , Low, G.H. 1976 Geology of the Perth Basin, Western Australia. Geological Survey of Western Australia. Bulletin 124

Playford, P.E. , Cope, R.W. , Cockbain, A.E. , Low, G.H. , Lowry, D.C. 1975 Perth Basin IN Geology of Western Australia Geological Survey of Western Australia. Memoir 2

Playford, P.E. , Low, G.H. 1972 Definitions of some new and revised rock units in the Perth Basin. Western Australia. Department of Mines. Report 1971 p88-90

Playford, P.E., 1971, Petroleum exploration in Western Australia: past, present and future., Royal Society of Western Australia. Journal, 54(1), p1-13. (Refid: 32641)

Playford, P.E., Cockbain, A.E., Low, G.H., 1976, Geology of the Perth Basin, Western Australia., Geological Survey of Western Australia. Bulletin, 124

Playford, P.E., Willmott, S.P., 1958, Stratigraphy and structure of the Perth Basin, Western Australia, West Australian Petroleum Pty Ltd Report (unpublished), . (Refid: 12769)

Powell, T.G. , McKirdy, D.M. 1973 Crude oil correlations in the Perth and Carnarvon Basins. APEA Journal 13(1) p81-85

Prider, T. 1979 The geology of Western Australia in relation to its mineral resources in Prider R.T.(ed) - Mining in Western Australia. University of Western Australia Press 1v p24-38

Quaife, R., Rosser, J. and Pagnozzi, S. 1994 The structural architecture and stratigraphy of the offshore northern Perth Basin. IN: The Sedimentary Basins of Western Australia (Edited by Purcell, P.G. and Purcell, R.R.). Proceedings of the West Australian Basins Symposium, Western Australia PESA, Perth, 1994, 811-822

Quaife, R., Rosser, J., Pagnozzi, S., 1994, The structural architecture and stratigraphy of the offshore northern Perth Basin, in Purcell, P.G. & Purcell, R.R. (eds), The sedimentary basins of Western Australia. Proceedings of a PESA Symposium, Perth, 811-822. (Refid: 12770)

Rigg, A. 1979 Structural and stratigraphic settings of Australian fluvio-deltaic petroleum reservoirs.1979 Apea Conference Perth 11-14 March 1979 PESA Symposium: Fluvio-deltaic sediments and hydrocarbons APEA Journal 19(2) p31-36

Salles T., Marchès, E., Dyt, C., Griffiths, C., Hanquiez, V., Mulder, T., 2009, Simulation of the interactions between gravity processes and contour currents on the Algarve Margin (South Portugal) using the stratigraphic forward-model Sedsim. Reference: SEDGEO4050, Sedimentary Geology DOI information: 10.1016/j.sedgeo.2009.05.007]

Salles, T., 2009: Aeolian module in Sedsim. open file. CSIRO Predictive Geoscience Group: CSIRO report number 09-002

Salles, T., Cacas, M.C., Mulder, T., Li, F., Griffiths, C., Dyt, C., Sedimentary fill of submarine canyons and channels using a Cellular Automata process-based model. 2008, APPEA Journal.

Salles, T., Lopez, S., Eschard, R., Mulder, T., Euzen, T., Cacas, M.C., A turbidity currents model to simulate impact of basin-scale forcing parameters. SEPM Special publication, accepted.

Schlumberger-TerraTek, 2010. Petrographic Analysis of Eneabba Formation and Myalup and Wonnerup Member Samples- Pinjarra 1 Well - Western Australia. TR10-403014 January 2010

Smith, G.C. , Cowley, R.G. 1987 The tectono-stratigraphy and petroleum potential of the northern Abrolhos Sub-basin, Western Australia. APEA Journal 27(1) p112-136

Smith, D.G., 1983, Anastomosed fluvial deposits: modern examples from Western Canada, In: Collinson, J. and Lewin, J., Eds. Modern and ancient fluvial systems: Oxford: Blackwell (Special Publication of the International Association of Sedimentologists v. 6, p. 155-168.

Song, T and Cawood, P.A. 2000 Structural styles in the Perth Basin associated with the Mesozoic break-up of greater India and Australia. Tectonophysics. Vol. 317, Issues: 1-2, Pp 55-72

Song, T. and Cawood, P.A. 1999 Multistage deformation of linked fault systems in extensional regions; an example from the northern Perth Basin, Western Australia. Australian Journal of Earth Sciences. 46; 6, Pages 897-903

Song, T., Cawood, P.A., 2000, Structural styles in the Perth Basin associated with the Mesozoic breakup of Greater India and Australia, Tectonophysics, 317, 55-72. (Refid: 12771)

Spencer, L., Xu, Q., LaPedalina, F., Weir, G., 2006: Site characterization of the Otway Basin Storage Pilot in Australia. Proceeding of the 8th International Conference on Greenhouse Gas Control Technologies, 19-22 June 2006, Trondheim, Norway.

Stagg, H.H.J, Willcox, J.B., Symonds, P.A, OBrien, G.W., Colwell, J.B., Hill, P.J., Lee, C.S., Moore, A.M.G. and Struckmeyer, H.I.M. 1999 Architecture and evolution of the Australian continental margin. AGSO Journal of Australian Geology and Geophysics. 17; 5-6, Pages 17-33. 1999

Stagg, H.M.J., Willcox, J.B., Symonds, P.A., O'Brien, G.W., Colwell, J.B., Hill, P.J., Lee, C-S., Moore, A.M.G., Struckmeyer, H.I.M., 1999, Architecture and evolution of the Australian continental margin, AGSO Journal of Australian Geology and Geophysics, 17(5/6), 17-33. (Refid: 12772)

Stein, A., Lunn, G., Scott, J., Alexander, B., Sherlin, B., Dolan, R., 1989, Petroleum geology, offshore exploration potential and economic evaluation, Perth Basin, Western Australia, Perth, Dolan and Associates (unpublished), . (Refid: 12773)

Stein, A., Lunn, G., Scott, J., Alexander, B., Sherlin, B., Dolan, R., 1989, Petroleum geology, offshore exploration potential and economic evaluation, Perth Basin, Western Australia, Perth, Dolan and Associates (unpublished), . (Refid: 12773)

Summons, R.E., Boreham, C.J., Foster, C.B., Murray, A.P., Gorter, J.D., 1995, Chemostratigraphy and the composition of oils in the Perth Basin, Western Australia, APEA Journal, 35(1), 613-632. (Refid: 12774)

Symons, P.A. , Cameron, P.J. 1977 The structure and stratigraphy of the Carnarvon Terrace and Wallaby Plateau. APEA Journal 17(1) p30-41

Tetzlaff, D. M. and Harbaugh, J. W., 1989: Simulating Clastic Sedimentation; Computer Methods in the Geosciences, Van Nostrand Reinhold, New York, p 202.

Thomas, B.M. , Barber, C.J. 2004 A Re-evaluation of the Hydrocarbon Habitat of the Northern Perth Basin APPEA Journal 44(1) p59-91

Thomas, B.M. 1979 Geochemical analysis of hydrocarbon occurrences in northern Perth Basin, Australia. American Association of Petroleum Geologists. Bulletin 63(7) p1092-1107

Thomas, B.M., 1979, Geochemical analysis of hydrocarbon occurrences in northern Perth Basin, Australia., American Association of Petroleum Geologists. Bulletin, 63(7), p1092-1107. (Refid: 35653)

Thomas, B.M., 1984, Hydrocarbons, source rocks and maturity trends in the northern Perth Basin, Australia, In: G. Demaison and R.J. Morris (eds), Petroleum Geochemistry and Basin Evolution. AAPG, Memoir, 35, 341-403. (Refid: 12777)

Thyer, R.F., Everingham, I.B., 1956, Gravity survey of the Perth Basin, Western Australia., Bureau of Mineral Resources, Australia. Bulletin, 33, . (Refid: 44971)

Truswell, E.M. 1982 Palynology of seafloor samples collected by the 1911-14 Australasian Antarctic Expedition: implications for the geology of coastal East Antarctica. Geological Society of Australia. Journal 29(3/4) p343-356

Tyler, I.M., Hocking, R.M., 2001, Tectonic units of Western Australia (scale 1:2 500 000), Geological Survey of Western Australia, . (Refid: 12778)

Vanderhor, F. , Flint, R.B. , Tyler, I.M. , Hocking, R.M. 2006 1:500 000 interpreted bedrock geology of Western Australia, 2006 update. Dataset within GeoVIEW.WA (interactive geological map) Geological Survey of Western Australia map

Vanderhor, F., Flint, R.B., Tyler, I.M., Hocking, R.M., 2006, 1:500 000 interpreted bedrock geology of Western Australia, 2006 update. Dataset within GeoVIEW.WA (interactive geological map), Geological Survey of Western Australia, map

Varma, S., Underschultz, J., Dance, T., Langford, R., Esterle, J., Dodds, K., van Gent, D., 2009. Regional study on potential CO2 geosequestration in the Collie Basin and the Southern Perth Basin of Western Australia. Marine and Petroleum Geology. V26. p 1255-1273

Veevers, J.J., Li, Z.X., 1991, Review of seafloor spreading around Australia II, marine magnetic anomaly modelling, Australian Journal of Earth Sciences, 38 (4), 391-408. (Refid: 12779)

Warris, B.J. 1988 The geology of the Mount Horner oilfield, Perth Basin, Western Australia. APEA Journal 28(1) p88-99

West Australian Petroleum Pty Ltd 1964 Summary of data and results, Perth Basin, Western Australia - Eneabba No.1, Hill River Stratigraphic Wells, Woolmulla No.1. Petroleum Search Subsidy Acts. Publication 54 50pp

Wharton, P.H. 1981 The geology and hydrogeology of the Quindalup borehole line. Geological Survey of Western Australia. Annual Report 1980 p27-35

Wijns, C., Poulet, T., Boschetti, F., Dyt, C., Griffiths, C. M., 2005: Interactive Inverse Methodology Applied to Stratigraphic Forward Modelling. In: Curtis, A., and Woods, R., (eds) Geological Prior Information, Geological Society of London, Special Publication 239.

Wilde, S.A. , Walker, I.W. 1982 Collie, Western Australia, 1:250 000 geological series explanatory notes. Sheet SI/50-06. Geological Survey of Western Australia 1v

Wilde, S.A. , Walker, I.W. 1984 Pemberton-Irwin Inlet, Western Australia, 1:250 000 geological series explanatory notes. Sheets SI/50-10 and SI/50-14. Geological Survey of Western Australia 1v

Willmott, S.P. 1964 Revisions to the Mesozoic Stratigraphy of the Perth Basin. IN 'Summary of data and results, Perth Basin, Western Australia. Eneabba No.1.' Petroleum Search Subsidy Acts. Publication 54 p11-17

Willmott, S.P., 1964, Revisions to the Mesozoic Stratigraphy of the Perth Basin. IN 'Summary of data and results, Perth Basin, Western Australia. Eneabbba No.1.', Petroleum Search Subsidy Acts. Publication, 54, p11-17

Yeates, A.N. , Mulholland, S.M. 1991 Notes to accompany a 1:500 000 - scale structure and structural history map of the Australian Triassic. Bureau of Mineral Resources, Record 1991/32 p1-41

CONTACT US

t 1300 363 400
+61 8 6436 8500
e enquiries@csiro.au
w www.csiro.au

YOUR CSIRO

Australia is founding its future on science and innovation. Its national science agency, CSIRO, is a powerhouse of ideas, technologies and skills for building prosperity, growth, health and sustainability. It serves governments, industries, business and communities across the nation.

FOR FURTHER INFORMATION

CSIRO Earth Science and Resource Engineering/Rock Properties Group
Cedric M. Griffiths
t +61 8 6436 8784
e cedric.griffiths@csiro.au
w www.csiro.au/en/Organisation-Structure/Divisions/Earth-Science--Resource-Engineering.aspx